uOttawa

L'Université canadienne
Canada's university

FACULTÉ DES ÉTUDES SUPÉRIEURES ET POSTOCTORALES

uOttawa

L'Université canadienne
Canada's university

FACULTY OF GRADUATE AND POSDOCTORAL STUDIES

Nicolette Stanley
AUTEUR DE LA THÈSE / AUTHOR OF THESIS

M.Sc. (Earth Sciences)
GRADE / DEGREE

Department of Earth Sciences
FACULTÉ, ÉCOLE, DÉPARTEMENT / FACULTY, SCHOOL, DEPARTMENT

Effect of various biogeochemical processes on mercury methylation in Cu-Zn and Au mine tailings

TITRE DE LA THÈSE / TITLE OF THESIS

D. Fortin
DIRECTEUR (DIRECTRICE) DE LA THÈSE / THESIS SUPERVISOR

CO-DIRECTEUR (CO-DIRECTRICE) DE LA THÈSE / THESIS CO-SUPERVISOR

EXAMINATEURS (EXAMINATRICES) DE LA THÈSE / THESIS EXAMINERS

D. Lean

D. Paktunc

Gary W. Slater
LE DOYEN DE LA FACULTÉ DES ÉTUDES SUPÉRIEURES ET POSTDOCTORALES /
DEAN OF THE FACULTY OF GRADUATE AND POSTDOCORAL STUDIES

Effect of various biogeochemical processes on mercury methylation in Cu-Zn and Au mine tailings.

By
NICOLETTE STANLEY

Thesis submitted to the
Faculty of Graduate & Postdoctoral Studies
in partial fulfillment of the requirements for the
M.Sc. degree in Earth Sciences

OTTAWA-CARLETON GEOSCIENCE CENTRE
AND
UNIVERSITY OF OTTAWA,
OTTAWA, CANADA

Thèse soumise à
Faculté des études supérieures et postdoctorales
Université d'Ottawa
En vue de l'obtention de la maîtrise és sciences en science de la Terre

CENTRE GÉOSCIENTIFIQUE D'OTTAWA-CARLETON
ET
UNIVERSITÉ D'OTTAWA
OTTAWA, CANADA

Your file Votre référence
ISBN: 0-494-11415-0
Our file Notre référence
ISBN: 0-494-11415-0

Abstract

Mercury is a well known environmental pollutant. Anthropogenic sources include coal combustion, waste incineration and metal processing. In base metal mines, Hg is often left in the mining wastes (i.e., mine tailings). Once disposed of in open-air impoundments, these Hg-containing tailings can undergo various biogeochemical transformations, including Hg methylation. It is the methylated form of mercury (MeHg) that poses a threat to the environment, because it bio-accumulates at each level of the food chain. The present study was undertaken to assess the biogeochemical factors affecting Hg methylation in Cu-Zn and Au mine tailings. The study focused on the role of sulfate-reducing bacteria (SRB) because they are suspected to be associated with Hg methylation. Temperature, sulfate and organic carbon availability, along with SRB activity were tested as potential factors affecting Hg methylation in column experiments containing old Au tailings and fresh Cu-Zn tailings. The results first showed that SRB activity did not enhance Hg methylation in Cu-Zn tailings and Au tailings, indicating that iron reducing bacteria, and not SRB, along with abiotic methylation reactions played an important role. Cold temperatures did not slow down SRB activity and MeHg production, but the accidental freezing and thawing of the Cu-Zn tailings promoted the production of soluble MeHg. The mechanism responsible for this unexpected Hg methylation is however unknown. Elevated organic carbon and sulfate concentrations did enhance SRB activity, but not MeHg formation in the tailings, because increased sulfide production hindered Hg methylation. Tailings mineralogy played a significant role in the production of methyl mercury, Au tailings contained more soluble and solid-bound MeHg than Cu-Zn tailings. These results add to the increasing amount of information on Hg cycling in the environment, and indicate that SRB might not be the dominant Hg methylators in mining environments.

Sommaire

Le mercure (Hg) est un polluant environnemental notoire. Les sources anthropiques comprennent la combustion du charbon, l'incinération des déchets et la transformation des métaux. Dans les mines de métaux communs, le mercure est souvent laissé dans les résidus miniers. Une fois placés dans des bassins à ciel ouvert, ces résidus miniers contenant du mercure peuvent subir diverses transformations biogéochimiques, dont la méthylation du mercure. C'est cette forme méthylée de mercure (MeHg) qui représente une menace pour l'environnement en raison de sa bioaccumulation à chaque niveau de la chaîne alimentaire. Le but de la présente étude était d'évaluer les facteurs biogéochimiques qui ont une incidence sur la méthylation du mercure dans les résidus miniers de cuivre-zinc (Cu-Zn) et d'or (Au). L'étude se penchait sur le rôle des bactéries sulfato-réductrices (BSR) que l'on soupçonne d'être responsables de la méthylation du mercure. La température, la présence de sulfate ou de carbone organique, ainsi que l'activité des BSR ont été examinées en tant que facteurs susceptibles d'influer sur la méthylation du mercure dans le cadre d'expériences avec des colonnes contenant de vieux résidus miniers d'or et des résidus frais de cuivre-zinc. Les résultats ont d'abord démontré que l'activité des BSR n'a pas accru la méthylation du mercure dans les résidus de cuivre-zinc et d'or, ce qui indique que les bactéries réductrices de fer, et non les BSR, ainsi que les réactions de méthylation abiotique, ont joué un rôle important. Les basses températures n'ont pas ralenti l'activité des BSR et la production de MeHg, mais le gel accidentel et le dégel subséquent des résidus de cuivre-zinc ont favorisé la production de MeHg soluble. Le mécanisme responsable de cette méthylation inattendue du mercure demeure toutefois inconnu. Les concentrations élevées de carbone organique et de sulfate ont cependant accru l'activité des BSR, mais non la formation de MeHg dans les résidus, la production accrue de sulfides ayant entravé la méthylation du mercure. La minéralogie

des résidus a joué un rôle de premier plan dans la production de méthylmercure, les résidus miniers d'or contenant davantage de MeHg soluble et solide que les résidus miniers de cuivre-zinc. Ces résultats s'ajoutent à l'information toujours plus importante dont on dispose sur le cycle du mercure dans l'environnement, et indiquent que les BSR ne sont peut-être pas les facteurs dominants de la méthylation du mercure dans les environnements miniers.

Table of Contents

List of Tables

List of Figures

Acknowledgements

The present study was funded by an NSERC research grant and COMERN grants to D. Fortin. I would like to thank Kidd Metallerical Division in Timmins, Ontario for access to their tailings impoundment, and GSC Atlantic for help in funding the trip to Lower Seal Harbour, Nova Scotia.

I would also like to thank Dr. Tanmay Praharaj for his assistance in the geomicrobiology lab; Susan Winch for her assistance in the geomicrobiology lab, mercury lab, and many times in the field; Dr. David Lean for allowing me to use his mercury instruments; and Emmanuel Yumvihoze for his guidance in the mercury lab.

Danielle Fortin is greatly thanked for her comments and corrections to this thesis, and overall amazing supervision. Danielle is also thanked for making my MSc experience a very positive one, with a lot of traveling and extra experience in geomicrobiology.

Finally, I would like to thank Colin for his patience, encouragement, and technical help from beginning to end.

1. Introduction

1.1 Mining activities and mine tailings

There are over 10,000 abandoned mines in Canada, 6,015 of them are in Ontario alone (MacKasey, 2000). Some abandoned mines, especially those with mine tailings rich in sulfides, can be a source of acid mine drainage (AMD), an acidic plume of mine discharge that is enriched with soluble iron, various heavy metals and sulfate. AMD is generated during the oxidation of metal sulfides, more specifically pyrite and pyrrhotite. It is estimated that there are at least 1.8 billion tonnes of acidic tailings and 700 million tonnes of acid waste rock in Canada (Feasby and Jones, 1994). The release of AMD into the environment therefore poses a serious threat to the health of nearby ecosystems (Government of Canada, 1991).

Another potential environmental problem associated with abandoned and operational base-metal mines is mercury (Hg) contamination. In Canada, most of the research focus on Hg contamination has been on abandoned gold mines and their associated tailings. Hg-amalgamation was a process used between 1860 and 1890 in gold mining in Canada because of mercury's affinity for gold (Au), and its ability to form an amalgam with Au and leach it from the host rock. Hg can also form an amalgam with many other metals, except Fe and Pt. An amalgam is not an alloy, but a deep sorption of Hg with some interpenetration with the other metal (Veiga, 2004). After the amalgamation process, Hg was usually burned off to recover the Au and this mercury ended up in the atmosphere, which affected nearby water and soils (Malm, 1998). Large amounts of mercury were released into the atmosphere as a result of this process but Hg-amalgamation was later replaced with cyanide concentration in gold and silver mining processes (Pirrone et al., 1998). During cyanidation, Hg becomes oxidized and is

dissolved by cyanide along with Au. The problem is that if some Hg is left in old tailings from the cyanide concentration process or naturally occurring in the ore and it can be leached out if the tailings are disposed of improperly (Veiga, 2004).

As for other base metal mines (such as Cu-Zn mines), Hg contamination has never been really investigated because Hg generally represents a minor component of sulfide-rich tailings. Hg contamination from Cu-Zn tailings is however the focus of an ongoing investigation by D. Fortin, under the Collaborative Mercury Research Network (COMERN).

1.1.1 Mineral composition of sulfide-rich tailings

In Cu-Zn tailings, Hg is present in small amounts and generally originates from cinnabar (HgS) and as nano inclusions (likely HgS) in pyrite. On a weight by weight basis, Cu-Zn tailings contain more naturally occurring mercury than gold mine tailings because of the high affinity of Hg for zinc sulfides (Ku et al., 2002). The composition of Cu-Zn mine tailings depends on the composition of the host rock. In the case of the Kidd Creek Division Metallurgical Mining Site in Timmins, which is the location of the fresh Cu-Zn tailings used in this study, the processed ore is primarily composed of chalcopyrite, sphalerite, galena and pyrite. After processing, the tailings are 17% wt solid and are thickened to 62% wt solid before being deposited in the tailings impoundment. The tailings consist of 25 wt% pyrite, 1-2 wt% pyrrhotite, 1-2 wt% sphalerite and chalcopyrite, 75-85% gangue material (quartz and other silicate minerals), 7-8 wt% carbonates and other trace materials (Al et al., 1994).

1.1.2 Mineral composition of Au tailings

The mineralogical composition of Au tailings varies with the geological context. In the case of the Au ore from Lower Seal Harbour in Nova Soctia (i.e., the Au tailings used in this study), the geological setting is a wide slate dominated belt with interlacing quartz leads (MacKenzie, 1907). The main sulfide mineral in the mine tailings is arsenopyrite. Pyrrhotite, pyrite, galena, sphalerite, and chalcopyrite occur in lesser amounts in the ore and are present in the tailings. The tailings also contain trace amounts of iron and steel from the mining equipment wearing as the ore was processed (Roach, 1937; Roach 1940). The tailings also contain Hg from the mercury amalgamation process used in the early days of Au mining (the mill started in 1905) (MacKenzie, 1907). Mercury amalgamation process was later replaced in 1936 with cyanidation because a portion of the Au disseminated in the arsenopyrite was not recovered by amalgamation (leaving 30% of the ore in the tailings) (Roach 1940).

1.1.3 Chemical and microbial processes in mine tailings

Recent work on Cu-Zn and Au mine tailings have shown that there is a complex microbial community that exists under a wide range of physico-chemical conditions. Chemical and microbial iron oxidation by iron- and sulfur oxidizing bacteria has been found to occur mainly in the upper oxic portion of the tailings (Fortin et al., 1996 and references therein). Sulfate-reducing bacteria (SRB) occur deeper in the tailings, under neutral and acidic conditions and oxic and anoxic conditions (Fortin et al., 2000; 2002). In addition, the presence of iron-reducing bacteria in Cu-Zn mine tailings has also been reported (Rioux, 2004).

1.1.3.1 Microbial iron and sulfur oxidation

Iron and sulfur oxidation is very damaging to the environment because it can create toxic and acidic conditions called Acid Mine Drainage (AMD). Acidophilic chemolithotrophic bacteria greatly enhance the oxidation of iron and sulfur in mining environments (Fortin et al., 1996). These bacteria have been identified as *Acidithiobacillus ferrooxidans*, *Leptospirillum ferrooxidans* or related *Leptospirillum* spp. and *A. thiooxidans.* They are obligate acidophiles, autotrophic and aerobic microorganisms (Rawlings, 2001). Iron-oxidizing bacteria can be recovered from oxic and anoxic tailings, but maximum populations generally occur near the surface (Fortin et al., 1996).

1.1.3.2 Microbial sulfate reduction

Sulfate-reducing bacteria (SRB) were discovered in 1895 by a Dutch Biochemist, Beijerinck (Postgate, 1984). The SRB were found to be widely distributed, but only active under certain conditions, and a rotten egg smell is indicative of their presence. J.R. Postgate, a professor of Microbiology at the University of Sussex, described them as "Smelly, awkward to grow, intractable to isolate and count, but revealing intriguing novelties of biochemistry and physiology to those persistent enough to stick with them".

In order to understand the importance of SRB in carbon mineralization in natural systems, one must look at the redox sequence of carbon mineralization, as shown Figure1 (Drever, 1997). Under reducing conditions, the pH increases and net alkalinity is produced, as shown in Figure 1. Under anoxic environments where sulfate is present, microbial sulfate reduction is the dominant redox reaction taking place, if Fe(III)-rich minerals are depleted or if iron-reducing bacteria are not active. Although SRB generally

prefer anoxic and near-neutral pH conditions, they have been shown to tolerate oxygen and low-pH conditions (Fortin et al., 2000; Praharaj and Fortin, 2004).

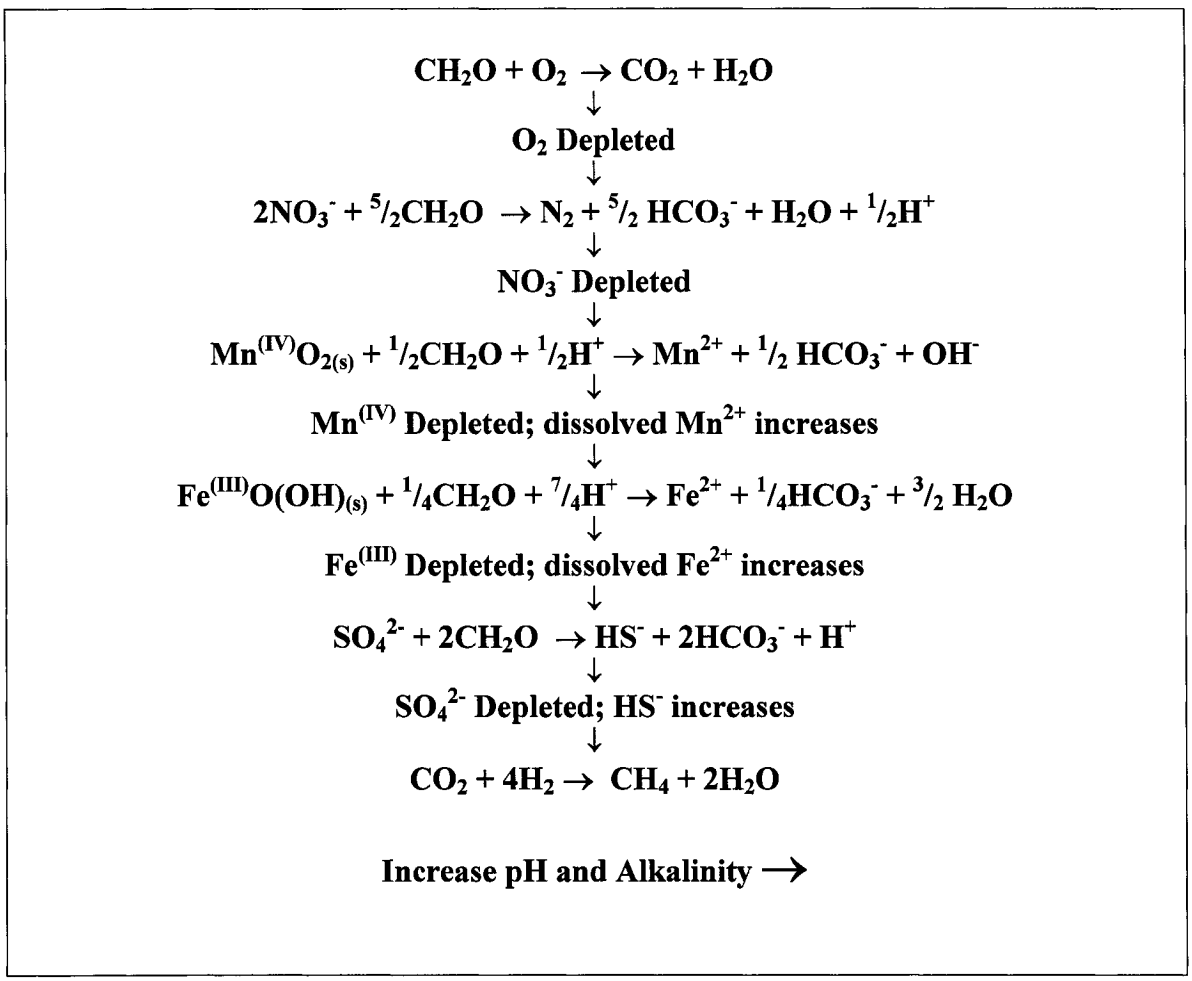

Figure 1. Controls on the redox state of water (Drever, 1997)

SRB carry out dissimilatory sulfate reduction, whereby they oxidize simple electron donors (such as lactate, formate, acetate) and transfer the electrons to sulfate, the final electron donor (Postgate, 1984). This is represented by the following reaction:

$$SO_4^{2-} + 2CH_2O \Leftrightarrow H_2S + 2HCO_3^- \qquad [1]$$

where CH_2O represents a simple form of organic carbon. During the reaction, sulfate is reduced and reduced sulfur species are produced along with bicarbonate alkalinity. The increase in sulfide species enhances the precipitation of metals from solution as metal sulfides, as shown in equation 2:

$$Me^{2+} + H_2S \Leftrightarrow MeS + 2H^+ \qquad [2]$$

where Me^{2+} represents metals such as Cd, Fe, Ni, Cu, Co, Zn, Hg (Waybrant, 1995). Combining equations [1] and [2] gives the overall reaction of sulfate reduction and precipitation of metal sulfides:

$$Me^{2+} + SO_4^{2-} + 2CH_2O \Leftrightarrow MeS_{(s)} + 2H_2CO_3 \qquad [3]$$

Desulfibrio sp. have been identified as important SRB in natural environments (Tsukamoto and Miller, 1999). The two most studied SRB genera are *Desulfovibrio* and *Desulfotomaculum,* because they are the easiest to isolate and purify (Ifill, 1999). SRB generally thrive in neutral anaerobic environments and are active up to a pH of 9.5. The presence of SRB with a high metabolic activity is revealed by the blackening of water and sediment due to the precipitation of iron sulfide, and by the smell of H_2S (Ifill, 1999).

In mining environments, sulfate-reducing bacteria could be used to remove soluble metals as biogenic metal sulfides (Adam and Edyvean, 1996). Reaction [3] shows that this reaction will occur spontaneously when the conditions favour sulfate-reducing bacteria.

Populations of SRB have been studied in Cu-Zn and Au mine tailings, and were found to vary with depth, generally preferring anoxic and near neutral pH conditions

(Praharaj and Fortin, 2004), but they can survive at low pH conditions and can tolerate oxic conditions (Fortin et al., 2000).

1.1.3.3 Microbial iron reduction

Iron reducing bacteria (IRB) are mainly active in acidic and anoxic zones of Cu-Zn and Au tailings (Fortin et al., 2002; Rioux, 2004). If iron(III)-oxides are available, microbial Fe-reduction is thermodynamically favoured over sulfate reduction (Figure 1). However, competition for common electron donors between SRB and IRB can occur and often limit the activity of iron reducers in mine tailings (Blodau et al., 1998; Rioux, 2004).

1.2 Mercury

Mercury is present in the environment in many forms. Elemental mercury (Hg^0), inorganic mercury (Hg^{2+}), and methyl mercury [$(CH_3)Hg^+$] are the most common forms and they are all toxic. However, methyl mercury is the form of Hg that is on the priority list of most environmental agencies (including Canada and the US), because it is the one that bioaccumulates in the food chain (Renzoni et al., 1998; King et al., 2002; Boening 2000). One of the most well known cases of mercury poisoning happened in Japan when thousands of people ate fish and shellfish that were highly contaminated with methyl mercury (MeHg) from in and around the Minamata Bay. The second case was in the 1970's in Iraq when farmers ate Hg-treated seeds that were supposed to be used for planting (Veiga, 2004).

1.2.1 Mercury sources

Mercury is the only metal that is liquid at room temperature and is very susceptible to volatilization. Cinnabar is the natural occurring mercury ore that has been used to impart the color red for dye. Mercury's high density and uniform expansion previously identified mercury as the ideal element to be used in household in such instruments as barometers, manometers, vacuum gauges, fluorescent lamps, switches, thermostats and thermometers. Mercury is also found in dental amalgams, and can contribute as much as 50% of the amalgam metal content. Old paint, some old athletic sneakers, and button-cell batteries also contain considerable amounts of mercury (Environment Canada, 2004).

Anthropogenic sources of mercury are very important to consider. In 2000, Canada emitted over 8 tons of mercury into the atmosphere (Environment Canada, 2004). Over 50% of this emission was from electric power generation and base-metal smelting (Figure 2). This quantity of mercury emitted per year is misleading because it does not take into account the amount of mercury released into water or soil from industrial processes or the amount emitted from pre-existing sources (i.e. land fills and mine sites).

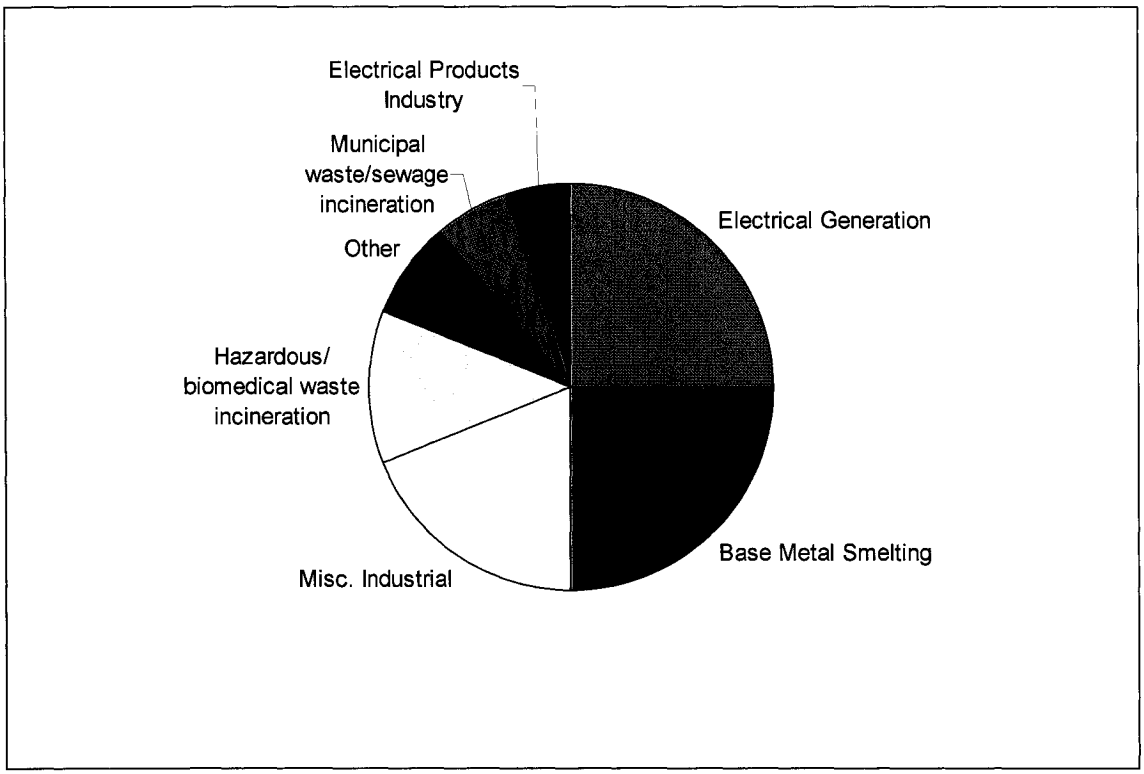

Figure 2. Canadian Atmospheric Mercury Emissions in 2000. (Environment Canada 2004).

1.2.2 Mercury cycling and transformation

Mercury cycles locally from the sediments to the water column to the atmosphere and back again by many biotic and abiotic processes (Poissant, 2004). Figure 3 shows the most important reactions regulating mercury cycling in the environment.

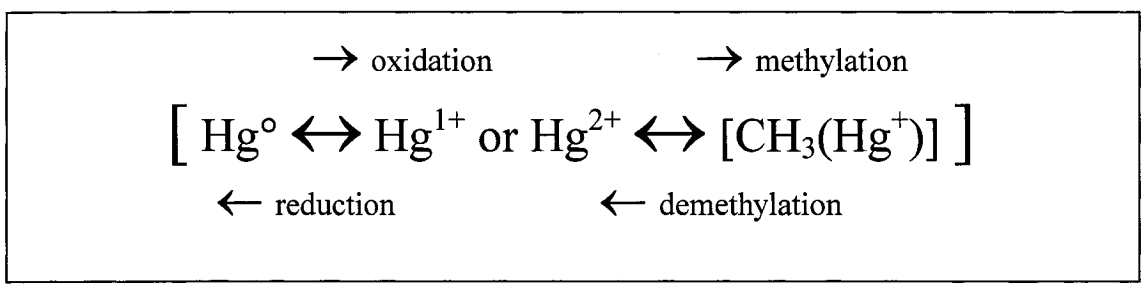

Figure 3. The cycling of mercury in local environments (Poissant, 2004).

Inorganic mercury (Hg^{2+}) is the most dominant form of Hg in water because it is the most soluble form and it usually forms complexes with dissolved organic carbon (DOC) or with sulfides (Gilmour et al., 1998). Methyl mercury is known to form in anoxic sediments but only accounts for less than 5% of the total mercury in the water column (Babiarz et al., 1998). Elemental mercury is largely insoluble, but recent work has shown that dissolved gaseous mercury plays a greater role than previously thought in the outflow of mercury (Sellers and Kelly, 2001).

1.2.3 Toxicity of MeHg

Exposure to Hg of people living in close proximity of mining sites is primarily via two pathways (Veiga et al., 2004):

1. Occupational Hg vapour exposure from amalgam burning or gold melting,
2. Methylmercury (MeHg) from dietary sources, especially fish.

Methylation of mercury produces the most toxic species of mercury because the chemical transformation leads to a structural mimic of an essential amino acid. Methyl mercury (MeHg) is then able to cross the brain blood barrier and generate neurological diseases. Methylation also makes mercury readily bioavailable and biomagnified in the food chain (Boening, 2000).

Once the MeHg crosses the brain blood barrier, it targets the central nervous system. Clinical symptoms of MeHg poisoning include (Dickman et al., 1997):

1. Parathesia (loss of sensation in the arms, legs, and around the mouth)
2. Dysarthria (impairment of speech)
3. ataxia (impairment of the ability to walk)
4. visual and hearing impairment
5. limb tremors

The severity of the symptoms depends on the amount of MeHg in the blood, and the duration of exposure.

1.2.4 Role of sulfate-reducing bacteria in MeHg formation

Over time, bacteria have evolved and developed protective mechanisms against high levels of toxic mercury. According to Boening (2000), bacteria use several mechanisms to prevent Hg toxicity:

- Efflux pumps that remove the ion from the cell
- Enzymatic reduction of the metal to Hg° (less toxic form)
- Chelation by enzymatic polymers
- Binding to cell surface (immobilizing)
- Precipitation of Hg as a sulfide
- Biomethylation

The first 5 mechanisms make mercury less toxic by converting it to volatile elemental mercury (Hg°) or immobilizing it within the sediment or on the cell wall. The sixth process converts mercury into methyl mercury, which is the form of Hg that has the ability to bioaccumulate and biomagnify in the food chain.

Sulfate-reducing bacteria have been labelled as mercury methylators, their respiration activity has been implicated in the methylation process. However, in pure culture, SRB do not methylate mercury in the absence of sulfate (King et al., 2002). The exact mechanism by which SRB actually produce methyl mercury is unknown. Several explanations have been put forward to explain why SRB methylate Hg. It might be a detoxification mechanism if the levels of mercury become toxic to SRB, or it might be that the methylation process is accidental, i.e., when sulfate-reduction produces soluble

mercury sulfides in the water column, this creates a significant source of mercury that is available for methylation (Mauro et al., 2002)

1.2.4.1 Biogeochemical factors affecting microbial sulfate reduction

1.2.4.1.1 Oxygen as an inhibitor of microbial sulfate reduction

Pure cultures of SRB have not been grown or isolated in the presence of oxygen, but in nature it has been shown that SRB can tolerate oxygen stress for several hours, and even respire with oxygen (Sass et al., 1997). The oxygen can be used as an electron acceptor and the respiration happens in the form of Adenosine triphosphate (ATP). This aerobic growth cannot be established over long periods of time, because the oxygen starts to deactivate the bacterial enzymes. SRB are able to sense oxygen concentrations, and usually move deeper in the anoxic sediments (Krekeler et al., 1997). Although SRB have been found in the oxic portion of sediments (Fortin et al. 2002), their activity is much more vigorous in anoxic, nutrient rich conditions (Sass et al. 1997).

1.2.4.1.2 Effect of pH

SRB are considered neutrophilic, but they have been recovered in acidic environments (Fortin et al., 1996) and found to be active in acidic lake sediments (Koschorreck et al., 2003). Pure SRB cultures can not be grown in a lab under pH 6 unless pre-treated, but SRB from natural environments have been recovered in AMD impacted sites and thrive in low pH conditions ($pH < 4$) (Kolmert et al., 2001).

Another organic form of mercury is Dimethylmercury (DMM) which is even more toxic than methylmercury and is much more dangerous to fish and aquatic life under acidic conditions than under neutral water, because DMMis more volatile under neutral

pH conditions. Therefore a lower pH, DMM is stable and available to enter the food chain (Hakanson, 1980). Acidophilic SRB are therefore very important in the cycling of mercury to MeHg and DMM because of the increased threat of MeHg or DMM contamination to the surrounding ecosystem in a low pH environment.

1.2.4.1.3 Effect of temperature

Most bacteria are temperature sensitive (Pomeroy et al, 2001). It is expected that cold temperature should slow down the metabolic activity of SRB and therefore slow down the formation of MeHg, whereas high temperature should enhance SRB activity and promote Hg methylation. In a temperate climate region, this implies that in the winter, there might be less methyl mercury production in the environment, such as wetlands and mine tailings. In a recent study on Cu-Zn mine tailings, Praharaj and Fortin (2004) showed that the rate of microbial sulfate reduction was indeed reduced in the spring when compared to summer months. However, temperature did not appear to be the sole factor responsible for the decline of microbial sulfate reduction rates, pH, sulfate and organic carbon availability might have also played important roles. Temporal differences in monomethylmercury (MMHg) were however observed in salt marsh pore waters (i.e., May>September>November) indicating that warmer temperatures favoured organic mercury accumulation (Langer, 2001).

1.2.4.1.4 Effect of sulfate availability

The effect of sulfate levels on methyl mercury formation is disputed in the literature. Some studies have shown that high sulfate levels in the presence of active SRB populations could result in high levels of methyl mercury (King et al., 2002). High sulfate concentrations promote the formation of large levels of soluble mercury sulfide (HgS)

which act as available mercury for methylation (King et al., 2002). On the other hand, other studies have indicated that even though methylation is mediated by SRB, the process could be limited in high sulfate environments. High levels of sulfate and consequently sulfide, could restrict mercury methylation because of the binding of Hg to sulfides and the decrease of Hg available for methylation (Langer et al., 2001).

1.2.4.1.5 Availability of organic carbon

The addition of high levels of organic substrates should promote Hg methylation because SRB activity is directly dependent on the availability of electron donors to bring the sulfur atom from its fully oxidized state to its fully reduced state (Postgate 1984). In the presence of low levels of electron donors, sulfate would not be reduced and Hg methylation should be hindered. Dissolved organic carbon (DOC) in the water is known to correlate with high levels of methylmercury and dissolved total mercury because of the high affinity of mercury for DOC (Boening 2000). In addition, in the presence of organic material, elemental mercury (Hg^0) may be oxidized to inorganic mercury (Hg^{2+}), creating a pool of mercury available for microbial methylation in the proper environment (Boening 2000).

Not all SRB methylate mercury at the same rate. There are more than 19 genera of SRB (Postgate 1984) and they all have different ability to breakdown different organic carbon sources. The SRB groups that can easily breakdown acetate have a higher methylmercury formation rate than those groups that can not breakdown acetate at all (King et al. 2002). Recent work by Rioux (2004) has shown that mixed SRB isolated from Cu-Zn mine tailings can use acetate as a simple organic electron donor and oxidize it completely to CO_2. The same study has also shown that the same SRB can partially

oxidize lactate to acetate, which then becomes available to acetate-using SRB. Acetate has also been detected in the porewater of Cu-Zn mine tailings (Fortin et al., 1996)

1.2.4.1.6 Effect of tailings mineralogy

There are no known studies on the effect of tailings mineralogy on MeHg formation. However, it is known that Cu-Zn tailings contain on average more sulfide minerals than Au tailings and that SRB populations are more active in Cu-Zn tailings (Fortin et al., 2000). Given the fact that mercury has a high binding affinity for sulfides (Langer, 2001), there might be more natural Hg in Cu-Zn tailings. Reaction [4] shows that inorganic mercury ions (Hg^{2+}) can actually be precipitated as elemental Hg in the presence of Zn (Ku et al., 2002).

$$Zn_{(s)} + Hg^{2+} \Leftrightarrow Zn^{2+} + Hg_{(s)} \qquad [4]$$

Reaction 4 explains why high concentrations of Hg in sediments are well correlated with high concentrations of Zn.

1.2.5 Abiotic factors involved in Hg methylation

Mercury has the potential to be methylated by small organic molecules i.e. acetic acid. MeHg formation has been reported when acetic acid was used as an analytical chemical compound with oxidized Hg present (Gardfeldt et al., 2003). Formation of MeHg was also reported to have formed from mercuric acetate when exposed to UV light (Akagi et al., 1973). Atmospheric MeHg is formed abiotically when volatile organic compounds are oxidized by OH or ozone reactions (Gardfeldt et al., 2003). MeHg in sediment can be formed biotically and abiotically. While most of the literature is written

about biotic MeHg formation, there is little known about the abiotic formation that is due to the presence of reductant substances produced by micro-organisms. If the microbial activity is inhibited in MeHg producing sediments, then MeHg should still be produced at a reduced rate because of the reductants left behind by the micro-organisms (Chen et al., 1995).

2. Objectives and Hypotheses

The following objectives and hypotheses were made prior to beginning the experiments:

2.1 Objectives

1. Determine the effect of SRB activity on Hg methylation in Cu-Zn and Au mine tailings.
2. Determine the effect of temperature (4^{o} and 25^{o} C) on Hg methylation in Cu-Zn tailings containing active SRB populations in order to simulate winter and summer conditions.
3. Determine the effect of sulfate concentrations (high and low levels) on Hg methylation in Cu-Zn tailings containing active SRB populations.
4. Determine the effect of organic carbon substrate availability (high and low DOC levels) on Hg methylation in Cu-Zn mine tailings containing active SRB populations.
5. Determine the effect of tailings mineralogy , i.e., Cu-Zn tailings and Au tailings, on Hg methylation.

2.2 Hypotheses

1. It is expected that the column containing inhibited SRB populations should not contain MeHg, if SRB are entirely responsible for Hg methylation
2. Cold temperature should slow down the metabolic activity of SRB and therefore slow down the formation of MeHg whereas high temperature should enhance SRB activity and promote Hg methylation

3. It is expected that high sulfate levels in the presence of active SRB populations should promote high concentrations of soluble sulfide which will prevent Hg methylation as a result of HgS formation. Under limited sulfate levels, Hg methylation should proceed.
4. The addition of high levels of organic substrates should promote Hg methylation because SRB activity is directly dependent on the availability of electron donors. In the presence of low levels of electron donors, Hg methylation should be hindered.
5. Au tailings should contain more Hg and potentially more MeHg than Cu-Zn tailings because of past ore extraction processes which used Hg amalgamation. But Hg has a high affinity for Zn, therefore the Cu-Zn tailings may in fact contain more Hg than the Au tailings because the Hg is less mobile in the Cu-Zn tailings.

3. Methods

3.1 Field sampling

3.1.1 Timmins, Ontario

Twenty liters of fresh Cu-Zn tailings (from the discharge pipe) were collected at the Kidd Creek Division Metallurgical site in Timmins, Ontario in May 2003. The tailings were collected into an ethanol washed bucket that was then sealed immediately and taken back to the lab and kept in a cold room after being purged with N_2. The tailings were kept in a cold room until they could be homogenized on a shaker and then put into the plexiglass column setup in October 2003. The tailings were kept under anaerobic conditions in the columns with nitrogen gas.

3.1.2 Lower Seal Harbour, Nova Scotia

Fifteen liters of sixty year old Au tailings from a saturated tailings pile in Lower Seal Harbour, Nova Scotia were collected in September 2003. The top 2 cm of semi-vegetated soil was removed and sediments from a depth of 5 to 20 cm were collected and roughly homogenized in an ethanol washed bucket. The tailings were kept in a cold room in a sealed container under N_2 until they could be homogenized on a shaker for 2 days and then put into the plexiglass column setup in January 2004. The tailings were kept under anaerobic conditions in the columns with nitrogen gas.

3.2 Column experiments with Cu-Zn and Au tailings

A laboratory column setup (Figure 4) was designed to test the role played by SRB in Hg methylation in fresh Cu-Zn tailings old Au tailings. Plexiglass columns used in the

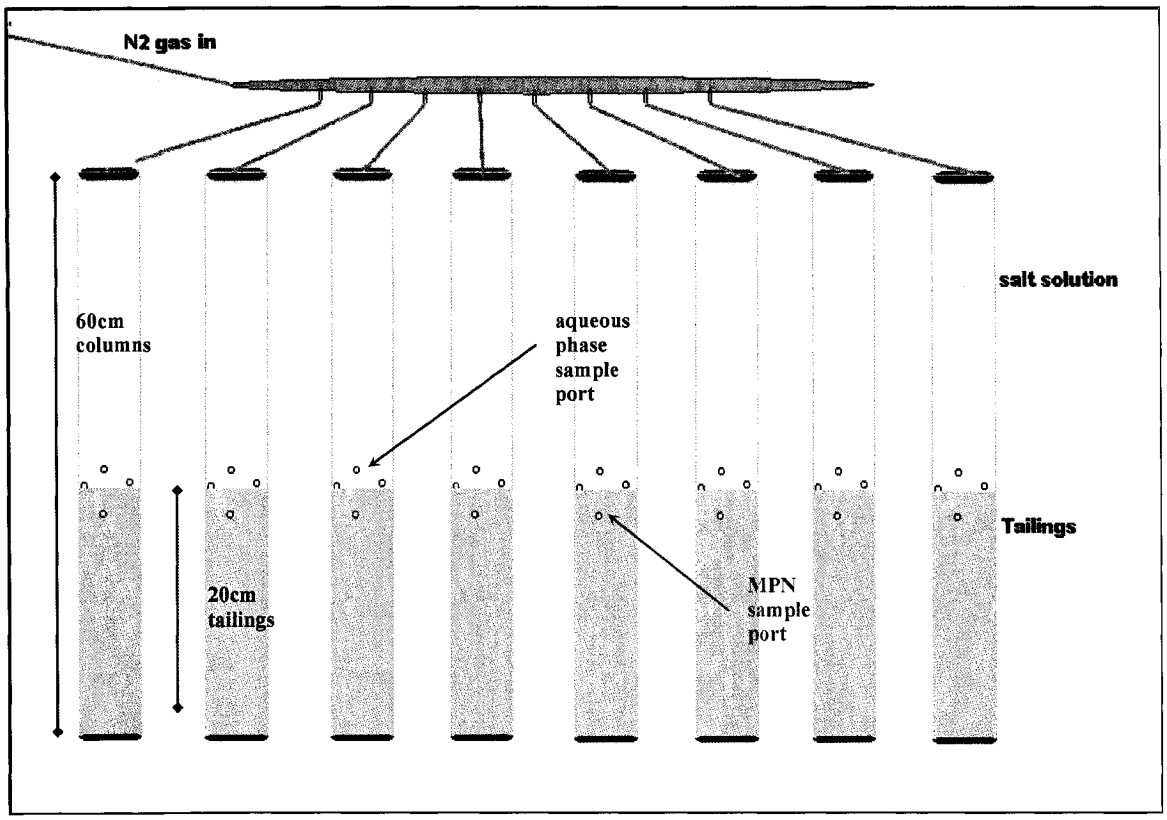

Figure 4. Column setup for laboratory experiment on mercury methylation in mine tailings.

experiment had a diameter of 7cm and a height of 60cm. The columns were first acid washed to remove any metal contamination and then ethanol washed to remove any bacteria present. Sampling ports were located on the side of each column between 27 and 36cm of depth. The sampling port at the top of the column was used to purge the column with N_2 gas and the bottom port of the column was sealed with a rubber stopper and silicon to prevent leakage, and all the side ports had silicon stoppers inserted to seal them.

Fresh homogeneous Cu-Zn tailings slurries (containing 60% solid and 40% water) were poured into individual columns. The sediments were allowed to settle for several days while bubbling N_2 into the water above the sediments. This removed all soluble oxygen and promoted reducing conditions in the columns. After the sediments settled, there was about 20cm of tailings in each column, bringing the sediment/water interface to

the middle sampling port. The Au tailings were treated the same way as the Cu-Zn tailings, but only poured into 2 individual plexiglass columns. The initial aqueous phase above the sediments was removed and replaced with a chemically defined liquid medium as described in section 3.3.

3.2.1 Physico-chemical and microbial conditions in the columns

The physico-chemical composition of the liquid growth medium added to the columns was modified to assess how SRB activity, temperature, sulfate and organic carbon concentrations affected Hg methylation. The various systems tested in this study are listed in Table 1.

Table 1. Physico-chemical parameters of the various column experiments with Cu-Zn and Au tailings.

System	Temperature (°C)	SRB activity	$[SO_4^{2-}]$ (mg/L)	[DOC] (mg/L)
Cu-Zn tailings				
Warm Active Cu-Zn*	22	non-inhibited	18.8	1862
Warm Non-Active Cu-Zn	22	inhibited	18.8	1862
Warm Active Cu-Zn*	22	non-inhibited	18.8	1862
Cold Active Cu-Zn	4	non-inhibited	18.8	1862
Low Sulfate Active Cu-Zn	22	non-inhibited	0	1862
High Sulfate Active Cu-Zn	22	non-inhibited	10144	1862
Low DOC Active Cu-Zn	22	non-inhibited	18.8	0
High DOC Active Cu-Zn	22	non-inhibited	18.8	37,249
Au tailings				
Warm Active Au	22	non-inhibited	18.8	1862
Warm non-active Au	22	inhibited	18.8	1862

* Same column

3.2.1.1 Warm Active and Non-active Cu-Zn columns

For both the active and non-active Cu-Zn columns, the medium contained 1862 mg/L of dissolved organic carbon (DOC) as Na-Acetate, Na-Formate, Na-Pyruvate and Na-Lactate, and 27 mg/L Na_2SO_4 (18.8 mg/L SO_4^{2-}), which corresponded to the initial concentration of sulfate in the tailings slurry. The medium also contained various salts, such as, 1.2 g/L NaCl, 0.3 g/L NH_4Cl, 0.4 g/L $MgCl_2*6H_2O$ and 0.2 g/L KH_2PO_4. In order to inhibit SRB activity in one of the columns, Na-Molybdate was added for a final concentration of 4.9 g/L. The pH was adjusted to 6.5 with NaOH. After the liquid medium was poured over the tailings, the columns were bubbled with N_2 for 48 hours in order to establish anoxic conditions and kept at room temperature for the remainder of the experiment.

3.2.1.2 Warm and Cold active Cu-Zn columns

The growth medium added to the warm and cold active columns containing Cu-Zn tailings was identical to the medium described in section 3.2.1.1. However, it did not contain Na-Molybdate to inhibit SRB activity. After the solution was added, the columns were bubbled with N_2 for 48 hours to establish anoxic conditions. One column was left at room temperature (~ 22 °C), whereas the second one was kept around 4 °C. The column placed in the fridge at 4 °C was periodically taken out in order to bubble N_2 and maintain anoxic conditions.

3.2.1.3 Low and High sulfate active Cu-Zn columns

For these experiments, the composition of the growth medium (i.e., salts and DOC) was identical to the one described in the 2 previous sections, but the concentration of

sulfate was varied. In one column, there was no sulfate added to the medium, whereas the second column contained 10,144 mg/L of sulfate (500 times the original molar concentration of sulfate). The columns were not inhibited for SRB activity and they were both kept at room temperature (22 °C). After the addition of the medium, the columns were bubbled with N_2 for 48 hours to establish anoxic conditions.

3.2.1.4 Low and High DOC active Cu-Zn columns

The chemical composition of the growth medium added to the low and high DOC columns was identical to the one in the active Cu-Zn column described in section 3.2.1.1. However, DOC was not added to the medium in one column, whereas the second column contained 37,249 mg/L total of DOC (i.e., 100 mM of each Na-Acetate, Na-Formate, Na-Pyruvate and Na-Lactate). The term "low DOC active Cu-Zn column" is used here despite the fact that no organic carbon was added to the medium because the original tailings might have contained some DOC. SRB activity was maintained in both columns. After the addition of the medium, N_2 was bubbled in the columns to help develop anoxic conditions. Both columns were kept at room temperature for the remainder of the experiment.

3.2.1.5 Warm active and Non-active Au columns

These columns contained Au tailings and the same growth medium as in the warm active and non-active Cu-Zn columns described in section 3.2.1.1. SRB activity was inhibited in the warm non-active column with Na-Molybdate (final concentration 4.9 g/L). After the addition of the medium, the columns were degassed with N_2 for 48 hours to insure the development of anoxic conditions. Both columns were left at room temperature over the course of the experiment.

3.2.2 Column sampling and analyses

3.2.2.1 Sampling

Prior to the column experiments, the fresh Cu-Zn tailings and the old Au tailings were analyzed for various physico-chemical and microbial parameters. In addition, after the addition of the chemically defined growth medium to the columns (every 2-3 weeks over a period of 4 months), approximately one liter (1L) of the aqueous phase from above the sediment-water interface was collected with a sterile syringe and needle through the sampling ports on the side of the column. The aqueous sample was used for the analyses described below. After each sampling, the volume of medium removed from the columns (1L) was replenished with an identical growth medium specific to each column.

3.2.2.2 Aqueous analysis

3.2.2.2.1 pH and Eh

pH and Eh measurements were performed on unfiltered water samples shortly after sampling, with a VWR portable pH meter and a VWR symphony Ag/AgCl gel filled pH probe calibrated with VWR pH 4 and 7 buffers. Eh measurements were performed with the same meter and a Corning platinum combination redox probe (model 476516). The Eh probe was checked with the ZoBell's solution (Nordstrom, 1977). Correction with respect to the hydrogen reference electrode was performed for each reading, by adding +199 mV to each reading.

3.2.2.2.2 Major cations

A sub-sample of 15 mL was filtered (0.22 μm) and acidified with 100μl of concentrated trace metal grade HNO_3 and stored until analysis. Dissolved total metal and elemental concentrations (Ca, K, Mg, Mn, Na,) were determined with an ICP-OES

(Varian-Pro CCD Simultaneous Inductively Coupled Plasma – Optical Emission Spectroscopy) in the department of Earth Sciences, at the University of Ottawa. Other elements (Al, Cd, Co, Cr, Cu, Ni, Pb, Sr, Zn) were analyzed but they were all below the detection the instrument.

3.2.2.2.3 Sulfate and sulfide

Total sulfate and sulfide concentrations were determined on filtered samples (0.22 μm) with a spectrophotometer-analyzer HACH DR / 2010 with a detection range of 0 - 70 mg/L and 0 - 0.600 mg/L, respectively. Sulfide analyses were performed within minutes after the samples were collected in order to prevent oxidation.

3.2.2.2.4 Total and dissolved Fe

Unfiltered and filtered (0.22 μm) samples were analyzed for total Fe and dissolved Fe with a spectrophotometer-analyzer HACH DR / 2010 with a detection limit of 0 – 3.00 mg/L. Fe analyses were performed within minutes after sampling to prevent oxidation of Fe(II) into Fe(III).

3.2.2.2.5 DOC

Un-filtered samples were analyzed for DOC with a 1010 model TOC-TIC analyzer calibrated with sodium persulfate standards in the Department of Biology at the University of Ottawa.

3.2.2.2.6 Soluble total Hg

Samples were subjected to EPA method 1631, Revision B; for total mercury analysis on the TEK-RAN (Model 2500 System control module + CVAFS mercury

detector). The mercury in the water was determined by oxidation, purge and trap, and cold vapour atomic fluorescence spectrometry. Serial dilution standards were prepared with a 1000ppm Hg stock solution then the standards and samples were oxidized with 500 μL BrCl to convert all Hg to Hg(II). Before running the samples and standards, 100 μL of 30% hydroxylamine was added to neutralize any excess oxidant BrCl. In the TEK-RAN, any existing Hg(II) in the samples was reduced to Hg(0) with $SnCl_2$. The Hg(0) was then separated from solution by purging N_2 onto a gold-coated sand trap. The trapped Hg is thermally desorbed from the gold trap into an inert gas stream that carries the released Hg(0) into the cell of a cold-vapour atomic fluorescence spectrometer (CVAFS) for detection. All preparation and anlaysis was done in the Department of Biology at the University of Ottawa.

3.2.2.2.7 Soluble MeHg

500 mL of unfiltered and acidified sample (with 2.5 mL of trace metal grade HCl) was analyzed for MeHg on a capillary Gas Chromatograph (HP 6890 series GC/AFS) after pre-concentration of the organomercurials onto sulfydryl-cotton fibers, elution with acidic KBr and $CuSO_4$ and extraction with dichloromethane (DCM) (Cai et al. 1996). Analyses were done at the Department of Biology at the University of Ottawa.

3.2.2.3 Microbial enumeration

3.2.2.3.1 Growth medium for SRB enumaration

The growth medium for SRB enumeration was prepared using a modified version of Postgate medium G (Postgate, 1984). The growth medium was prepared with the following ingredients; Bacto Tryptone (10g/L), $MgSO_4.7H_2O$ (2g/L), $FeSO_4.7H_2O$ (0.5g/L), Na_2SO_3 (0.5g/L), 60% Na-Lactate (0.59 mL/L), Na-formate (0.34g/L), Na-

Acetate (0.41mL/L), and Na-pyruvate (0.55mL/L). The growth medium was adjusted to a pH of 7.5 using 2M NaOH. 9 mL of the prepared growth medium was dispensed into culture tubes, sealed with caps and autoclaved at 121°C for 15 minutes. A reducing agent supplement (RAS) was prepared on a daily basis prior to SRB inoculation. It was prepared with thioglycolic acid (7.5 mL/L) and L-ascorbic acid (7.5g/L). The pH of the solution was adjusted to 7.5 with 2M NaOH and the solution was transferred into 125 mL Erlenmeyer flask and autoclaved at 121°C for 15 minutes. RAS (1mL) was then aseptically added to each MPN tube containing the growth medium. Dilution water was prepared with NaCl (2.1 g/L) and RAS 100 (mL/L). The solution pH was adjusted to 7.5 using 2 M NaOH, and 9 mL was transferred to culture tubes. Culture tubes were autoclaved at 121°C for 15 minutes and cooled prior to inoculation.

3.2.2.3.2 MPN technique

Serial dilution series (1:10) were prepared using the dilution water. A 1-mL unfiltered sub-sample was taken from the columns and transferred to 9 mL of sterile dilution water for the first 10-fold dilution using the flame-sterilization technique. A sequence of 10-fold serial dilutions was performed for all systems where bacterial populations were active. Between each dilution, the suspension was vortexed to disperse the particles uniformly in the dilution tube. All MPN tubes were stored in the dark for a period of two weeks. SRB growth was assessed by the formation of a black Fe-sulfide precipitate in the tubes. MPN values were calculated from statistical tables (Cochran, 1950) and expressed as colony forming units per milliliter (CFU/mL), which was then corrected for the samples dry weight (CFU/g dry wt.). Note that MPN will under-estimate the number of bacteria actually present because of the growth mediums preference for certain strains of SRB and MPN does not reflect the activity of the SRB.

3.2.2.4 Solid phase geochemistry

The original Cu-Zn tailings slurry and Au tailings, along with the sediments in the columns at the end of the 4-month experiments were analyzed for acid volatile sulfides (AVS), total Hg, MeHg and organic carbon content. After 4 months, the columns were sampled for a final time at 125 days, not replenished with the medium, and exposed to air to dry out for 2 - 4 months. The sediment was then manually extruded from the plexiglass holder, cut into 6 sections (i.e., 3 cm thick section) and stored until analysis.

3.2.2.4.1 Acid-volatile sulfide (AVS) extraction

The presence of AVS in natural sediments is an indication of the activity of SRB, following the reduction of sulfate into sulfide and the subsequent precipitation of Fe-monosulfides (Berner, 1984). To determine the fraction of sulfides that is acid-volatile, 2 g of sediment was weighed into the extraction apparatus and the whole setup was flushed with N_2 before starting the extraction. 10 mL of 90% ethanol was added to wash the sediment before extraction. AVS was extracted at room temperature for 1 hour with 8 mL of 12N HCl under continuous flow of N_2. The evolving H_2S was trapped in a 10 mL 20% ZnAc solution (Praharaj et al. 2004). The AVS fraction was then determined by colorimetry using the Cline's method (Cline, 1969) with a spectrophotometer (Beckman DU-65). AVS extractions were performed in the Department of Earth Sciences at the University of Ottawa.

3.2.2.4.2 Solid total Hg

Total Hg was analyzed in duplicate samples that were air-dried using a Nippon Mercury SP-3D (mercury analyzer) using the cold vapour atomic absorption method to determine the quantity of Hg. Standards were made from $HgCl_2$ with a 0.001% L-

cysteine solution to produce a final concentration of 1ppm Hg. No treatment was needed for the solid phase before analysis, the sample (S) was weighed into a ceramic boat with additives M (Calcium hydroxide and Sodium carbonate anhydrous) and B (Aluminum oxide) layered above and below the sample with the pattern M+S+M+B+M. The Nippon Mercury SP-3D measures the quantity of Hg in the sample in the form of liquid, solid, and gas. The sample was then heated to 850 °C to liberate the mercury atoms and analyze with the MA-1 analyzer which has a detection limit of 0.05 ppb. All analysis was done in the Department of Biology at the University of Ottawa.

3.2.2.4.3 Solid MeHg

MeHg analysis was done on triplicate samples that were air dried using the same capillary Gas Chromatograph as mentioned in section 3.2.2.2.7, but the samples were first cleaned with sodium thiosulfate and the MeHg was isolated as a bromide derivative by acidic KBr and $CuSO_4$ and similarly extracted as in section 3.2.2.2.7 into a small volume of dichloromethane (DCM) (Cai et al. 1997).

3.2.2.4.4 Water and organic carbon content

The water content of the tailings was determined by drying the sediments for 12 hours at 100°C, whereas the organic carbon content was estimated by loss on ignition (LOI), by heating the samples at 400 °C for 8 hours.

3.2.2.4.5 Granulometry

Grain size fractions were determined using 3 sizes of sieves, i.e., >250μm, 63μm-250μm , and <63μm. Sediments were dried in the oven at 70°C overnight to remove any moisture that could hinder partitioning through the sieves. 10g of sediments was weighed

and poured into the top of the sieve apparatus and shaken vigorously by hand for 5 minutes. Each size fraction was weighed out and converted into a percentage of the total amount.

3.2.2.5 Statistical analyses (*t test*)

A statistical t test was used to compare values and to choose between two hypotheses. The statistical work for the t test is shown in Appendix A.

The hypothesis that μ_1 and μ_2 are equal is called a null hypothesis and is abbreviated H_0. It can be written as

$$H_0: \mu_1 = \mu_2$$

The alternative hypothesis would then be written as

$$H_A: \mu_1 \neq \mu_2$$

The null hypothesis says that the two items compared are equal, which is the same as saying the difference between them is zero. The alternative hypothesis would then say that the difference is not zero.

The *t test* is a standard method of choosing between the two hypotheses.

$$t_s = \frac{|X_a - X_n| - 0}{SE_{(Xa - Xn)}}$$ where; $SE_{(Xa - Xn)} = \sqrt{[((sd_a)^2/n_a) + ((sd_n)^2/n_n)]}$, X = average value

sd = standard deviation, n = # of samples

If $t_s < 1$, the null hypothesis is not rejected

If $t_s > 1$. the null hypothesis is rejected and the alternative hypothesis is accepted

Note that the $|X_a - X_n|$ is subtracted from zero because H_o states that μ_a - μ_n equals zero; writing "$|X_a - X_n| - 0$" reminds us of what we are testing (Sameuls et al., 1999).

4. Results

The result section first presents the physico-chemical and microbial characteristics of the original tailings (section 4.1) used in this study and then the changes that occurred in the aqueous and solid phases of the tailings systems over time (sections 4.2 to 4.7). The last part of the results looks at possible relationships between the parameters measured in this study. Some additional data are presented in appendices A to E.

In order to present the results in a consistent manner, the vertical axis of all the bar graphs is identical between systems for each parameter measured in this study.

In the results, dissolved refers to the filtered aqueous fraction, and dissolved total refers to the unfiltered aqueous fraction.

4.1 Physico-chemical, mineralogical and microbial parameters of the tailings used in the columns.

4.1.1 Fresh Cu-Zn tailings

The chemical composition of the aqueous phase of the fresh Cu-Zn tailings slurry is shown in Tables 2 and 3, whereas the physico-chemical and microbial properties of the solid phase is shown in Table 4. The fresh tailings slurry was neutral pH, contained little dissolved iron, sulfide and DOC, but large concentrations of sulfate, calcium sodium and potassium (Tables 2 and 3). Dissolved total and methyl mercury were not detected in the aqueous phase, but the solid phase contained 118 ppb of total mercury and no methylmercury (Tables 3 and 4). The initial population of SRB in the fresh tailings was around 2.8×10^4 CFU/g dry wt. sed. (Table 4).

Table 2. Initial chemical composition of the aqueous phase of the fresh Cu-Zn tailings slurry used in the column experiments.

pH	Eh	SO_4^{2-}	HS^-	Fe(diss)	THg	MeHg	DOC
	mv	ppm	ppm	ppm	ppt	ppt	ppm
6.82	166	192	0.05	0.62	b/d	b/d	0.30

Table 3. Initial concentration of soluble major cations in the fresh Cu-Zn tailings used in the column experiments.

Ca	K	Mg	Mn	Na	Fe(total)
ppm	ppm	ppm	ppm	ppm	ppm
727	26	b/d	b/d	130	2.08

* b/d = below detection

Table 4. Initial physico-chemical and microbial characteristics of the solid phase of the fresh Cu-Zn tailings.

organics	AVS	THg	MeHg	SRB
%	μmol/g S^{2-}	ppb	ppt	CFU/g dry wt.
4.15	0.21	117.9	b/d	2.8×10^4

4.1.2 Old Au tailings

A full geochemical analysis was also performed on the aqueous and solid fractions of the old Au tailings collected from Lower Seal Harbour, Nova Scotia prior to the column experiments. The initial physico-chemical properties of the aqueous phase of the Au tailings are shown in Tables 5 and 6, whereas the physico-chemical and microbial properties of the solid phase are presented in Table 7. The tailings were slightly below pH neutral and contained low concentrations of dissolved iron, sulfide and DOC, but high level of soluble total Hg and no detectable dissolved methyl mercury (Table 5). Dissolved Ca, Mg, K and Na concentrations were very low, whereas dissolved Mn and Fe were higher than the concentrations measured in the fresh Cu-Zn tailings (Table 6). The sulfate

concentration in the Au tailings was half of that measured in the Cu-Zn tailings (Table 5), but the organic carbon content of the solid phase was similar for both types of tailings. The Au tailings contained less total Hg in the solid phase than the Cu-Zn tailings and no MeHg (Table 7). The SRB populations were one order of magnitude higher than the Cu-Zn tailings (Table 7).

Table 5. Initial chemical composition of the aqueous phase of the Au tailings used in the column experiments.

pH	Eh	SO_4^{2-}	HS^-	Fe(diss)	THg	MeHg	DOC
	mv	ppm	ppm	ppm	ppt	ppt	ppm
6.30	151	91.35	0.45	3.83	92.2	b/d	0.3

Table 6. Initial concentration of soluble major cations in the Au tailings used in the column experiments.

Ca	K	Mg	Mn	Na	Fe(total)
ppm	ppm	ppm	ppm	ppm	ppm
0.15	0.11	0.60	276	b/d	32.38

* b/d = below detection

Table 7. Initial physico-chemical and microbial characteristics of the solid phase of Au tailings.

organics	AVS	THg	MeHg	SRB
%	µmol/g S^{2-}	ppb	ppt	CFU/g dry wt.
0.32	0.211	86.9	b/d	8.0×10^5

4.2 Warm Active and Non-active Cu-Zn columns

4.2.1 Statistics

A statistical t-test was performed on the data from the Warm Active and Non-active Cu-Zn aqueous phases to determine if the data were statistically similar or statistically different throughout the experimental period (Appendix E). Table 8 is a summary of the results from the test.

Table 8. Statistical summary of results from the Warm Active and Non-active Cu-Zn aqueous phases.

	same	different
pH		•
Eh	•	
SO_4^{2-}	•	
S^{2-}		•
Fe_{diss}		•
DOC	•	
Hg_{tot}	•	
MeHg	•	
SRB		•

4.2.2 Aqueous geochemistry

4.2.2.1 pH and Eh

The initial pH of the Warm Active and Non-active Cu-Zn columns was near neutral pH (Table 2), and the Eh was 166 mV (Table 2) The pH of the Non-active SRB Cu-Zn column remained fairly stable over time (Figure 5 a), whereas the pH of the active SRB Cu-Zn slightly increased over time. pH values of both systems are statistically different from each other (Table 8). The Eh values (Figure 5 b) for both systems stayed statistically similar (Table 8) and did not increase or decrease very much over the course of the experiment.

a)

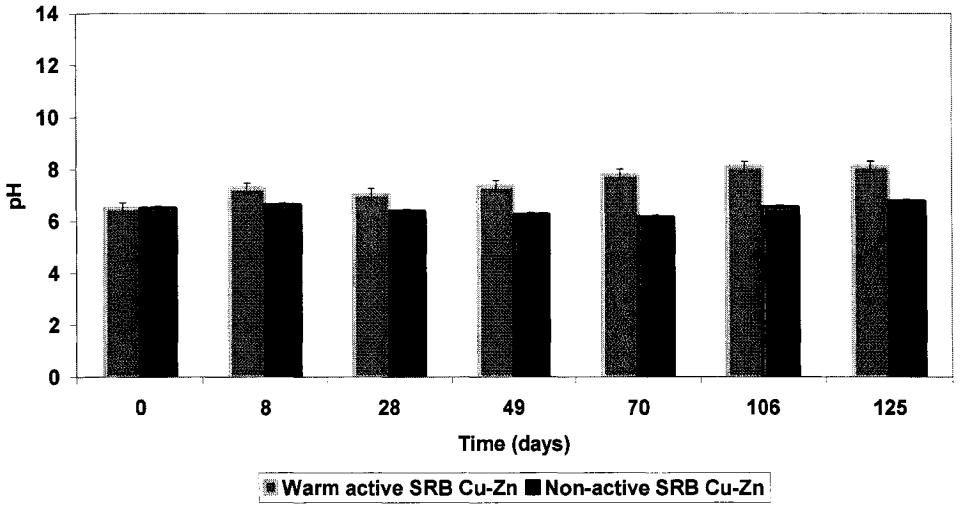

b)

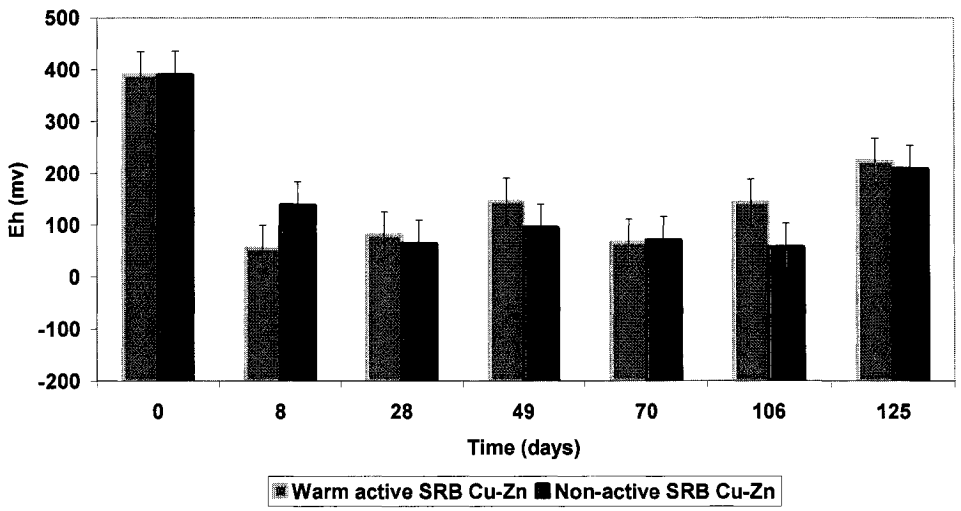

c)

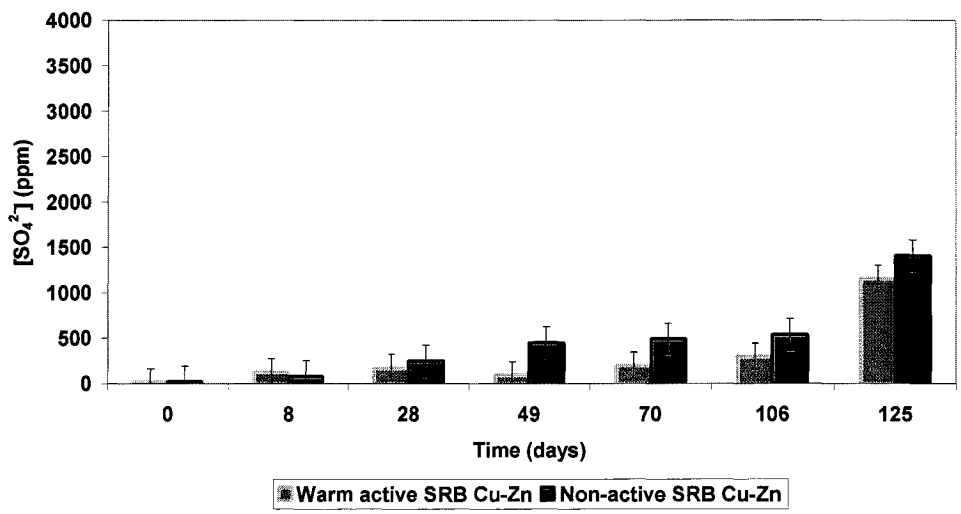

Figure 5. pH (a), Eh (b) and Sulfate (c) trends of the aqueous phase in the Warm Active SRB Cu-Zn and Non-active SRB Cu-Zn columns over 125 days.

4.2.2.2 Major cations

The major dissolved cations were measured at the same intervals as the other geochemical parameters, and appear in Appendix A. The data showed a release of some major cations into the aqueous phase over 125 days.

4.2.2.3 Sulfate and sulfide

The sulfate concentrations in both the Warm Active SRB and the Non-active SRB Cu-Zn columns gradually increased over time (Figure 5 c). The concentrations in the non-active SRB Cu-Zn appeared to be generally higher than in the active SRB columns, but statistically the values were not different (Table 8).

Very low levels of sulfide were detected in both the Warm Active SRB and Non-active SRB Cu-Zn columns, with the exception of time 8 and 125 days (Figure 6 a). At the end of 4 months, sulfide levels were however statistically higher in the Non-active SRB columns than in the Warm Active column (Table 8).

4.2.2.4 Dissolved Iron

The Warm Active SRB Cu-Zn had negligible levels of dissolved iron over the 125 days (Figure 6 b), whereas the Non-active SRB Cu-Zn column released dissolved iron in the aqueous phase by day 28, followed by little change.

4.2.2.5 DOC

DOC was rapidly consumed in the Warm Active and Non-active SRB Cu-Zn column within the first 8 days and then slightly declines until day 106, after which it increased (Figure 6 c). The concentration of DOC in both systems was fairly similar over time,

a)

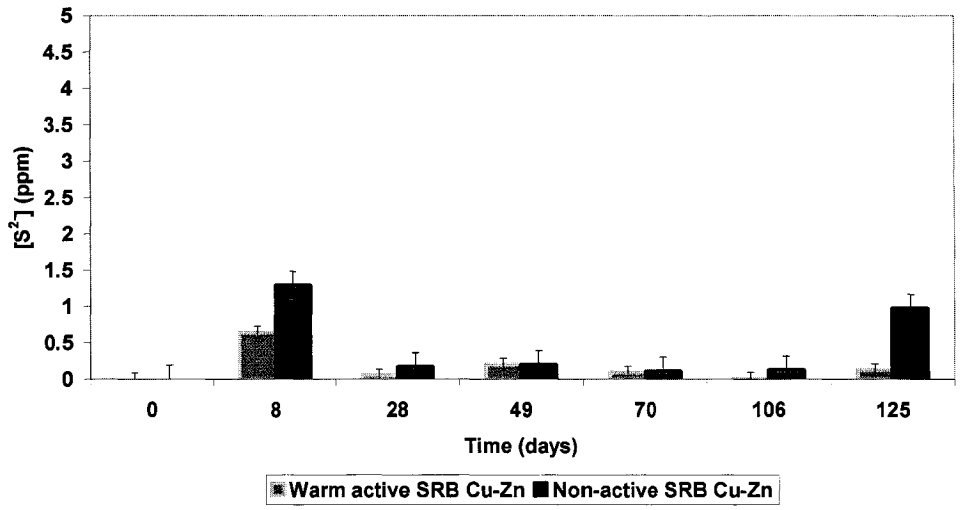

b)

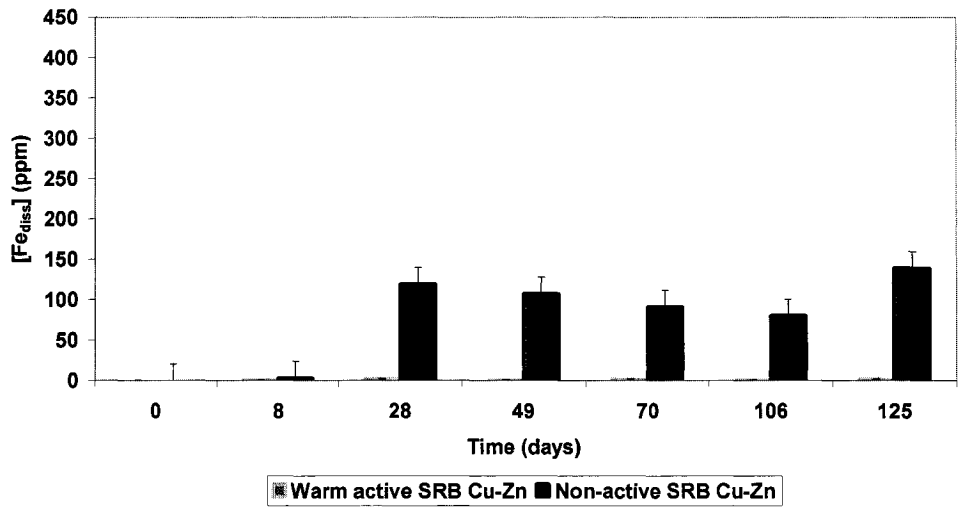

c)

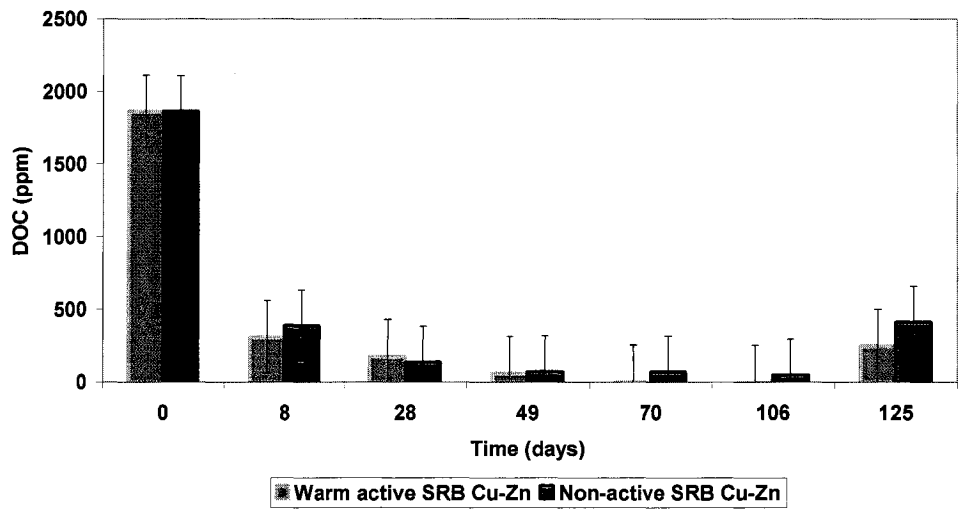

Figure 6. Sulfide (a), dissolved iron (b), and DOC (c) concentrations in the aqueous phase of the Warm Active SRB Cu-Zn and the Non-active SRB Cu-Zn columns over 125 days.

with the exception of time 70 and 106 days, when DOC levels were higher in the Non-active column than in the Warm Active one, but statistically the values were the same (Table 8).

4.2.2.6 Soluble total Hg

Both the Warm Active SRB Cu-Zn and Non-active SRB Cu-Zn columns released soluble Hg from 8 to106 days (Figure 7 a). The Warm Active SRB Cu-Zn column had a release at 70 days, whereas the Non-active SRB Cu-Zn column released soluble total Hg at 28 days. Even though the Non-active SRB Cu-Zn column had higher soluble total Hg, the values in the two columns were statistically the same (Table 8).

4.2.2.7 Soluble MeHg

Both the Warm Active and Non-active SRB Cu-Zn systems had no detectable MeHg in the water above the tailings until 125 days (Figure 7 b). The MeHg values were statistically the same in both columns (Table 8).

4.2.2.8 SRB enumeration

SRB populations in the Warm Active SRB column increased over time, whereas the SRB population in the Non-active columns remained fairly stable over time, with the exception of a slight increase at day 49 (Figure 7 c). The Non-active columns had some SRB colonies at the sediment/water interface that were not inhibited by the Na-molybdate, but the number of SRB was statistically lower than that of the Active SRB Cu-Zn column (Table 8).

a)

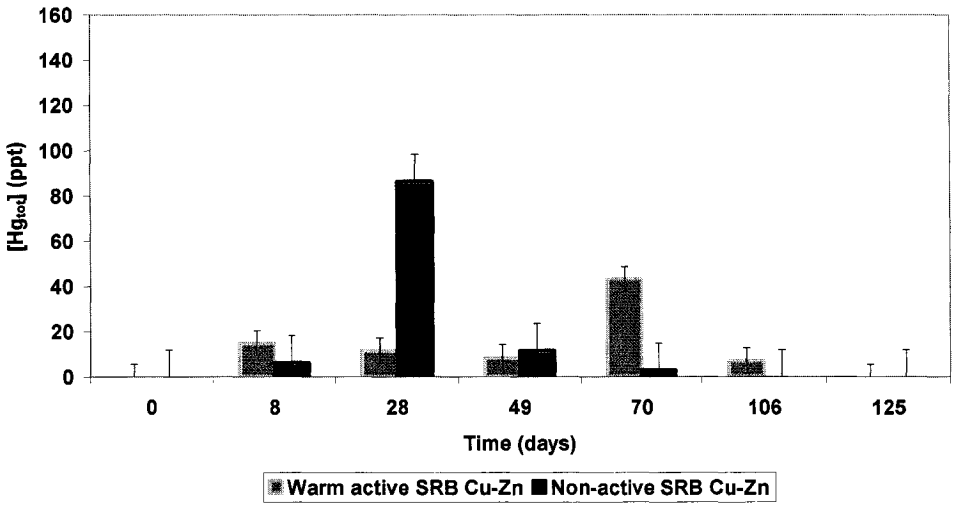

b)

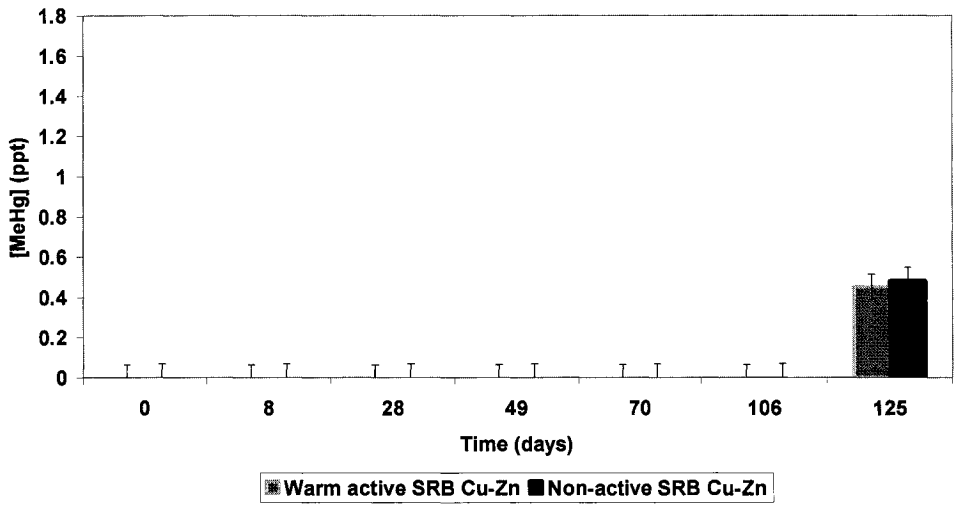

c)

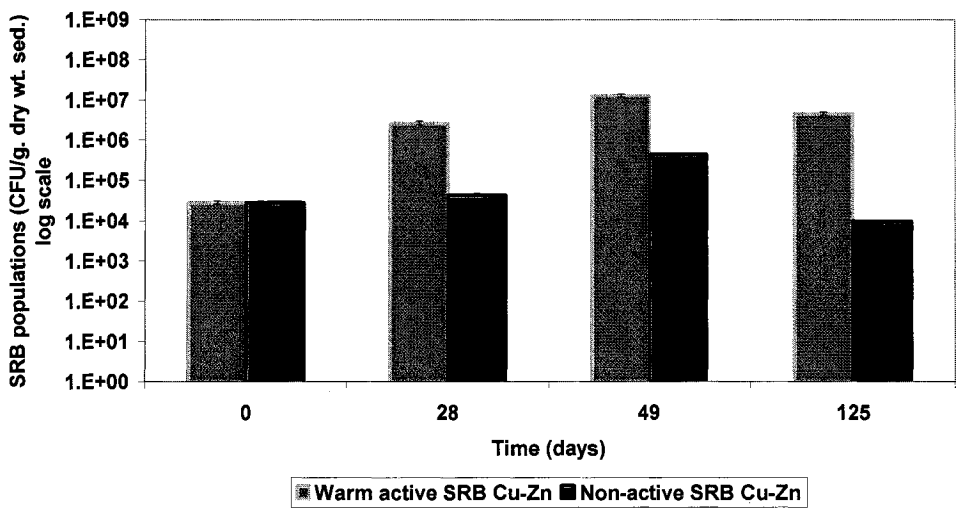

Figure 7. Total mercury (a), and methyl mercury (b) concentrations in the aqueous phase of the Warm Active SRB Cu-Zn and the Non-active SRB Cu-Zn columns over 125 days, and SRB populations (c) at the sediment/water interface in the Warm Active SRB Cu-Zn and the Non-active SRB Cu-Zn columns over 125 days.

4.2.3 Solid phase geochemistry

4.2.3.1 Acid-volatile sulfide (AVS) extraction

The initial concentration of acid volatile sulfides (AVS) in the fresh Cu-Zn tailings was 0.21μmol/g S^{2-} (Figure 8 a). The AVS concentration in the column at the end of the experiment fluctuated with depth in both systems, but the statistical t-test (Appendix B-1) showed that the values in the Active column versus the Non-active column were not different from each other. The Active column did however appear to decrease in AVS production with depth.

4.2.3.2 Solid total Hg

The total Hg concentration at the end of the experiment in both the Warm Active SRB Cu-Zn and Non-active SRB Cu-Zn columns was similar, but slightly higher than the initial concentration of Hg in the fresh Cu-Zn tailings, which was 118 ppb (Figure 8 b). The statistical t-test showed that the values for the Active and Non-active columns were not significantly different (Appendix B-2). Given the high standard deviation of the Hg concentration of the fresh Cu-Zn tailings, solid total Hg concentrations measured in the Warm Active SRB Cu-Zn and Non-active SRB Cu-Zn columns may not be different than the original amount.

4.2.3.3 Solid MeHg

Both the Warm Active SRB Cu-Zn and Non-active SRB Cu-Zn produced methylmercury with depth in the columns (Figure 9 a). The fresh tailings contained no MeHg, but after 4 months, concentrations reached 20 and 26 ppt in the Active SRB column and the Non-active SRB column, respectively. MeHg was not detected in the

a)

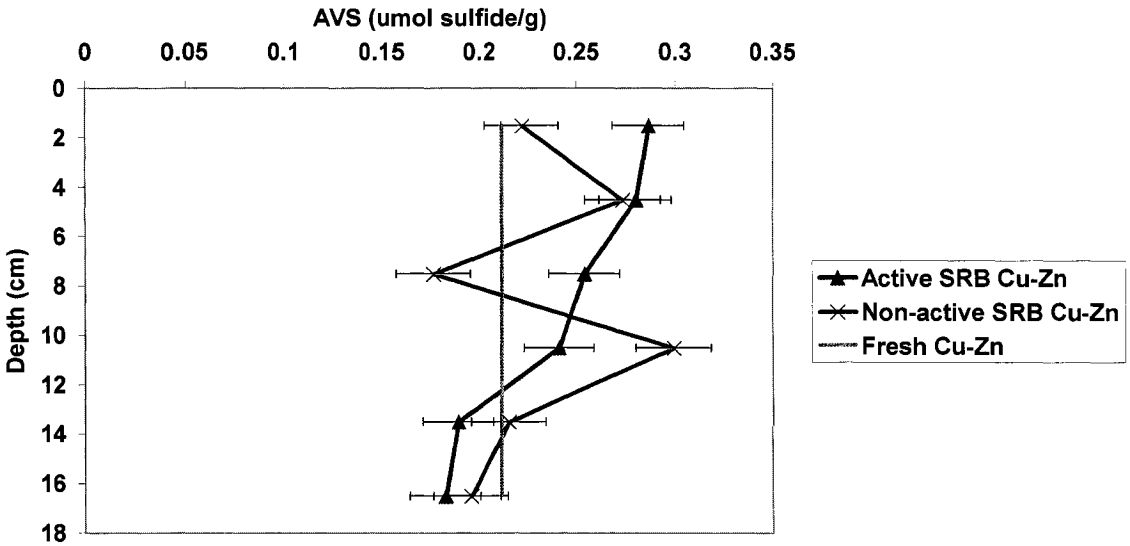

b)

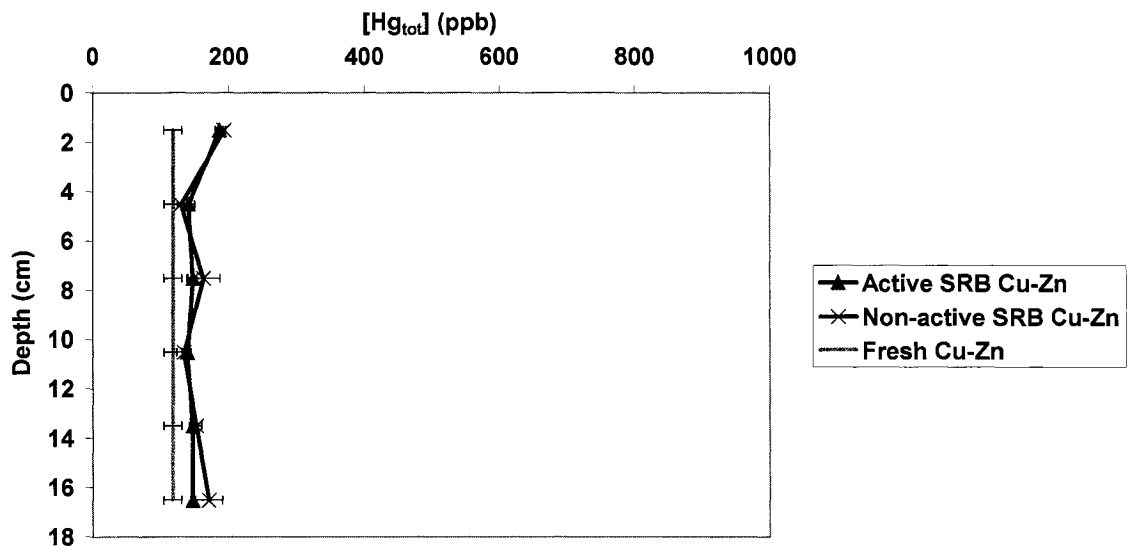

Figure 8. Acid volatile sulfide concentration in the solid phase of the Warm Active SRB Cu-Zn column and Non-active SRB Cu-Zn column at the end of the experiment and initial AVS concentration of the fresh Cu-Zn tailings (a), total mercury concentration in the solid phase of the Warm Active SRB Cu-Zn column and Non-active SRB Cu-Zn column at the end of the experiment and initial concentration in the fresh Cu-Zn tailings (b).

first 7.5cm of the Active SRB column, whereas the Non-active column had MeHg production down the entire column. The statistical t-test showed that the difference in MeHg concentrations in the Active and Non-active columns were statistically significant (Appendix B-3).

4.2.3.4 Organic carbon content (LOI)

The organic carbon contents of the Warm Active SRB and Non-active SRB Cu-Zn columns were lower than in the fresh Cu-Zn tailings, i.e., 4.1% (Figure 9 b). In the Non-active SRB system, there was an organic carbon enrichment in the upper portion of the column, whereas the organic carbon content of the Active SRB column remained unchanged with depth. Based on the t-test (Appendix B-4), the organic carbon content of the Active column and Non-active columns were significantly different.

4.3.1.1 Granulometry

The grain size of the tailings in both the Active and Non-active SRB columns was determined as a function of depth. The results are presented in Appendix D.

a)

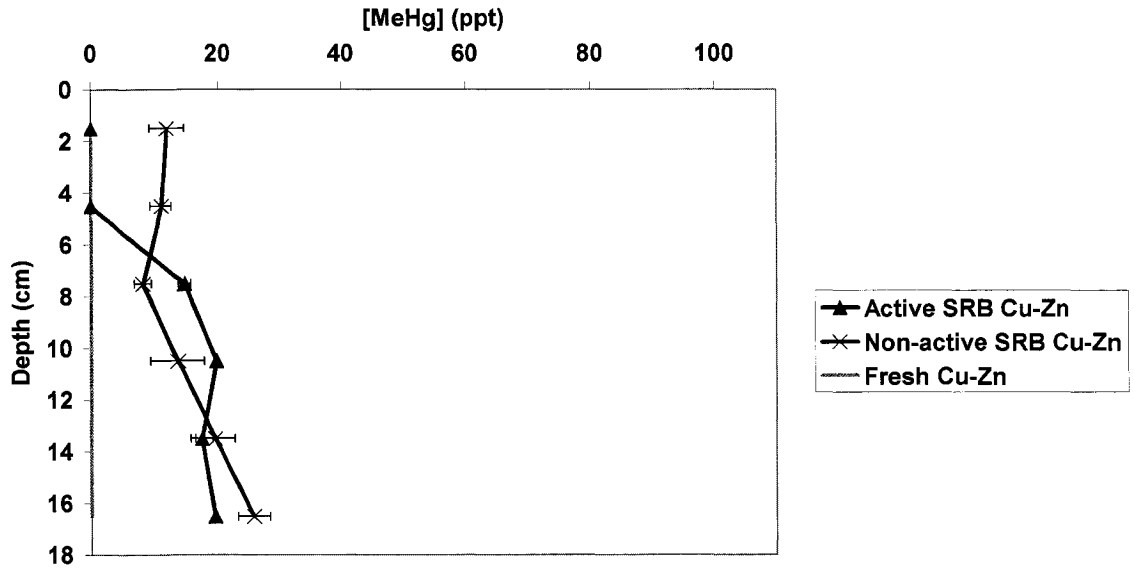

b)

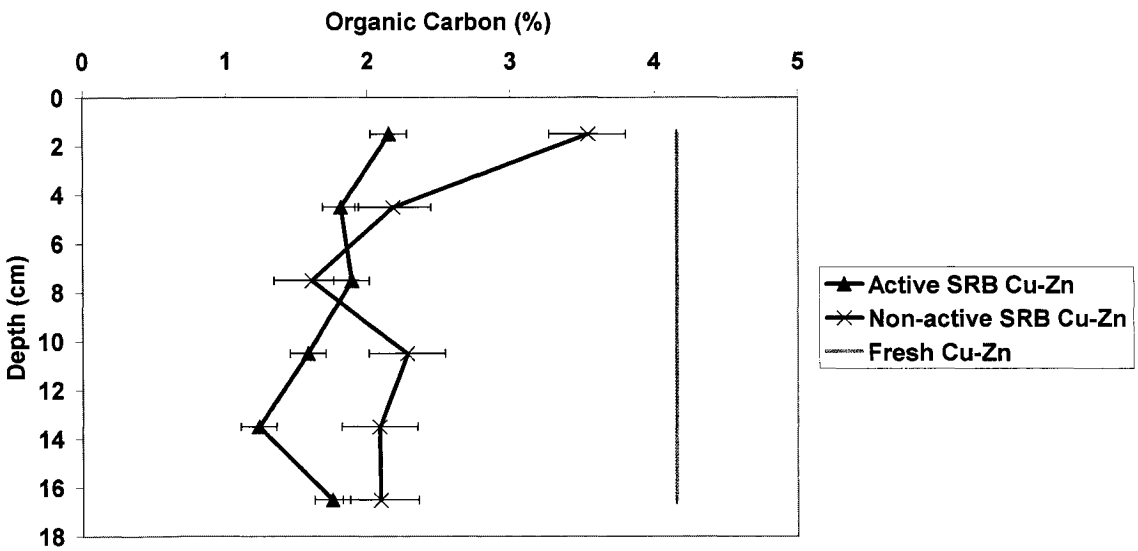

Figure 9. Methylmercury concentration in the solid phase of the Warm Active SRB Cu-Zn column and Non-active SRB Cu-Zn column at the end of the experiment and initial concentration in the fresh Cu-Zn tailings (a) and percentage of organic carbon in the solid phase of the Warm Active SRB Cu-Zn column at the end of the experiment and Non-active SRB Cu-Zn column and in the fresh slurry of Cu-Zn tailings (b).

4.4 Warm and Cold Active Cu-Zn columns

4.4.1 Statistics

A statistical t-test was performed on the data from the Warm Active and Cold Active Cu-Zn aqueous phases to determine if these were different (Appendix E). Table 9 is a summary of the results from the test.

Table 9. Statistical summary of results from the Warm Active and Cold Active Cu-Zn aqueous phases.

	same	different
pH		•
Eh	•	
SO_4^{2-}	•	
S^{2-}	•	
Fe_{diss}		•
DOC	•	
Hg_{tot}		•
MeHg	•	
SRB		•

4.4.2 Aqueous geochemistry

4.4.2.1 pH and Eh

The pH of both the Warm Active SRB and Cold Active SRB Cu-Zn columns was near pH neutral (Figure 10 a). pH conditions remained fairly stable over time in the Cold Active column, but slightly increased over time in the Warm Active one (Figure 10 a). Eh values were similar for both columns (Table 9). Values decreased in the first 8 days of the experiment and then increased slightly (Figure 10 b).

4.4.2.2 Major cations

The major dissolved cations were measured at the same intervals as the other geochemical parameters, and appear in Appendix A. The data showed a release of some major cations into the aqueous phase over 125 days.

4.4.2.3 Sulfate and sulfide

Sulfate concentrations in both columns increased within the first week (Figure 10 c). The Warm Active and Cold Active columns showed similar sulfate levels until 49 days, but at day 70, sulfate concentrations increased in the Cold Active column (Figure 10 c). This corresponded to the accidental freezing of the column. After thawing, sulfate levels returned to previous levels, whereas sulfate increased near the end of the experiment in Warm Active column. Statistically, sulfate concentrations in the two columns were not different despite the accidental freezing/thawing episode (Table 9).

The Warm Active SRB Cu-Zn column had sulfide levels that were near the detection limit for the entire experiment, with the exception of day 8 when sulfide concentrations were slightly elevated (Figure 11 a). Sulfide levels in the Cold Active SRB Cu-Zn column increased over time until day 70, but then declined and hovered near the detection limit of the method. Despite the fluctuations in sulfide levels in both columns, values reported for both the Cold Active and Warm Active SRB Cu-Zn columns were similar (Table 9).

a)

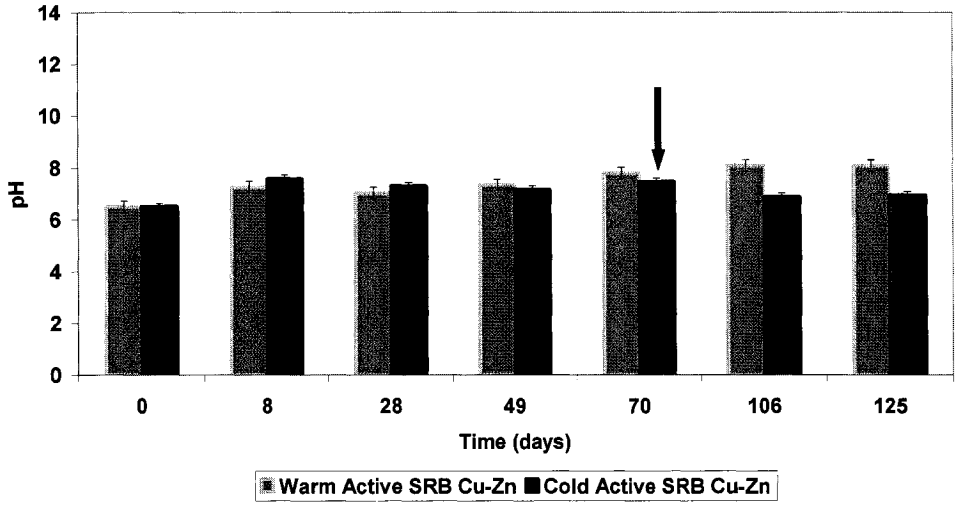

b)

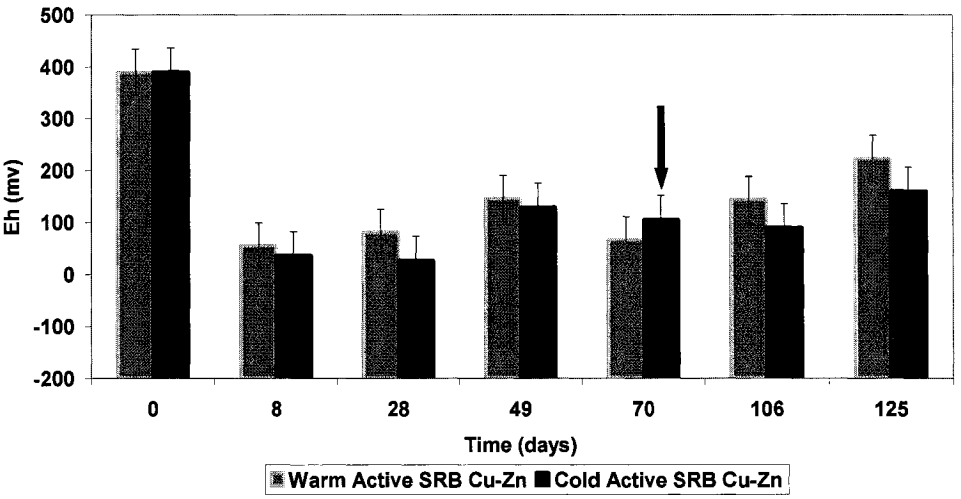

c)

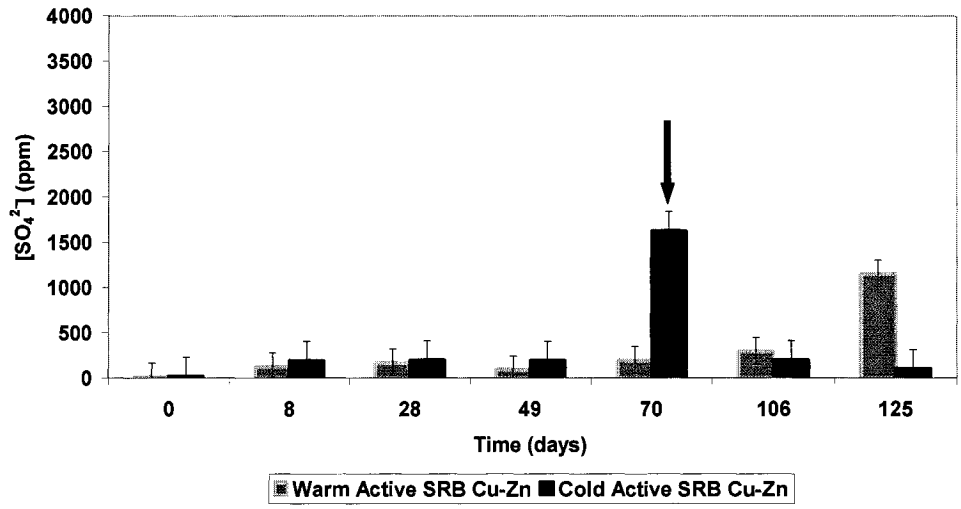

Figure 10. pH (a), Eh (b) and Sulfate (c) trends of the aqueous phase in the Warm Active SRB Cu-Zn and Cold Active SRB Cu-Zn columns over 125 days. Blue arrow corresponds to sample taken after accidental freezing of the Cold Active SRB Cu-Zn column.

4.4.2.4 Dissolved Iron

Both of the Warm Active and Cold Active SRB Cu-Zn columns, regardless of the temperature, did not release any significant Fe into the water above the tailings (Figure 11 b). The small values measured are however statistically different (Table 9), despite their insignificance.

4.4.2.5 DOC

DOC concentrations drastically declined within the first 8 days and then more gradually until day 106 in both columns. Near the end of the experiment, DOC values increased again (Figure 11 c). DOC values reported for both the Cold Active and Warm Active SRB Cu-Zn columns were statistically similar (Table 9).

4.4.2.6 Soluble total Hg

Both the Warm Active SRB Cu-Zn and Cold Active SRB Cu-Zn columns released soluble Hg from days 8 to 106 (Figure 12 a), with the Warm Active column releasing a statistically larger amount (Table 9), especially on day 70.

4.4.2.7 Soluble MeHg

The Warm Active SRB Cu-Zn, as previously described in section 4.2.2.7, had no soluble MeHg in the aqueous phase until 125 days (Figure 12 b). The Cold Active SRB Cu-Zn column had no measurable MeHg either, except at day 70 when the column thawed after being accidentally frozen the day before. Statistically the MeHg production in the Warm Active and Cold Active columns were the same (Table 9).

a)

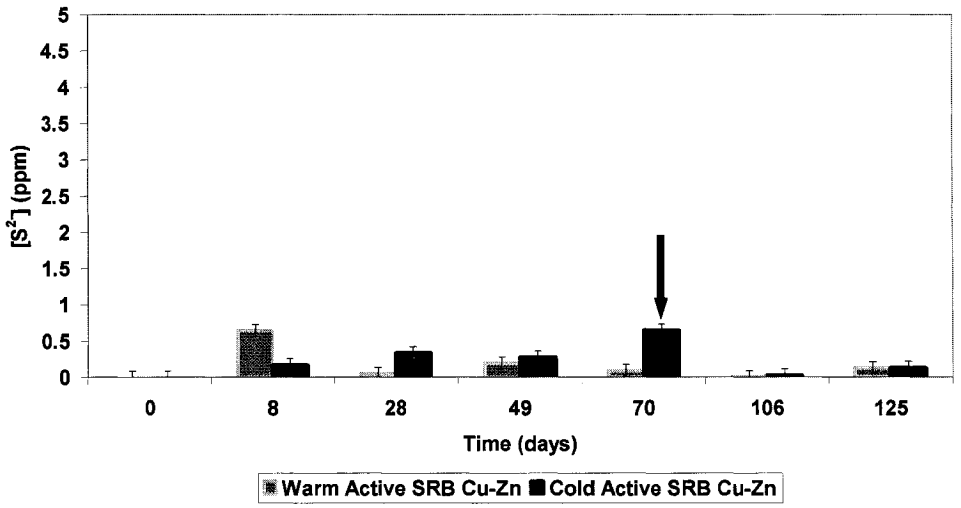

b)

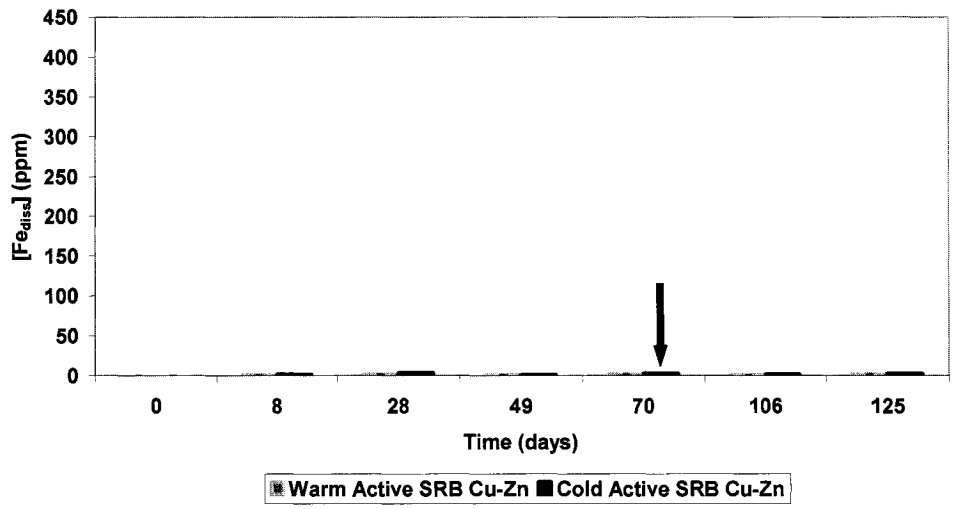

c)

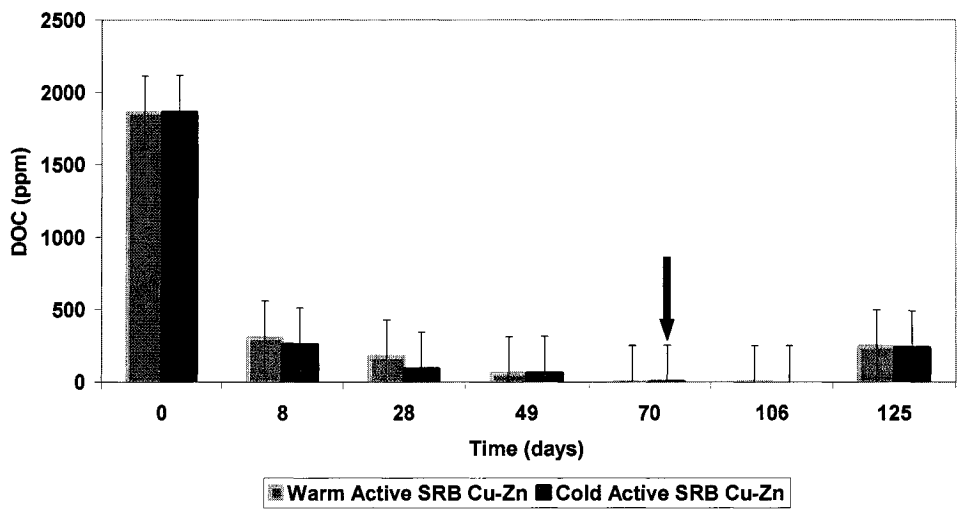

Figure 11. Sulfide (a), dissolved iron (b), and DOC (c) concentrations in the aqueous phase of the Warm Active SRB Cu-Zn and the Cold Active SRB Cu-Zn columns over 125 days. Blue arrow corresponds to sample taken after accidental freezing of the Cold Active SRB Cu-Zn column.

4.4.2.8 SRB enumeration

SRB populations in both the Warm and Cold Active SRB columns increased over the course of the experiment (Figure 12 c). At 125 days, populations were two orders of magnitude higher than the initial SRB population. SRB populations in the Cold Active column were statistically higher than the SRB than in the Warm Active column (Table 9).

a)

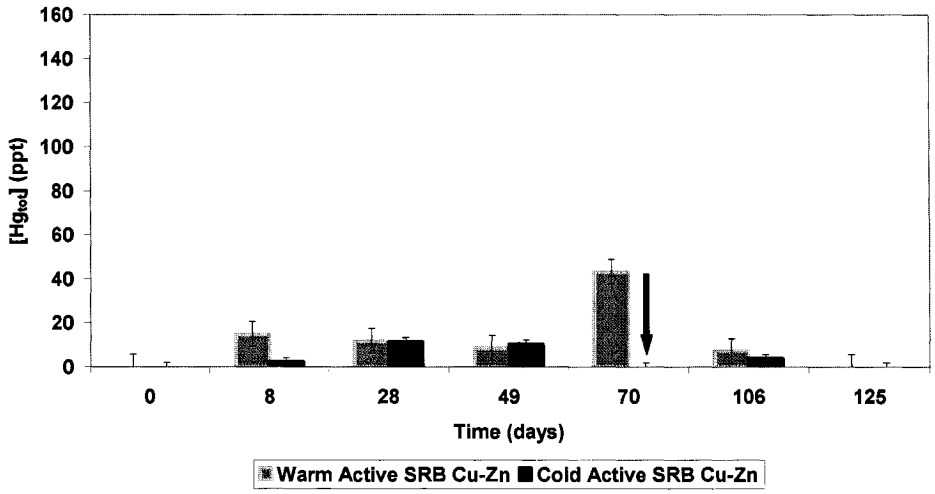

b)

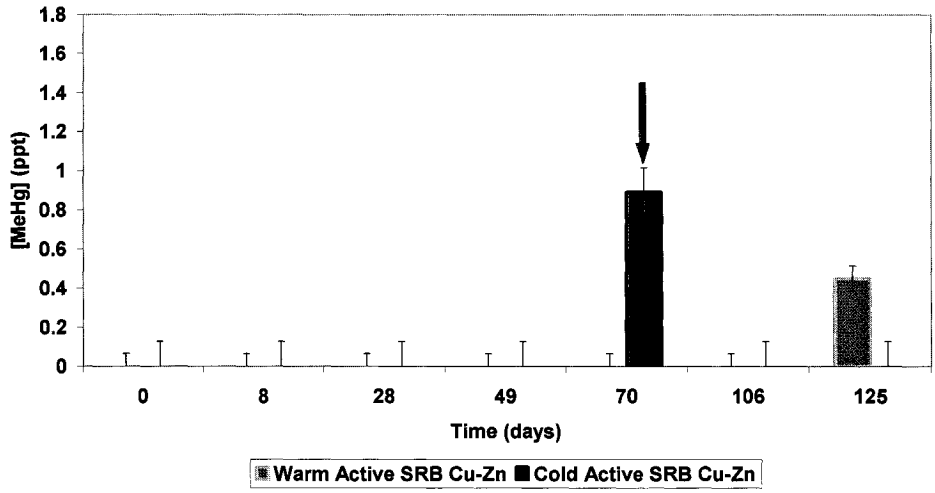

c)

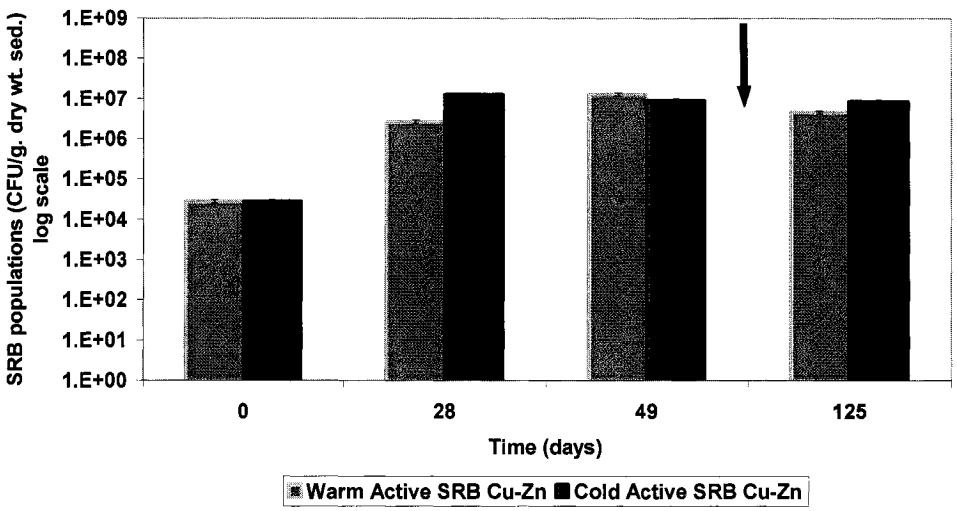

Figure 12. Total mercury (a), methyl mercury (b) concentrations in the aqueous phase of the Warm Active SRB Cu-Zn and the Cold Active SRB Cu-Zn columns over 125 days, and SRB populations (c) at the sediment/water interface in the Warm Active SRB Cu-Zn and the Cold Active SRB Cu-Zn columns over 125 days. Blue arrow corresponds to sample taken after accidental freezing of the Cold Active SRB Cu-Zn column.

4.5 Low and High Sulfate active Cu-Zn columns

4.5.1 Statistics

A statistical t-test was performed on the aqueous phase results from the High Sulfate and Low Sulfate Cu-Zn columns to determine if the data were statistically the same or statistically different (Appendix E). Table 10 is a summary of the results from the test.

Table 10. Statistical summary of results from the High Sulfate and Low Sulfate Cu-Zn aqueous phases.

	same	different
pH	•	
Eh	•	
SO_4^{2-}		•
S^{2-}	•	
Fe_{diss}	•	
DOC		•
Hg_{tot}	•	
MeHg	•	
SRB		•

4.5.2 Aqueous geochemistry

4.5.2.1 pH and Eh

The pH and redox trends overtime for both the High Sulfate and Low Sulfate columns were statistically similar (Table 10). The initial pH of 6.82 slightly increased to 8.2 and 8.6 for the High Sulfate and Low Sulfate columns, respectively (Figure 13 a). Both columns developed reducing conditions within the first 12 days, but the redox values increased thereafter, indicating establishment of more oxidizing conditions (Figure 13 b).

a)

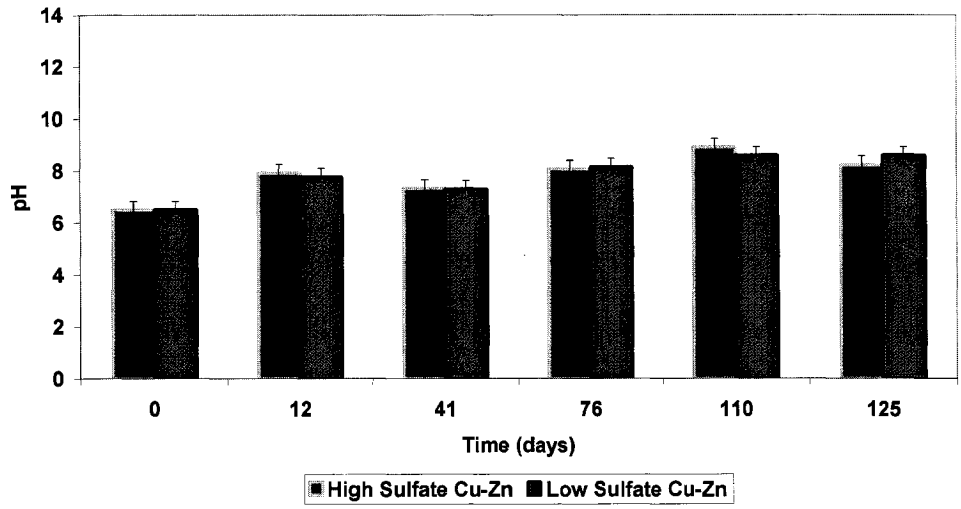

b)

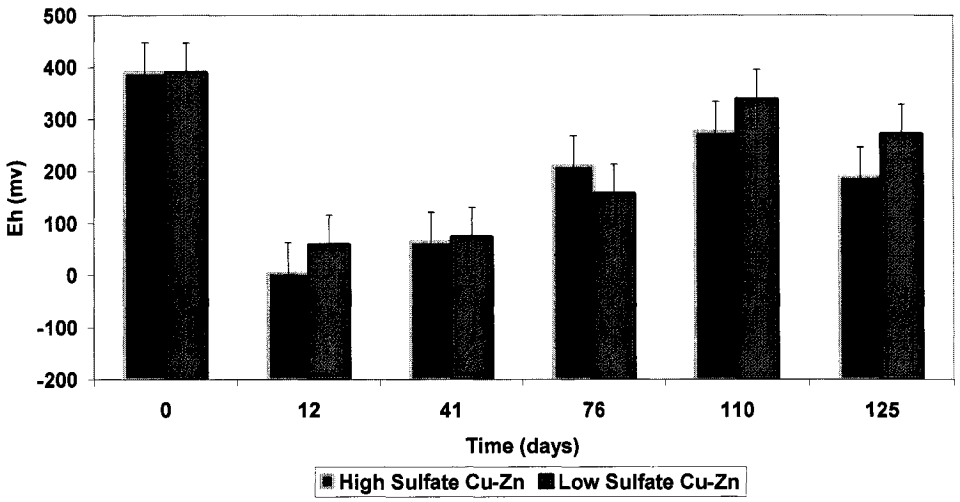

c)

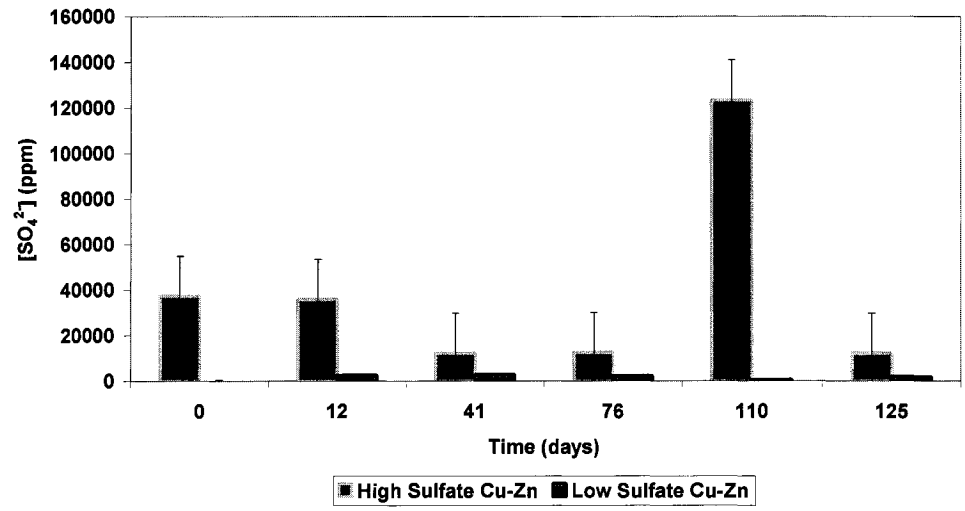

Figure 13. pH (a), Eh (b), and Sulfate (y-axis scale is x4 to include larger values) (c) trends of the aqueous phase in the High Sulfate Cu-Zn and Low Sulfate Cu-Zn columns over 125 days.

4.5.2.2 Major cations

The major dissolved cations were measured at the same intervals as the other geochemical parameters, and appear in Appendix A. The data showed releases of some major cations into the aqueous phase over 125 days.

4.5.2.3 Sulfate and sulfide

High Sulfate Cu-Zn column had a rapid release of sulfate at 110 days, whereas sulfate levels in the Low Sulfate column remained comparatively low over the course of the whole experiment (Figure 13 c). Given the difference in the initial sulfate concentration, values reported for both columns were statistically different (Table 10).

Sulfide levels in both columns were statistically similar (Table 10), despite the relatively high sulfide concentration recorded in the High Sulfate column on day 125. In both columns, sulfide concentrations increased gradually with time but the High Sulfate Cu-Zn system increased at a greater rate (Figure 14 a).

4.5.2.4 Dissolved Iron

Dissolved iron concentrations in the High Sulfate Cu-Zn and the Low Sulfate Cu-Zn columns were statistically identical (Table 10). Iron concentrations were generally below the detection limit, but some iron was released into solution in both columns at day 12 and 41 (Figure 14 b).

a)

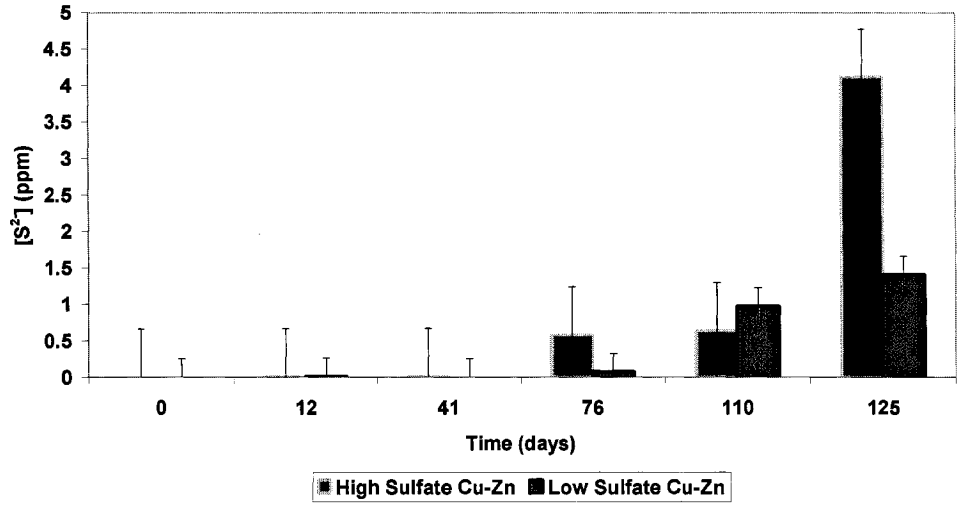

b)

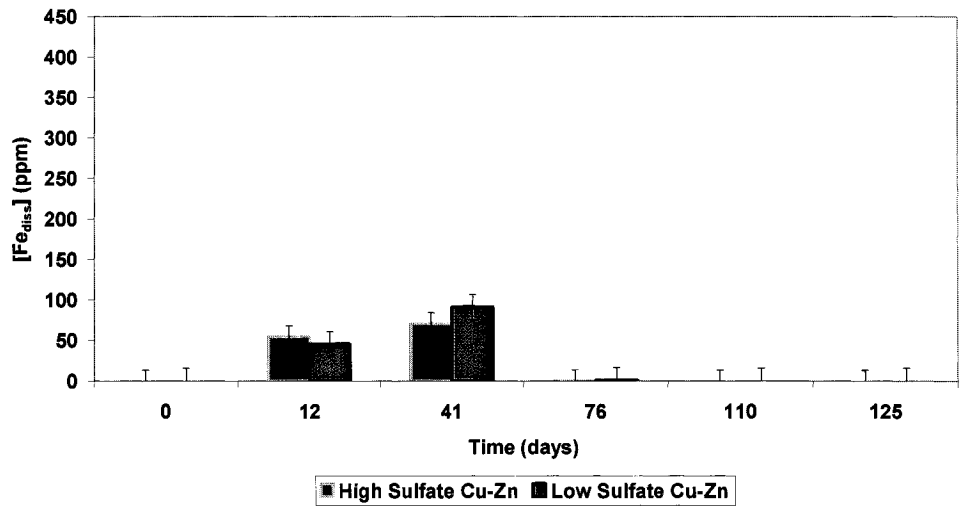

c)

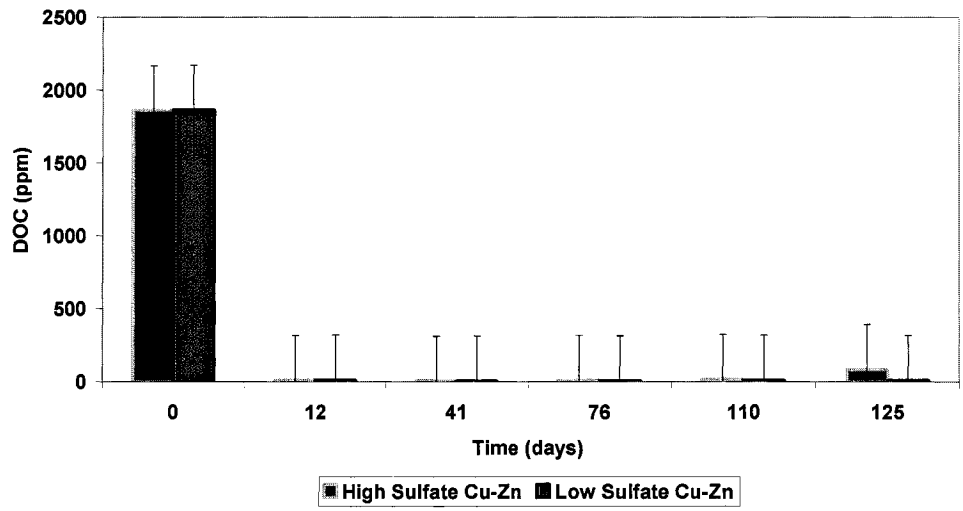

Figure 14. Sulfide (a), dissolved iron (b), and DOC (c) concentrations in the aqueous phase of the High Sulfate Cu-Zn and Low Sulfate Cu-Zn columns over 125 days.

4.5.2.5 DOC

DOC concentrations measured in both the High Sulfate Cu-Zn and Low Sulfate Cu-Zn systems during the course of the experiment were generally lower than the concentrations reported for all the other columns (Figure 14 c). DOC levels in the High and Low Sulfate columns showed a sharp decrease within the first 12 days and then slightly increased over time. DOC concentrations in the High Sulfate column were higher than the ones in the Low Sulfate column at the end of the experiment, and were statistically different (Table 10).

4.5.2.6 Soluble total Hg

The High and Low Sulfate Cu-Zn Columns had statistically similar dissolved Hg concentrations (Table 10). They both had soluble Hg at 12 days but the concentrations dropped to below the detection limit after 41 days, and then increased from 76 days to 125 days (Figure 15 a).

4.5.2.7 Soluble MeHg

There was no detectable MeHg in either columns (Figure 15 b).

4.5.2.8 SRB enumeration

Both the High Sulfate Cu-Zn and the Low Sulfate Cu-Zn columns showed an increase in SRB populations with time (Figure 15 c). The Low Sulfate Cu-Zn column had statistically more SRB than the High Sulfate Cu-Zn column (Table 10).

a)

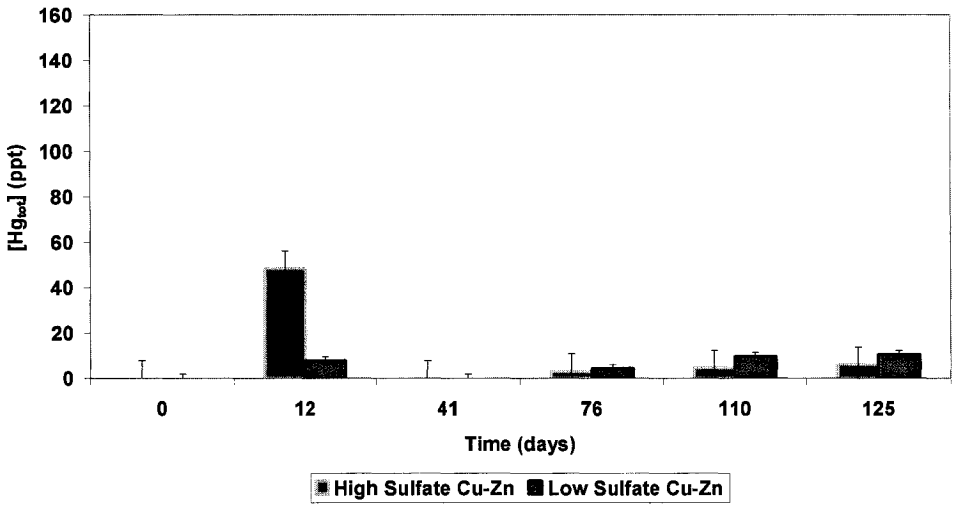

b)

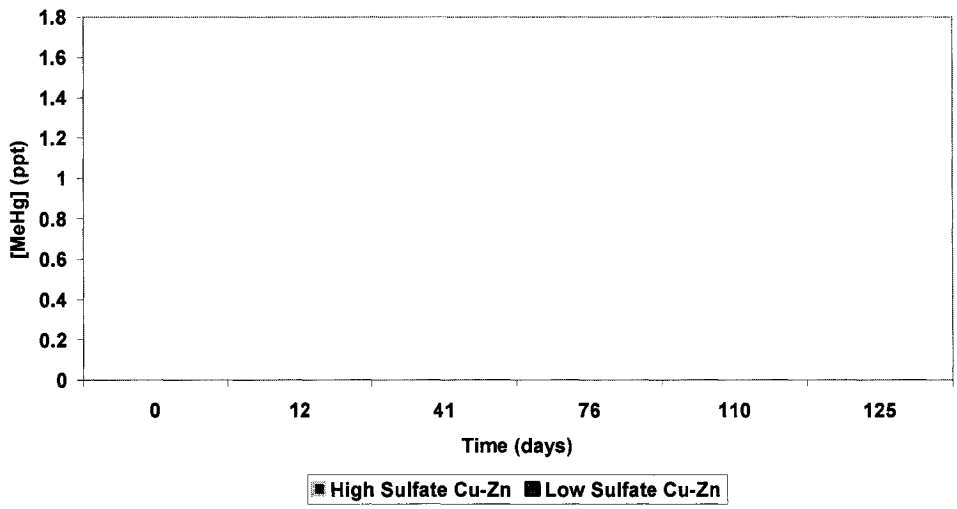

c)

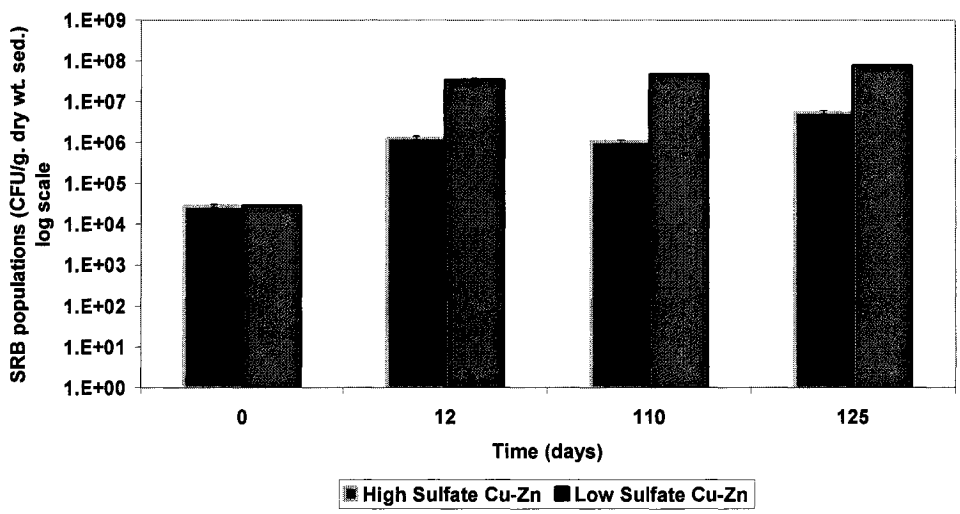

Figure 15. Total mercury (a), methyl mercury (b) concentrations in the aqueous phase of the High Sulfate Cu-Zn and Low Sulfate Cu-Zn columns over 125 days, and SRB populations at the sediment/water interface in the High Sulfate Cu-Zn and Low Sulfate Cu-Zn columns over 125 days.

4.6 Low and High DOC active Cu-Zn columns

4.6.1 Statistics

A statistical t-test was performed on the data from the High DOC and Low DOC Cu-Zn aqueous phase results to determine if the data were statistically similar or different (Appendix E). Table 11 is a summary of the results from the test.

Table 11. Statistical summary of results from the High DOC and Low DOC Cu-Zn aqueous phases.

	same	different
pH		•
Eh		•
SO_4^{2-}	•	
S^{2-}		•
Fe_{diss}		•
DOC		•
Hg_{tot}	•	
MeHg	•	
SRB		•

4.6.2 Aqueous geochemistry

4.6.2.1 pH and Eh

The pH of the High DOC Cu-Zn column increased until 110 days, then decreased slightly, whereas the pH of the Low DOC Cu-Zn column decreased until 76 days then increased slightly (Figure 16 a). pH values for both columns were statistically different (Table 11). The High DOC columns became reducing between 0 and 41 days, but the Eh values increased thereafter (Figure 16 a). In the Low DOC columns, slightly reducing conditions developed in the 12 days of the experiment, but Eh values increased afterward until 110 days. The Eh of the Low DOC Cu-Zn column appeared to increase and decrease

a)

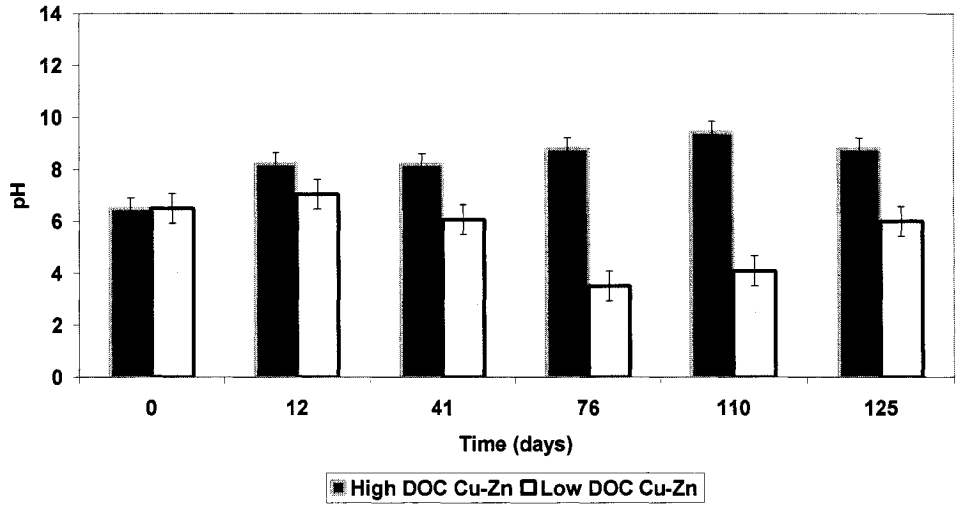

b)

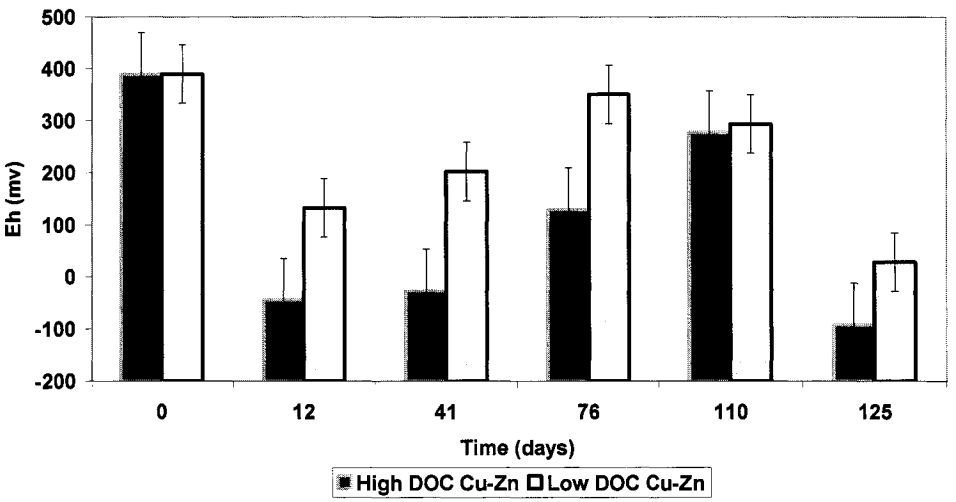

c)

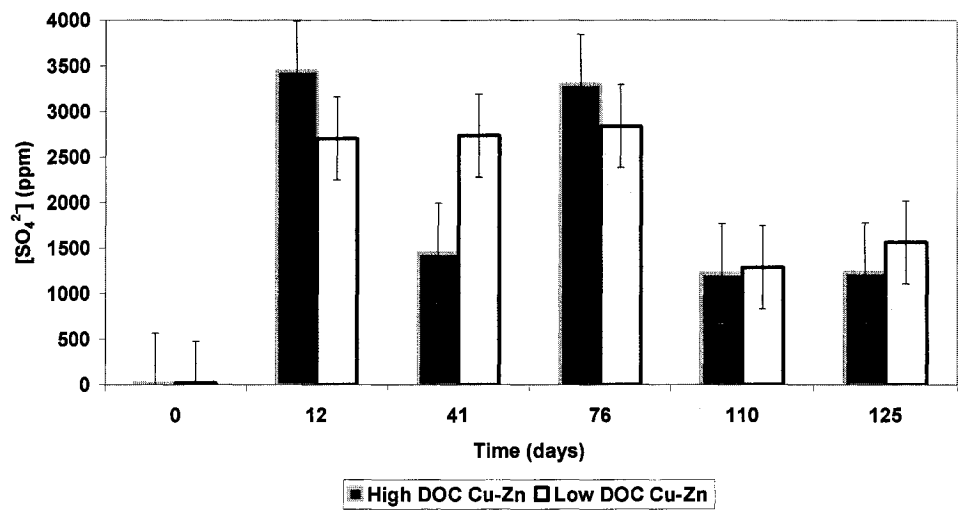

Figure 16. pH (a), Eh (b), and Sulfate (c) trends of the aqueous phase in the High DOC Cu-Zn and Low DOC Cu-Zn columns over 125 days.

at the same time as the High DOC column but was statistically more oxic than the High DOC column.

4.6.2.2 Major cations

The major dissolved cations were measured at the same intervals as the other geochemical parameters, and appear in Appendix A. The data showed a release of some major cations into the aqueous phase over 125 days.

4.6.2.3 Sulfate and sulfide

Both the High DOC Cu-Zn and Low DOC Cu-Zn columns had statistically similar sulfate concentrations (Table 11). Sulfate concentrations in both columns sharply increased to above 1200 ppm SO_4^{2-} within the first 12 days and then remained fairly stable for the remainder of the experiment.

However, the High DOC Cu-Zn and Low DOC Cu-Zn columns were statistically very different with respect to sulfide concentrations (Table 11). There was some sulfide production in the High DOC column, especially at days 41 and 110, whereas no sulfide was detected in the Low DOC (Figure 17 a).

4.6.2.4 Dissolved Iron

The High DOC Cu-Zn column had very low levels of dissolved Fe above the sediment-water interface during the course of the experiment, whereas there was a net production of soluble Fe in the Low DOC column from days 12 to 125 (Figure 17 b). Fe values reported for both columns were statistically different (Table 11).

a)

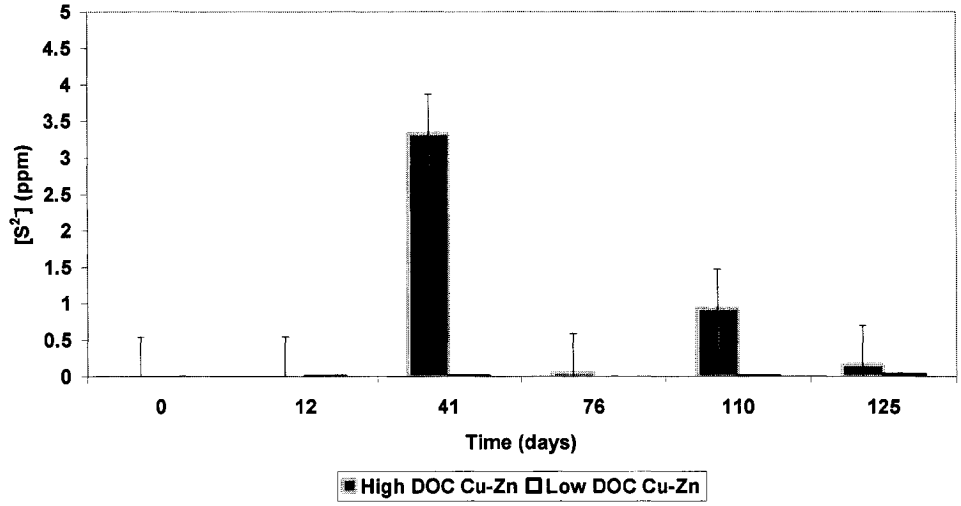

b)

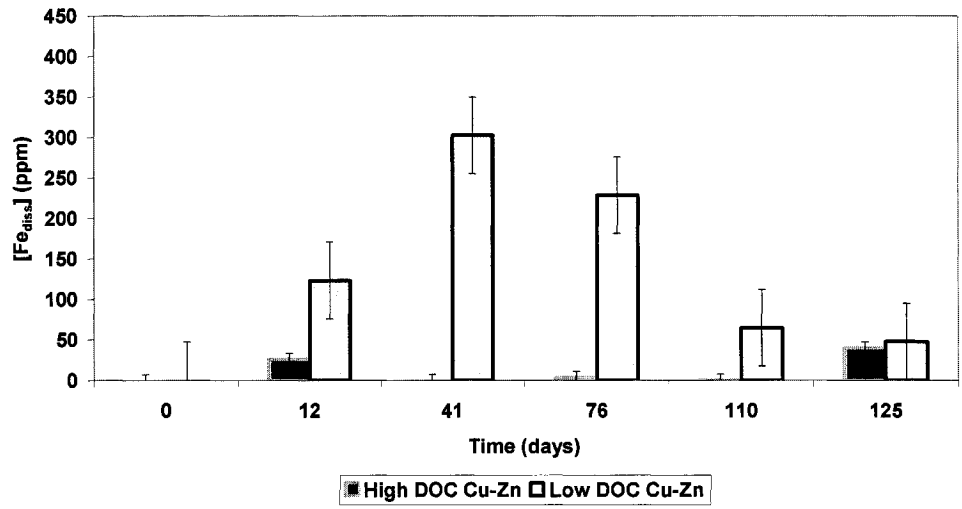

c)

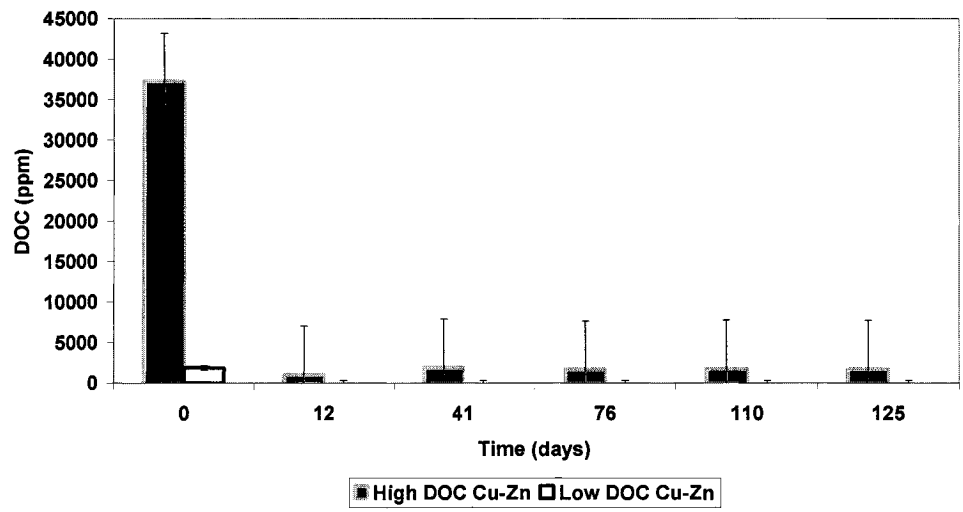

Figure 17. Sulfide (a), dissolved iron (b), and DOC (y-axis scale is x18 to include larger values) (c) concentrations in the aqueous phase of the High DOC Cu-Zn and Low DOC Cu-Zn columns over 125 days.

4.6.2.5 DOC

Given the difference in initial concentration of DOC, values reported for both columns were statistically different (Table 11). DOC concentrations in the High DOC Cu-Zn column declined within the first week and remained above 1000 ppm DOC for the remainder of the experiment (Figure 17 c). The Low DOC column showed a DOC increase at day 12 and then a slight decline for the rest of the experiment.

4.6.2.6 Soluble total Hg

The High DOC Cu-Zn and the Low DOC Cu-Zn columns both had no detectable soluble Hg during the 125 days, with the exception of day 12 in the High DOC Cu-Zn column and day 125 in the Low DOC Cu-Zn column (Figure 18 a). Hg values for both the High DOC and Low DOC columns were statistically identical (Table 11).

4.6.2.7 Soluble MeHg

The High DOC Cu-Zn column released some dissolved MeHg from day 41 until the end of the experiment (Figure 18 b), whereas the Low DOC Cu-Zn system had no detectable MeHg, except at day 111. MeHg values reported for both the High DOC and Low DOC columns were however statistically similar (Table 11).

4.6.2.8 SRB enumeration

Both the High DOC and Low DOC Cu-Zn columns had increasing SRB populations during the course of the experiment (Figure 18 c). The High DOC Cu-Zn column had the highest SRB populations of all the Cu-Zn systems studied here and the Low DOC Cu-Zn column had the lowest SRB populations. SRB values reported for both systems were statistically different (Table 11).

a)

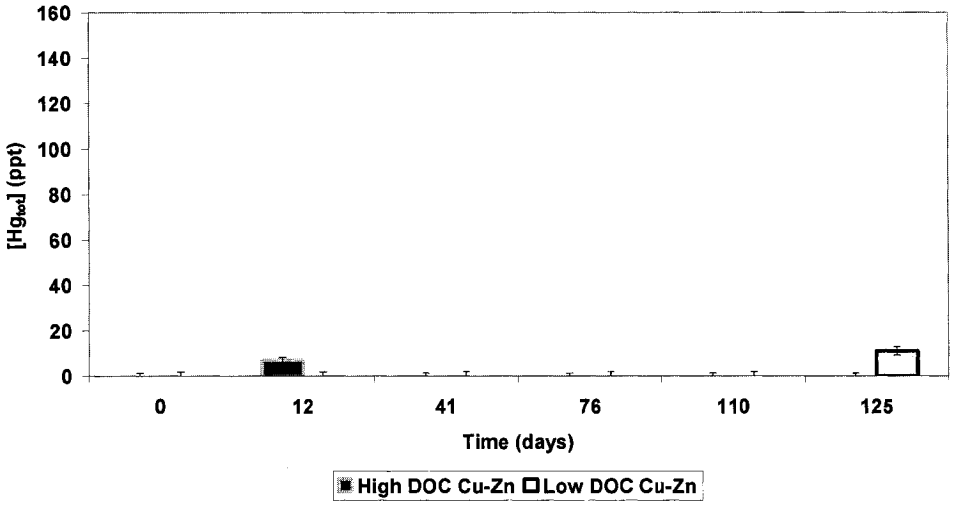

b)

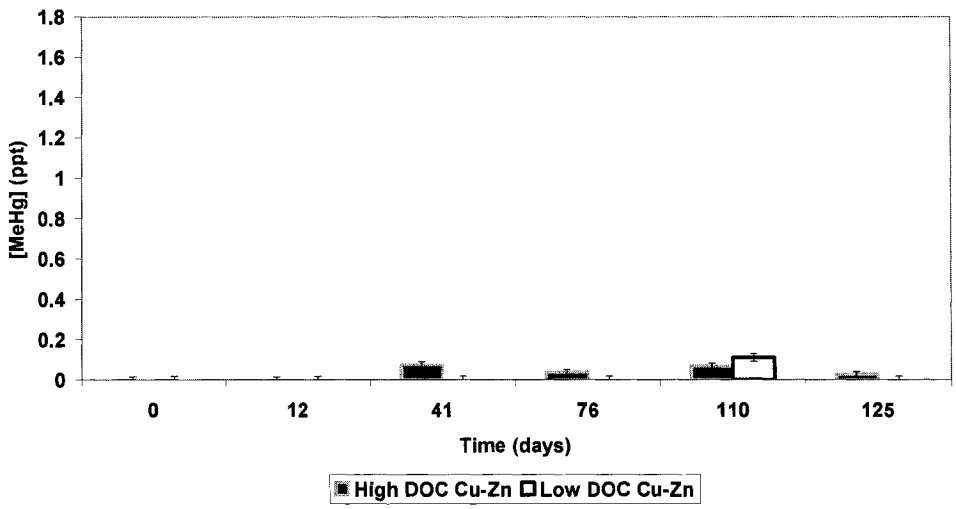

c)

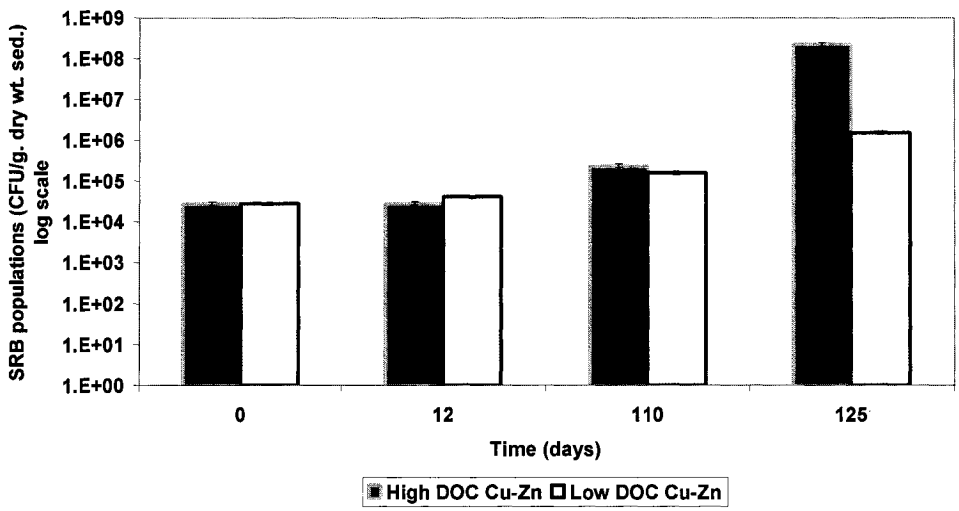

Figure 18. Total mercury (a), methyl mercury (b) concentrations in the aqueous phase of the High DOC Cu-Zn and Low DOC Cu-Zn columns over 125 days, and SRB populations at the sediment/water interface in the High DOC Cu-Zn and Low DOC Cu-Zn columns over 125 days.

4.7 Warm Active and Non-active Au columns

4.7.1 Statistics

A statistical t-test was performed on the aqueous phase results from the Active SRB Au and Non-active SRB Au columns to determine if the data were statistically the same or statistically different (Appendix E). Table 12 is a summary of the results from the test.

Table 12. Statistical summary of results from the Active SRB Au and Non-active SRB Au aqueous phases.

	same	different
pH		•
Eh		•
SO_4^{2-}		•
S^{2-}	•	
Fe_{diss}		•
DOC		•
Hg_{tot}		•
MeHg		•
SRB		•

4.7.2 Aqueous geochemistry

4.7.3.1 pH and Eh

For the gold tailings collected in Nova Scotia, the initial pH was near neutral. Both the Active SRB Au and Non-active SRB Au columns increased in pH (Figure 19 a) for the entire experiment but at different rates, the Active SRB Au had a statistically higher value (Table 12). Both systems displayed reducing conditions at the beginning of the experiment, but the redox values increased over time in the Active SRB column, where the redox potential remained fairly stable in the Non-Active columns, with the exception of day 125 (Figure 19 b). The Eh values of the Active SRB Au column were statistically different than the values reported for the Non-active SRB Au column (Table 12).

a)

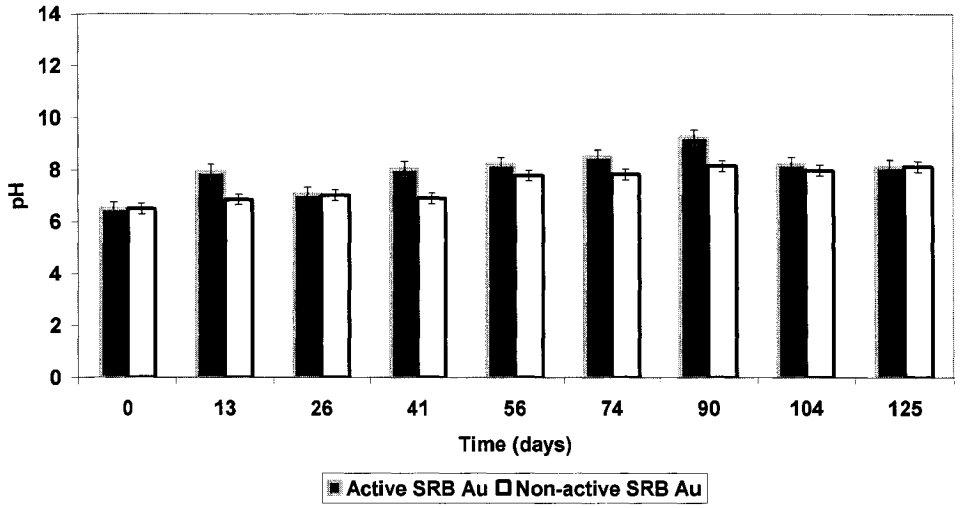

b)

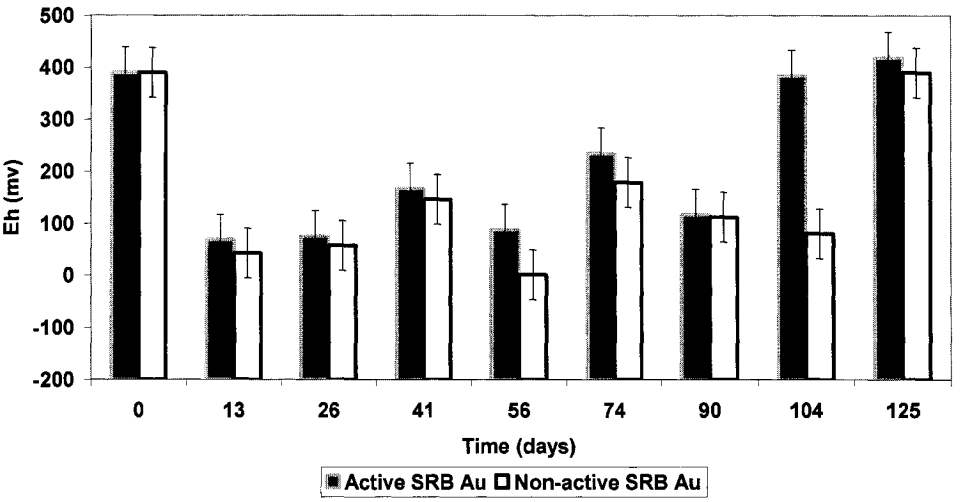

c)

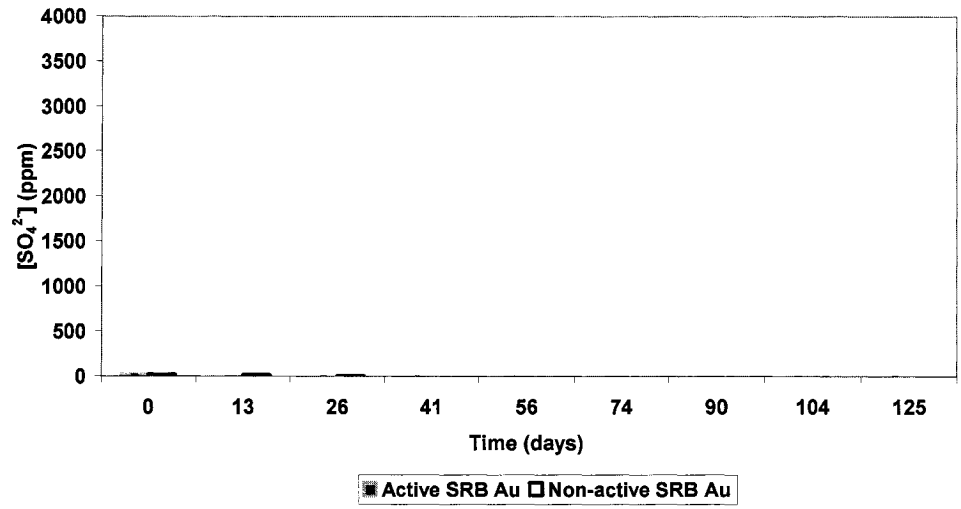

Figure 19. pH (a), Eh (b) and Sulfate (c) trends of the aqueous phase in the Active SRB Au and Non-active SRB Au columns over 125 days.

4.7.3.2 Major cations

The major dissolved cations were measured at the same intervals as the other geochemical parameters, and appear in Appendix A. The data showed a release of some major cations into the aqueous phase over 125 days.

4.7.3.3 Sulfate and sulfide

Sulfate levels of the Active SRB Au columns rapidly declined within the first 2 weeks and remained below the detection limit for the remainder of the experiment (Figure 19 c). Sulfate was detected in the Non-active SRB Au column until day 26, and then declined below detection limit, the sulfate concentrations for the Non-active SRB Au column and the active SRB Au column are statistically different (Table 12).

Sulfide concentrations in the Active SRB Au column were very low throughout the experiment, with the exception of day 90 (Figure 20 a). On the other hand, sulfide was detected in the Non-active SRB Au column during the course of the experiment, with the highest concentration measured at day 13 (Figure 20 a).. However, sulfide concentrations in the Non-active SRB Au column were not high enough to be statistically different from the Active SRB Au column (Table 12).

4.7.3.4 Dissolved Iron

The Active SRB Au system had no significant soluble Fe into the aqueous phase over the 125 days (Figure 20 b), whereas the Non-active SRB Au column released iron to the solution during the course of the experiments, with concentrations reaching almost 200 ppm at days 41 and 56 (Figure 20 b). Fe values for both columns were statistically different (Table 12).

a)

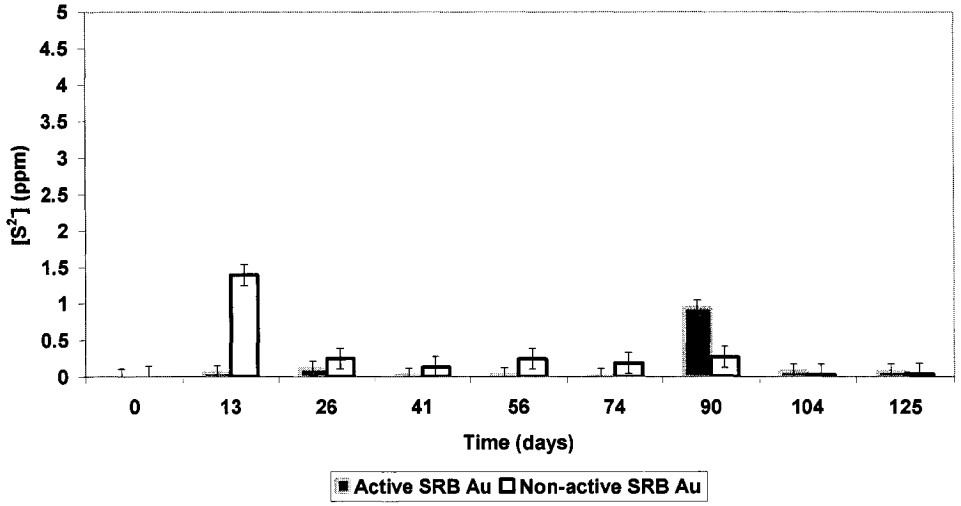

b)

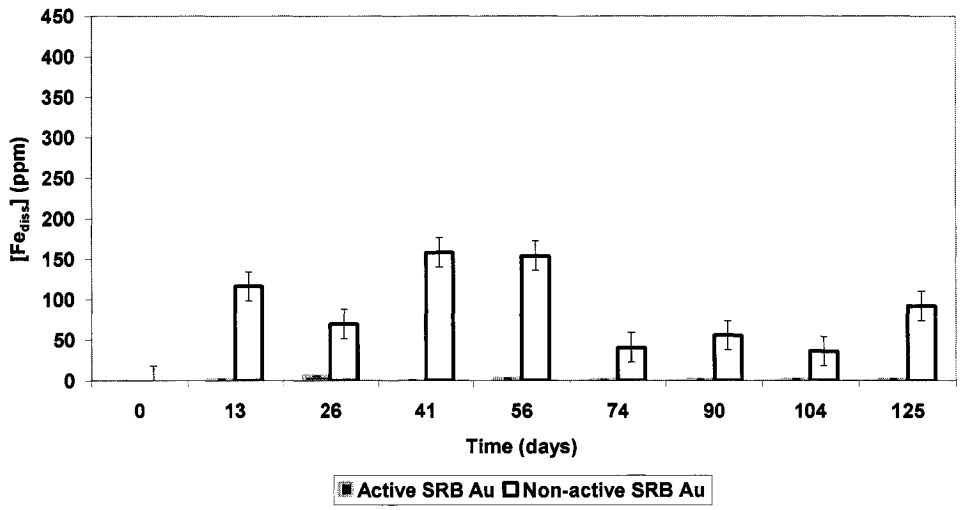

c)

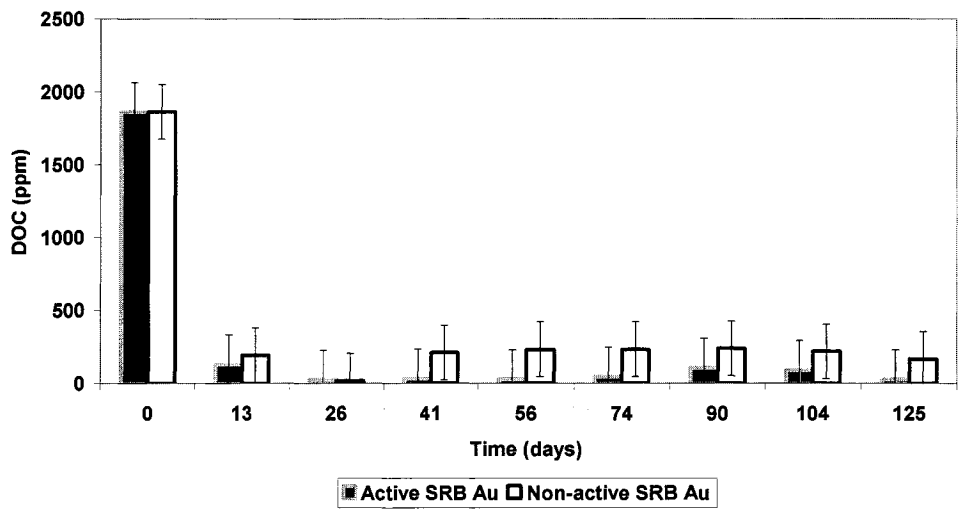

Figure 20. Sulfide (a), dissolved iron (b), and DOC (c) concentrations in the aqueous phase of the Active SRB Au and Non-active SRB Au columns over 125 days.

4.7.3.5 DOC

DOC concentrations declined within the first 2 weeks in both systems (Figure 20 c). In the Active SRB Au tailings column, DOC was consumed until day 56 and then increased thereafter. In the Non-active SRB Au column, DOC concentrations remained fairly stable over time, with the exception of day 26 (Figure 20 c). DOC values for both columns were statistically different (Table 12).

4.7.3.6 Soluble total Hg

Neither the Active SRB Au or the Non-active SRB Au column released any significant Hg into solution after the experiment started, with the exception of the Active SRB Au column at 74 and 125 days (Figure 21 a). The soluble Hg concentrations in the Active SRB Au and the Non-active SRB Au columns were statistically different (Table 12).

4.7.3.7 Soluble MeHg

Both the Active and Non-active SRB Au columns released MeHg during the course of the experiment (Figure 21 b), but the concentrations were statistically higher in the Active SRB column (Table 12). MeHg concentrations were particularly high at 90 and 104 days in the Active SRB Au system.

4.7.3.8 SRB enumeration

SRB populations in the Active SRB Au column increased within the first 2 weeks of the experiment, then declined at day 41 and increased again at the end of the experiment (Figure 21 c). In the Non-Active SRB column, SRB populations slightly declined over time. Values reported for SRB populations in both columns were statistically different (Table 12).

a)

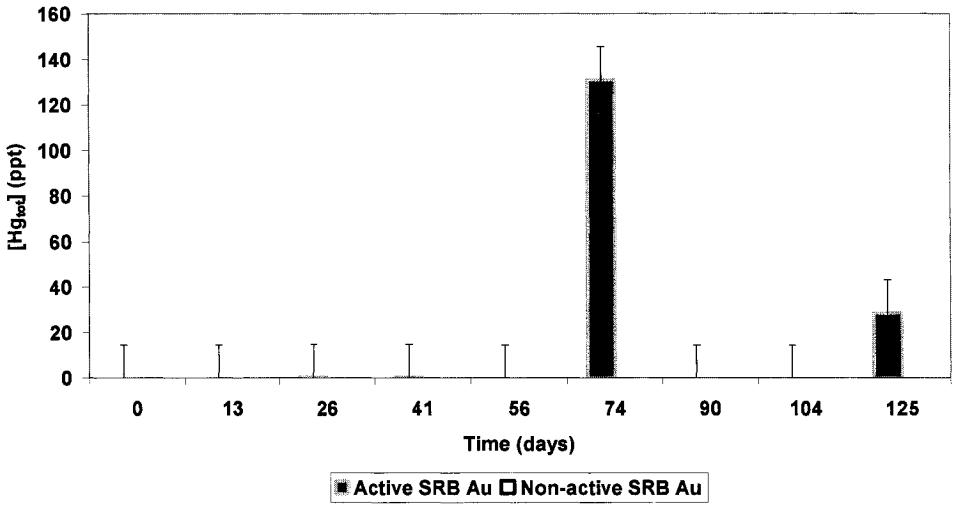

b)

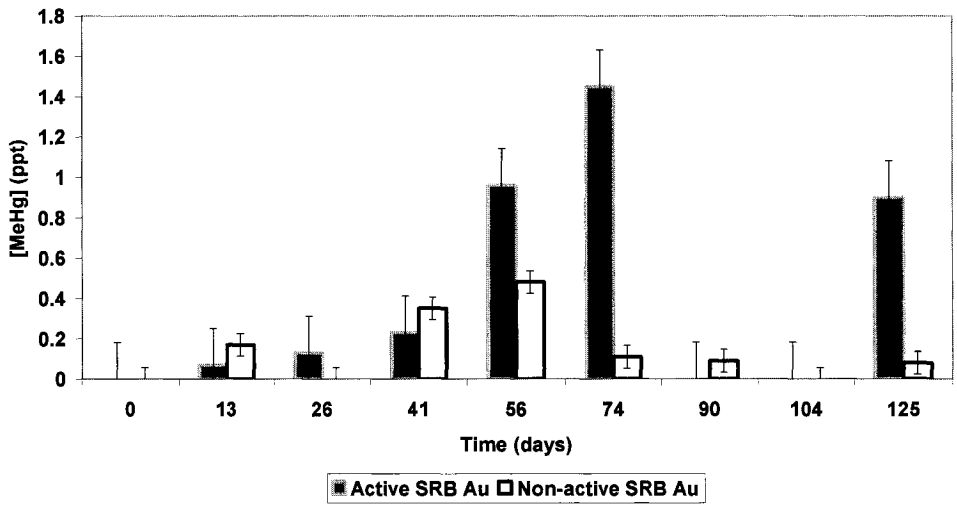

c)

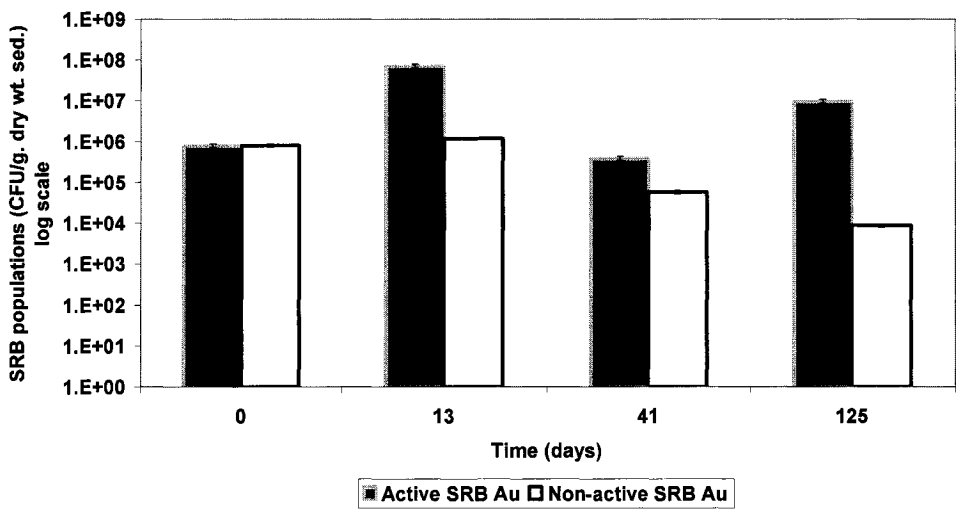

Figure 21. Total mercury (a), methyl mercury (b) concentrations in the aqueous phase of the Active SRB Au and Non-active SRB Au columns over 125 days, and SRB populations at the sediment/water interface (c) in the Active SRB Au and Non-active SRB Au columns over 125 days.

4.7.3 Solid phase geochemistry

4.7.3.1 Acid-volatile sulfide (AVS) extraction

The acid volatile sulfide levels in the Active SRB Au column increased at depths of 6 to 12 cm with respect to the original AVS concentration in the initial tailings (Figure 22 a). In the Non-active SRB Au column, AVS levels were higher at the surface of the column when compared to the initial concentration in the Au tailings, but then declined with depth (Figure 22 a). The statistical t-test (Appendix C-1) showed that the values for the Active SRB Au column were different from the ones in the Non-active SRB Au column.

4.7.3.2 Solid total Hg

The distribution of Hg with depth of both the Active SRB Au and Non-active SRB Au columns was similar, i.e., there was a net accumulation of Hg at the surface of the sediments in both columns, which was greater than the initial Hg concentration (Figure 22 b). The statistical t-test showed that the values reported for the Active SRB Au and Non-active SRB Au columns were identical (Appendix C-2).

4.7.3.3 Solid MeHg

Both the Active SRB Au and Non-active SRB Au columns showed an enrichment of MeHg in the solid phase at the surface of the columns, but the enrichment was far greater in the Non-active SRB column (Figure 23 a). The statistical t-test (Appendix C-3) indicated that the values in the Active SRB Au column and the Non-active SRB Au column were different from each other. The Non-active SRB Au column had significantly more MeHg produced in the top 6 cm than the Active SRB Au column.

a)

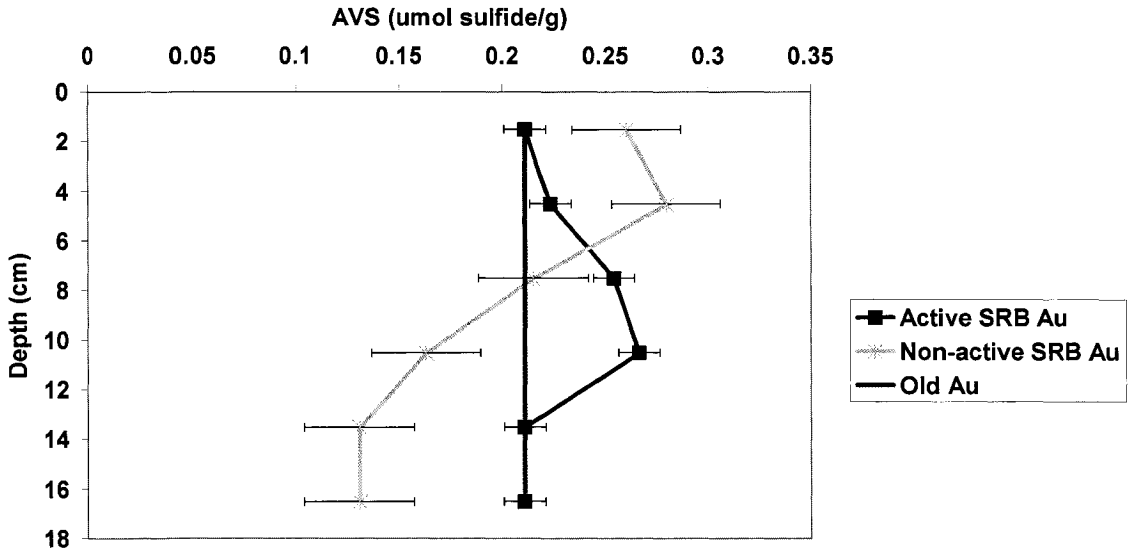

b)

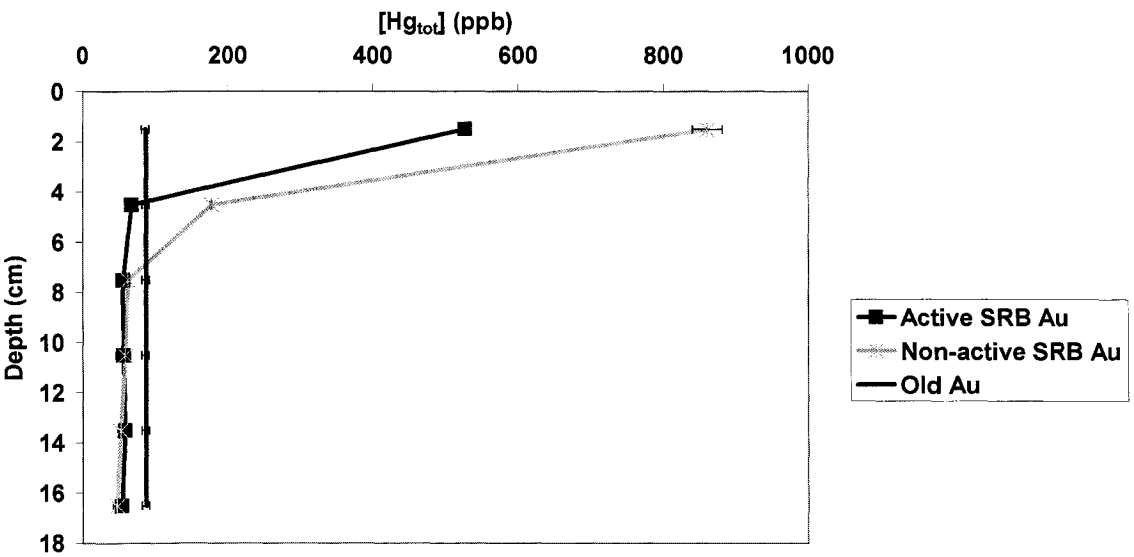

Figure 22. Acid volatile sulfide concentration in the solid phase of the Active SRB Au and Non-active SRB Au column at the end of the experiment and initial concentration in the Old Au tailings (a) and total mercury concentration in the solid phase of the Active SRB Au and Non-active SRB Au column at the end of the experiment and initial concentration in the Old Au tailings (b).

4.7.3.4 Organic carbon content (LOI)

Both the Active SRB Au and Non-active SRB Au columns showed a sharp enrichment of organic carbon in the surface sediments, when compared to the original concentration in the Au tailings (Figure 23 b). Interestingly, the organic carbon content of the solid phase followed the same trend with depth as MeHg (Figure 23 a and b). Based on the t-test (Appendix C-4), the organic carbon values in the Active SRB Au column and the Non-active SRB Au column were identical.

4.7.3.5 Granulometry

The grain size distribution as a function of depth for both columns is presented in Appendix D.

a)

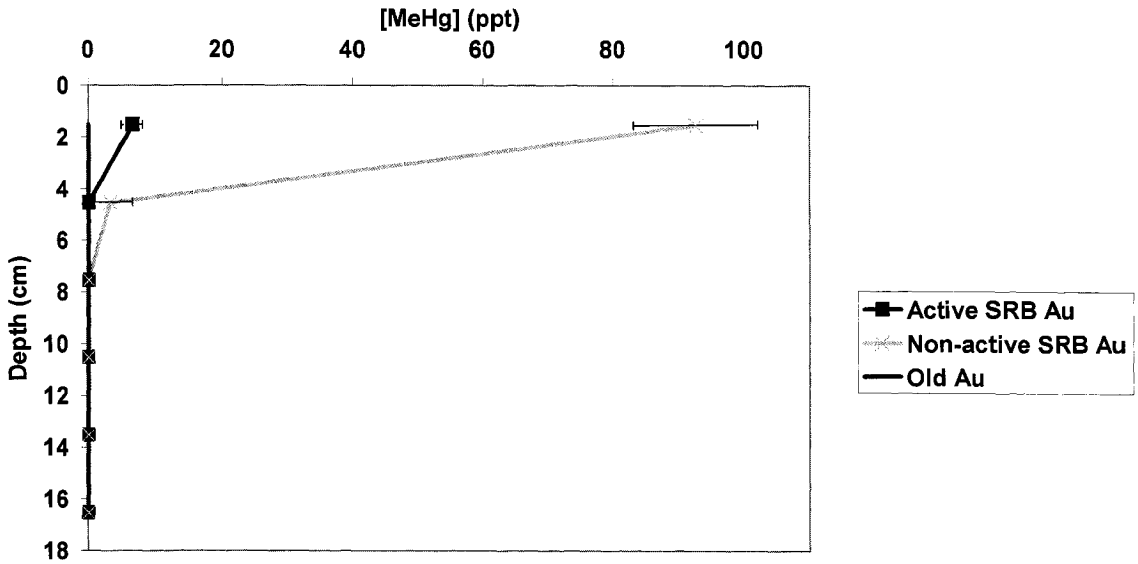

b)

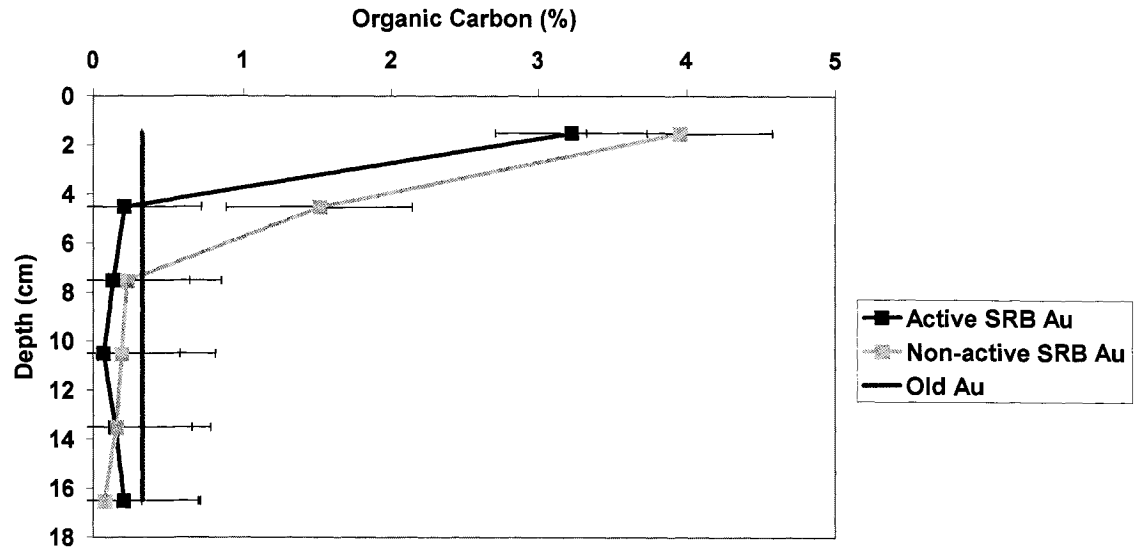

Figure 23. Methylmercury concentration in the solid phase of the Active SRB Au and Non-active SRB Au column at the end of the experiment and initial concentration in the Old Au tailings (a) and % organic carbon in the solid phase of the Active SRB Au and Non-active SRB Au column at the end of the experiment and original concentration in the Old Au tailings (b).

4.8 Relationship between Methylmercury production and other physico-chemical parameters in the Cu-Zn and Au columns.

The production of MeHg in the aqueous phase and in the sediments of all Cu-Zn and Au columns was compared to various measured chemical parameters in order to determine if Hg methylation was dependent on specific conditions.

4.8.1 Relationship with methylmercury

The results show that SRB abundance in the Cu-Zn and Au columns containing different treatments (i.e., warm and cold, low and high sulfate and low and high DOC) was not correlated to the concentration of soluble MeHg and total Hg (results not shown). There was also a lack of relationship between the abundance of MeHg and the concentration of organic material in the solid phase of the Cu-Zn tailings (Figure 24 a). On the other hand, there was a weak correlation between the abundance of organic material in the Au tailings and the levels of MeHg (Figure 24 a). For all Cu-Zn and Au tailings columns, no relationship was however observed between MeHg and soluble DOC (Figure 24 b).

The results also indicate the absence of a relationship between soluble MeHg and sulfate and sulfide levels in the Cu-Zn and Au columns (Figure 25 a and b). On the other hand, there was a clear correlation between the abundances of soluble Hg and MeHg in the water column and between total Hg and MeHg in the solid fraction of the columns containing Au tailings when the outliers are taken into account (Figure 26 a and b). With respect to the Cu-Zn columns, total soluble and solid Hg was not related to the concentration of MeHg in the soluble and solid fractions (Figure 26 a and b).

a)

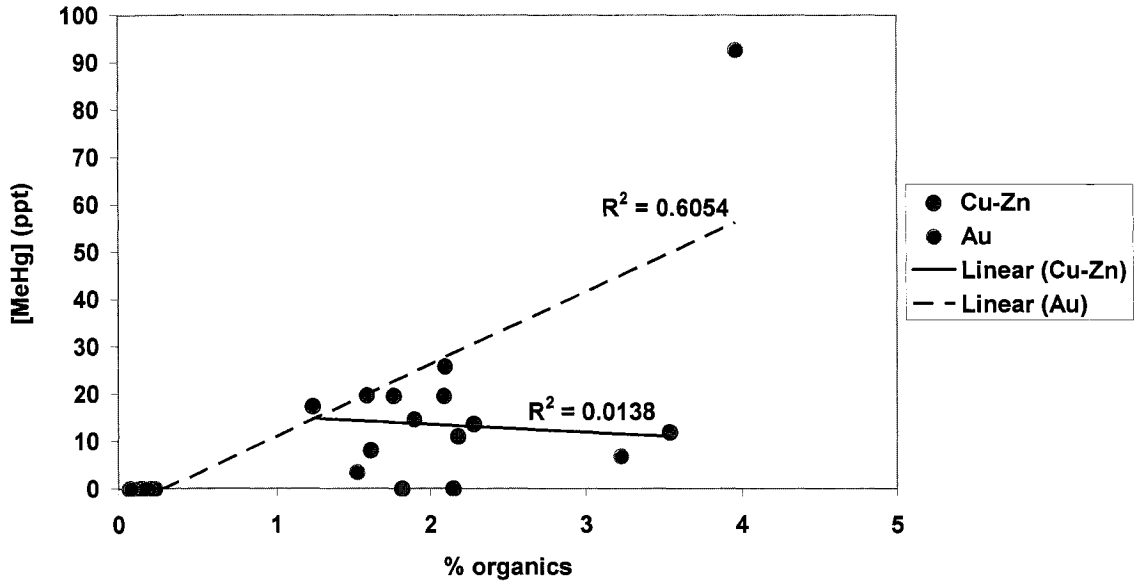

b)

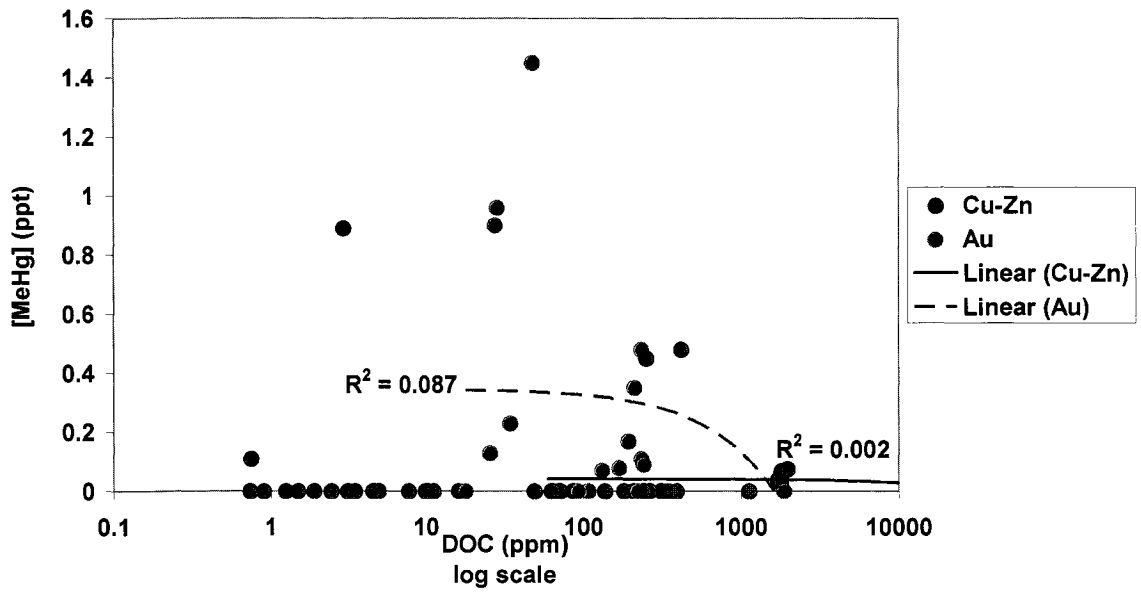

Figure 24. Relationship between solid methylmercury and % organics in the solids phase in all the Cu-Zn and Au columns (a) and soluble methylmercury and DOC concentrations in all the Cu-Zn and Au columns (b).

a)

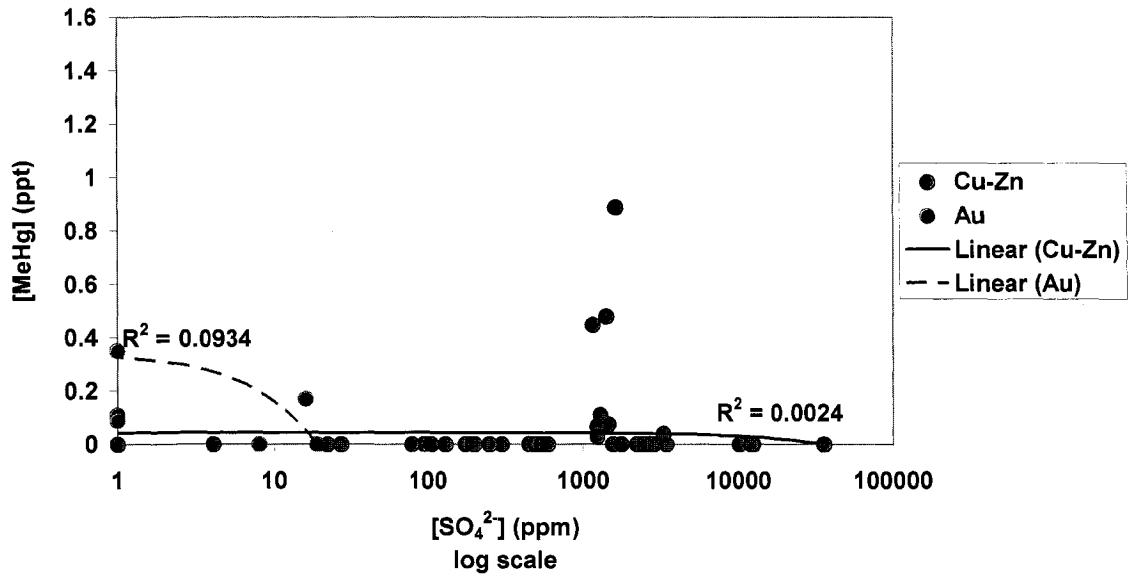

b)

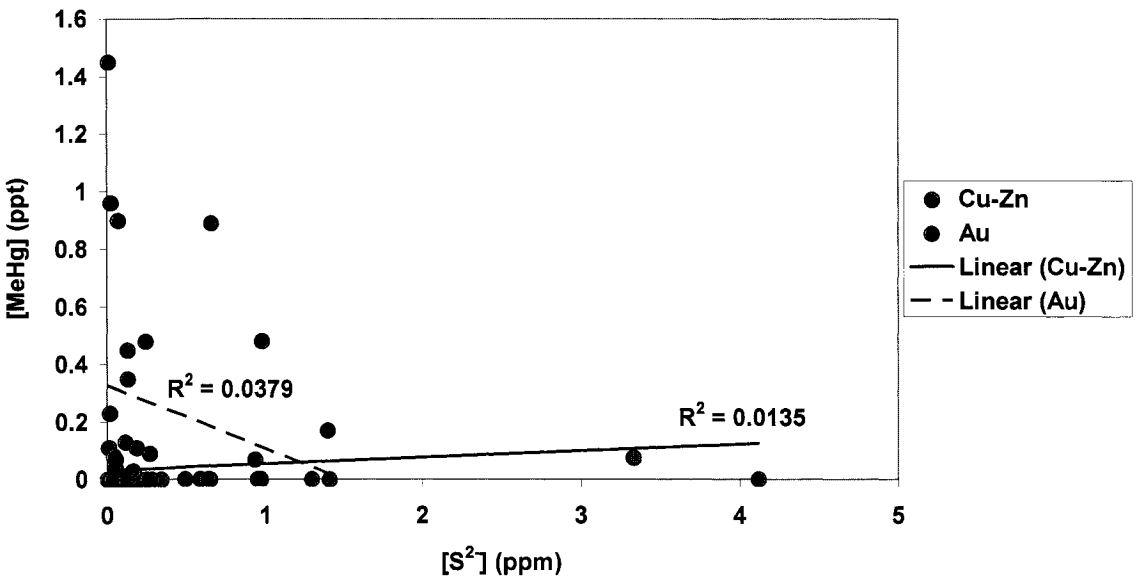

Figure 25. Relationship between soluble methylmercury and Sulfate concentrations in all the Cu-Zn and Au columns (a), and soluble methylmercury and Sulfide concentrations in all the Cu-Zn and Au columns (b).

a)

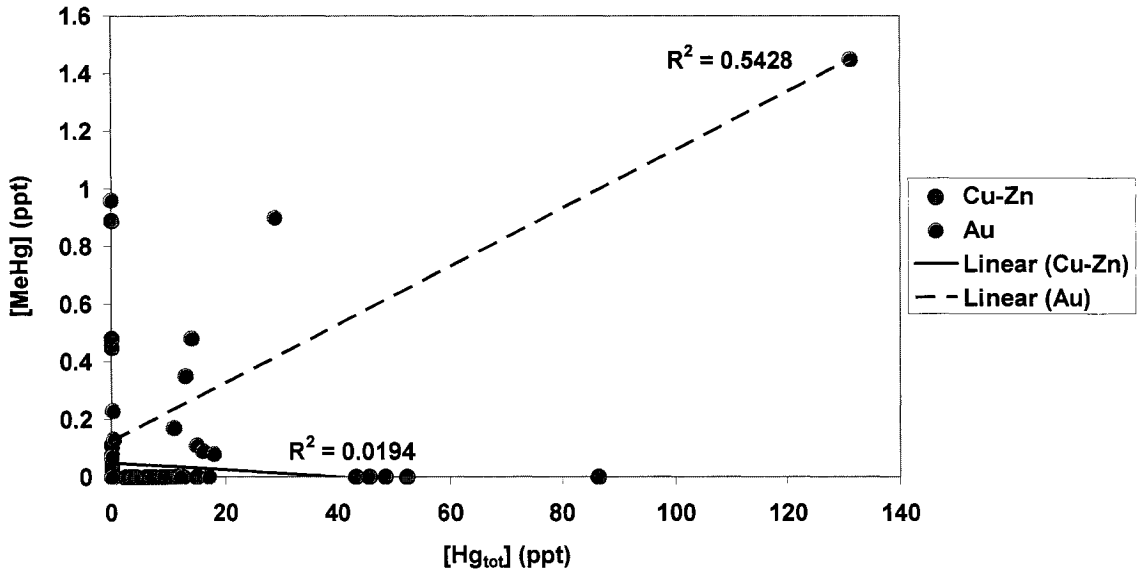

b)

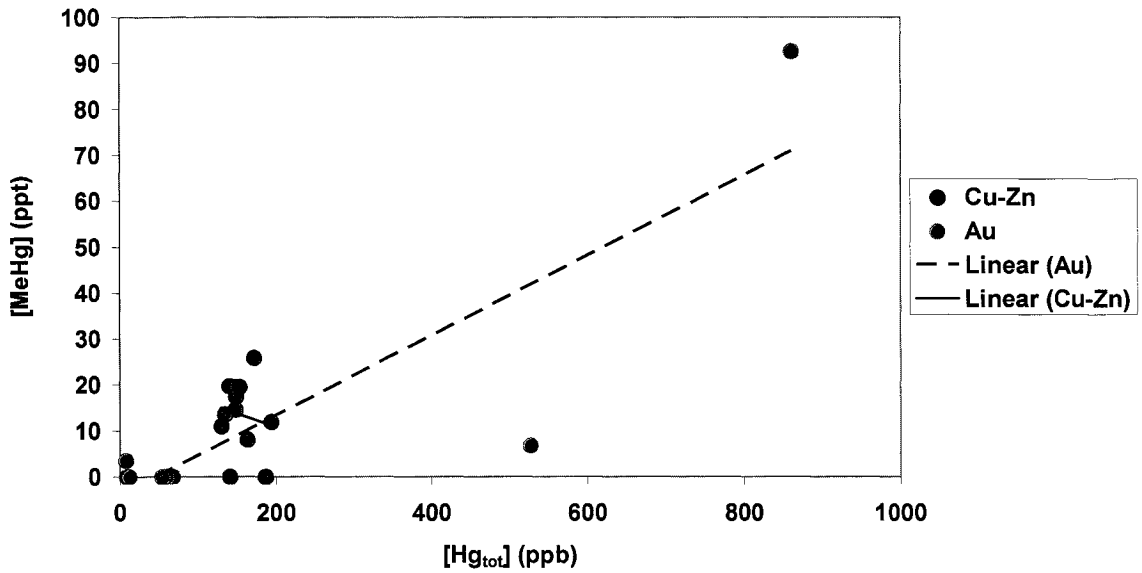

Figure 26. Relationship between soluble methylmercury and soluble total Hg concentrations (a), and solid Methylmercury concentrations and solid total Hg concentrations in the Warm Active SRB Cu-Zn and Non-active SRB Cu-Zn columns combined, and the Active SRB Au and Non-active SRB Au columns combined (b).

5. Discussion

5.1 Role of sulfate-reducing bacteria in MeHg formation in Cu-Zn and Au tailings

Several studies have shown a strong link between sulfate-reducing bacteria and Hg methylation (Compeau and Bartha, 1985, Gilmour et al., 1992; Pak and Bartha, 1998; Morel et al., 1998). In pure cultures, SRB can methylate Hg, but in natural sediments, the presence of mixed bacterial cultures, abiotic methylation pathways, along with demethylation processes make the role of SRB less clear (Morel et al., 1998; Warner et al., 2003). In order to assess the importance of SRB in MeHg formation in Cu-Zn and Au tailings, Na-molybdate was added to the mine tailings in order to stop microbial sulfate reduction and compare MeHg formation between active and non active SRB columns.

The results indicate that soluble MeHg was released to the overlying water in both the Active and Non-active SRB Cu-Zn and Au tailings (Figures 7 b and 21 b) and also accumulated in the solid phase (Figures 9 a and 23 a). These results imply that either the SRB populations were not completely inhibited in the Non-active SRB columns or that other biotic and abiotic factors were involved in Hg methylation. SRB populations were present in the Non-active SRB Cu-Zn and Au tailings, but they did not grow over the course of the experiment, unlike the SRB populations in the active columns (Figures 7 c and 21 c). This indicates that Na-molybdate inhibited the activity of SRB activity, as shown in other studies (Warner et al., 2003; Wendt-Potthoff et al., 2002). There was however a small release of S^{2-} from the tailings over time in both inhibited SRB columns (Figures 6 a and 20 a) which could have originated from the activity of some active SRB populations or from iron sulfide mineral dissolution. Saturation indices (results not shown) indicated that in the Non-active SRB Cu-Zn columns, the aqueous phase above

the sediments was slightly under-saturated with respect to amorphous FeS and mackinawite, which could explain the release of S^{2-} in solution. On the other hand, the solution was slightly saturated with respect to amorphous FeS and mackinawite in the Non-active SRB Au tailings, suggesting that some SRB could have been active despite the presence of molybdate. The release of S^{2-} from the Au inhibited tailings column could be from other metal sulfides in the tailings, such as arsenopyrite (a common sulfide associated with Au ore). However, Arsenic (As) concentrations were not determined in the present study, which prevents the calculation of the saturation indice of this specific mineral. Acid volatile sulfide (AVS) concentrations can be used to infer the formation of biogenic iron sulfides, as a result of microbial sulfate reduction (Morse et al., 1987). In sulfide-rich tailings, the AVS extraction protocol is however not selective and Pyrrhotite, a common minor iron sulfide mineral in mine tailings, can be extracted along with amorphous FeS and mackinawite, rendering the results difficult to interpret (Figures 8 a and 22 a) (Praharaj and Fortin, 2004a). As a result, the possibility that some SRB were active in the Au column cannot be ruled out completely. However, the use of 20 mM of Na-molybdate in this study exceeded the concentration generally used in other studies, i.e., 5 or 10 mM (Warner et al. (2003), making molybdate an abundant inhibitor. Molybdate is very specific because of its chemical similarity to sulfate, it is designed to inhibit adenosine triphosphate sulfurylase, the first enzyme in the sulfate-reducing pathway (Richard et al., 1981). Given the high concentration used in this study, it is believed that molybdate inhibited all SRB in the tailings.

Assuming that SRB populations were indeed inhibited in the Non-active Cu-Zn and Au tailings columns, then the production of MeHg (Figures 7 b, 9 a, 21 b and 22 a) in the same columns was either the result of other biotic or abiotic pathways. According

to Warner et al. (2003), a lack of microbial sulfate reduction does not necessarly preclude Hg methylation. In fact, these authors showed that MeHg formation occurred in riverine sediments where iron oxides were the dominant terminal electron acceptor, suggesting that iron-reducing bacteria could be involved in MeHg formation. However, the same study also indicated that in wetland sediments where microbial iron reduction was also an important redox process, Hg methylation was suppressed. The exact mechanism of Hg methylation under iron-reducing conditions is not known (Warner et al., 2003), but it might be representative due to another direct or indirect biotic process in natural sediments. In the inhibited SRB Cu-Zn and Au columns, the activity of iron-reducing bacteria was not assessed, but interestingly, the absence of active SRB populations led to the release of significant soluble Fe in both the Cu-Zn and Au columns (Figures 6 b and 20 b) when compared to the active SRB columns. In addition, DOC was consumed in the absence of active SRB populations (Figures 6 c and 20 c), which indicates that bacteria, other than SRB, were active in the tailings columns. In natural Cu-Zn tailings, iron-reducing bacteria have been recovered and can be as abundant as SRB populations (D. Fortin, pers. communication). In addition, Rioux (2004) showed that in laboratory Cu-Zn tailings batch systems where SRB activity was inhibited, iron-reducing bacteria were active and capable of reducing Fe(III) to Fe(II) in the presence of various electron donors, because they were not competing with SRB for available electron donors. Such findings indicate that iron-reducing bacteria could have indeed been active when microbial sulfate reduction was inhibited in the columns and that they might have been involved in MeHg formation. The other possibility is that MeHg sorbed onto iron-oxides was released during the microbial reduction of iron oxides, which implies that Hg was methylated prior to its sorption. At the present time, it is impossible to decipher between the two

processes (Regnell et al., 2001). These findings certainly warrant more research in order to really assess the role of iron-reducers in MeHg formation.

In the columns where SRB were not inhibited, MeHg was produced, but not necessary at a greater rate than in the non-active systems. This indicates that despite the fact that SRB are considered important Hg methylators in the environment, they do not significantly enhance MeHg formation in the mine tailings. Statistical analyses indicated that the MeHg values reported for the soluble and solid phases were often different between the active and not active systems, but not necessary greater, with the exception of the Active SRB Au tailings (Figure 21 b). In addition, no correlation could be found between the abundance of MeHg and the SRB populations (results not shown). This is in agreement with the results of Macalady et al. (2000), who showed that no relationship existed between MeHg and microbial diversity. Overall, the results from this study strongly indicate that Hg methylation in mine tailings is the result of complex biotic mechanisms, likely involving SRB and iron reducing bacteria, and possibly abiotic processes. Biotic methylation can also be carried out by certain methanogens (Bak and Bartha, 1998; Warner et al., 2003), but under the redox conditions prevailing in the Cu-Zn and Au columns (Figures 5 b and 19 b), it is unlikely that these strictly anaerobic bacteria were active because the columns were not reducing enough to support methanogenic activity. In addition, methanogens would not have been able to compete with iron reducing bacteria for acetate (Roden and Wetzel, 2003).

Abiotic Hg methylation in the systems studied here is also a possibility. According to Weber (1993), humic acids are the most suitable and significant Hg methylator in natural aquatic environments. In addition, formation of MeHg was also

reported under laboratory conditions when mercuric acetate was exposed to UV light (Akagi et al., 1973), and in rainwater, whereby oxidized Hg and small organic molecules, like acetic acid, react together to produce methyl mercury (Gardfeldt et al., 2003). The presence of humic acids in the Cu-Zn is not possible because the tailings were taken directly from the discharge area at the Kidd Metallurgical site. The presence of humic acids in the old Au tailings is on the other hand possible, but their abundance was not assessed in this study. With respect to the role of acetate, it could represent a methylation pathway since acetate was added to the columns, but the abiotic oxidation of acetate was not monitored in this study. Overall, abiotic methylation might be possible in the tailings, but given the low levels of organic material in the tailings (Figures 9 b and 23 b), it might not have played a significant role, as suggested by Loseto et al. (2004), for Arctic sediments low in organic carbon. True abiotic systems (containing autoclaved tailings or containing Na-azide to kill all bacteria) would be needed to fully ascertain the importance of abiotic Hg methylation with respect to biotic methylation in Cu-Zn and Au tailings.

It is also important to point out that MeHg concentrations measured in any sample represents the balance of the rates of methylation and demethylation (Harmon et al., 2004 and references therein). Demethylation processes are known to occur as a result of biotic reactions driven by sulfidogenic and methanogenic bacteria and abiotic processes (Warner, et al., 2003; Pak and Bartha, 1998; Oremland et al., 1991). Demethylation rates were not measured in the present study, but given the presence of sulfate reducing-bacteria, it can be assumed that it occurred in the columns where SRB populations were active (Warner et al., 2003). The relative importance of demethylation with respect to methylation is however not known.

Finally, the results reported here do not corroborate the first hypothesis stating that tailings containing inhibited SRB populations should not contain MeHg, if SRB are entirely responsible for Hg methylation. As explained above, other microbial populations, beside SRB, are likely to be responsible for MeHg formation in the Cu-Zn and Au tailings, along with potential abiotic methylation processes and demethylation processes.

5.2 Role of temperature on sulfate-reducing bacteria activity and MeHg formation in Cu-Zn tailings

Temperature is known to slow down microbial activity (Grossman and Desrocher, 2001). In mine tailings, microbial sulfate reduction generally decrease during the cold winter months when compared to summer months (Karnachuck et al., 2005; Praharaj and Fortin, 2004 b). On the other hand, Fortin et al. (2000b) reported that SRB populations increased in the winter in the sediments of a constructed wetland. In addition, Knoblauch et al. (1999) showed that the activity of SRB in Arctic sediments was not affected by permanently cold temperatures. According to Koretsky et al (2003), sulfate reduction rates in saltmarsh sediments vary with seasonal changes of temperature and are greater in the warm summer months than in the winter. On the other hand, iron-reducing bacteria populations in the same sediments are inhibited in the summer because of the high rate of sulfide production. Koretsky et al. also showed that the inhibition of SRB in the sediments under various temperatures was the only factor capable of increasing iron-reducing bacteria populations. The above studies therefore indicate that temperature

alone might not be a strong growth inhibitor for bacteria, but rather the competition between the various groups of bacteria for available electron donors.

The effect of temperature on MeHg formation in Cu-Zn tailings columns containing active SRB was tested, based on the promising results of a previous study on high arctic wetland sediments which had shown MeHg production in sediments incubated at low temperatures (Loseto et al., 2004). According to the results presented in this study, SRB activity was not affected by the cold temperature in the Cu-Zn tailings because SRB populations in both the Warm and Cold active columns were similar (Figure 12 c). In addition, DOC was consumed at a similar rate in both systems (Figure 11 c), which suggests that microbial activity was not inhibited by cold temperature, as shown by some previous studies (Fortin et al., 2000b; Knoblauch et al., 1999). The most interesting result is that MeHg was released into solution in the cold system after the column was frozen by accident and then thawed (at 70 days; Figure 12 b). The effect of freezing and thawing on Hg methylation in Cu-Zn tailings was further investigated (Wood, 2004) and the results showed that the concentration of soluble MeHg in the tailings kept frozen (at -12 °C) for 1 to 3 weeks and then thawed was greater than the levels measured in the systems kept at room temperature (i.e., 22 °C), which is in agreement with the results presented here (Figure 12 b). This has huge implications for Canadian mining environments because they are constantly undergoing freezing and thawing during the spring season, and could be releasing large pulses of MeHg into the environment. The exact mechanism responsible for MeHg release into solution is not known, but it is clear that the freezing and thawing effect was not limited to MeHg, because higher levels of sulfate (Figure 10 c) and soluble Ca (Appendix A), along with lower concentrations of soluble K were also observed after thawing (Appendix A). It is known that temperature

affects solubility (Stumm and Morgan, 1996). However, solubility calculations performed at 0 °C (T. Al pers. comm.) indicated that decreasing temperature should decrease the solubility of gypsum and therefore, lower the release of calcium and sulfate in the columns, which is the opposite trend of what was observed in the columns. At the present time, the exact mechanism responsible for MeHg release into solution after thawing events is not known, but it has serious implications for natural tailings impoundments in temperate regions which partially freeze in the winter and thaw in the spring. The only hypothesis that can be put forward at the present time is that freeze out weakens the bonds of sorbed MeHg onto the tailings particles and that it is released into solution during thawing. It is clear that more research is needed to investigate the mechanisms behind MeHg formation and release in frozen tailings, but it is beyond the scope of this study.

The results obtained on the effect of temperature are not consistent with the hypothesis which states that cold temperature should slow down the metabolic activity of SRB and therefore slow down the formation of MeHg whereas high temperature should enhance SRB activity and promote Hg methylation. Under both temperatures, SRB were active, but the release of soluble MeHg in the cold system occurred after thawing.

5.3 Role of organic carbon availability on MeHg formation in Cu-Zn and Au tailings

Under anaerobic conditions, the addition of suitable electron donors should enhance the activity of bacteria capable of oxidizing the organic substrates in the presence of available electron donors (Kusel and Dorsch, 2000). In the Cu-Zn columns, it was hypothesized that the addition of ample electron donors (up to 35 000 ppm) should

favor SRB activity since sulfate was the dominant electron acceptor (i.e., it was present in the growth medium added to the columns) and promote MeHg formation. The results indicate that the addition of large concentrations of electron donors did indeed favor SRB growth when compared to Cu-Zn columns where no organic carbon was added (Figure 18 c). The columns labeled as "low DOC" contained no added electron donors, with the exception of the dissolved organic carbon (0.3 ppm) originally present in the Cu-Zn tailings slurry (Table 2). Despite the difference in DOC, the concentration of soluble MeHg in both the High and Low DOC Cu-Zn columns was statistically similar (Table 11), indicating that increased SRB activity did not promote Hg methylation. To our knowledge, the effect of organic carbon addition on Hg methylation has never been reported in mine tailings and as a result, it is difficult to compare our results to other studies. We can only speculate that the increased SRB activity led to a built-up of dissolved sulfide in the column (Figure 17 a), which reacted with soluble Hg to form Hg sulfide precipitates and prevented MeHg formation (Regnell et al., 2001). The lack of soluble total Hg in the High DOC column (Figure 18 a) supports this assumption.

The lack of electron donors in the Cu-Zn column did however trigger the release of soluble Fe (Figure 17 b) and lowered the pH (Figure 16 a). In addition, low DOC concentrations led to the development of more oxic conditions in the columns (Figure 16 b). From these observations, it appears that the absence of available organic electron donors promoted to the development of oxidizing conditions in the column, which triggered metal sulfide oxidation, as indicated by the low pH conditions and the release of soluble Fe. The development of acidic and oxic conditions did not kill the SRB populations, because they were recovered from the columns (Figure 18 c). Their presence

is not surprising because SRB in mine tailings are able to survive under acidic and oxic conditions (Praharaj and Fortin, 2004 b; Fortin et al, 2002; 2000).

Several studies have reported a relationship between organic carbon (DOC and humic material) and MeHg because of the strong affinity of the latter for binding sites on organic material (Hintelmann et al., 1997; Macalady et al., 2000; Regnell et al., 2001; Karlsson et al., 2003). The results for all Cu-Zn tailings columns (i.e., all conditions tested in this study) showed no relationship between DOC and MeHg and solid organic material (LOI) and MeHg (Figure 24). The lack of correlation could be caused by the preferred binding of MeHg to sulfide complexes (Regnell et al., 2001). On the other hand, there was a correlation between MeHg and organic material in the solid fraction of the Au tailings (Figure 24 a). Given the fact that the Au tailings were old, they might have contained a different type of natural organic material (from plants debris growing on the tailings) which preferentially bound MeHg over dissolved sulfide complexes. The organic carbon material in both the Cu-Zn and Au tailings was however not characterized.

The results therefore contradict the original hypothesis and indicate that organic carbon availability does enhance SRB activity, but not MeHg formation. This further supports the view that biotic factors, other than SRB activity, and abiotic processes are responsible for MeHg formation in mine tailings.

5.4 Role of sulfate availability on MeHg formation in Cu-Zn and Au tailings

The abundance of sulfate in natural environments is often the limiting factor affecting the growth and activity of SRB populations (Postgate, 1984). In the absence of

sulfate, some SRB can however use alternate electron acceptors, such as iron oxides (Coleman et al., 1993). It is also known that SRB grown in pure culture will not methylate mercury in the absence of sulfate (King et al. 2002). As a result, it is expected that MeHg formation (resulting from SRB activity) should be a function of the availability of sulfate in a sample. In order to test the effect of sulfate availability, two Cu-Zn tailings columns were set up, one with no sulfate added (but still containing very low sulfate levels from the initial Cu-Zn slurry and sulfate-rich minerals) and one with about 10 000 ppm of sulfate, which is characteristic of acid mine drainage conditions (Fortin et al., 2000; 2002).

It has been reported that the addition of sulfate to wetland sediments can increase the formation of soluble MeHg, but not its accumulation in sediments, as shown by Harmon et al. (2004). Their results are however in contrast to what was observed in the Cu-Zn tailings columns containing high levels of sulfate. Results indicate that soluble MeHg was not produced in either the low or high sulfate Cu-Zn columns (Figure 15 b). The absence of MeHg under the concentrations used in this study is however compatible with previous studies which showed that MeHg formation is favored when sulfate levels range between 20 and 50 ppm (Morel et al., 1998). The concentration in the high sulfate Cu-Zn column (Figure 13 c) far exceeded the concentration range favorable to MeHg formation, whereas the low sulfate column contained no added sulfate, which is below the range reported by Morel et al. (1998). Interestingly, the absence of added sulfate in the tailings column did not hinder SRB growth (Figure 15 c), in fact SRB populations in the absence of added sulfate increased over the course of the experiment, but did remain lower than the populations in the high sulfate column (Table 10). SRB growth in both columns was also accompanied by DOC consumption (Figure 14 c), suggesting that

microbial activity was happening. The presence of large concentrations of sulfate generated high levels of sulfide in the water column (Figure 14 a), especially near the end of the experiment. Some sulfide was also produced in the column containing no added sulfate, which is compatible with the fact that SRB populations increased in the system, therefore indicating that they were active. The source of sulfate in the low sulfate column likely included some of the sulfate originally present in the fresh Cu-Zn slurry, but it is also possible that SRB were able to use gypsum, a mineral present it the Kidd Cu-Zn tailings (Al et al., 1994), as a source of sulfate, as shown by Karnachuck et al. (2002).

The present results indicate that sulfate concentrations (and sulfide concentrations) do affect MeHg formation, possibly as a result of complexation and precipitation reactions between sulfide species and soluble Hg. Active SRB populations produce soluble sulfide which can sequester available Hg into HgS precipitates, and therefore lower MeHg formation. MeHg formation appears to be dependent on specific sulfide and Hg concentrations in the sample, which can greatly vary with the activity of SRB, which in return depends on the availability of electron donor and electron acceptor.

The results from this study are somehow in agreement with the hypothesis stating that high sulfate levels in the presence of active SRB populations should promote the formation of large levels of soluble sulfide which will prevent Hg methylation as a result of HgS formation. However, the results indicate that under limited sulfate levels, Hg methylation did not occur either, indicating that Hg transformation is driven by complex reactions, involving more that sulfate availability.

5.5 Role of tailings mineralogy on MeHg formation

Cu-Zn and Au tailings differ in terms of mineralogical composition and total Hg concentrations. Base-metal mine tailings, such as the Cu-Zn tailings used in this study, generally contain large quantities of pyrite (up to 25% on a weight basis (Al et al., 1994)), whereas Au tailings, such as the ones from Nova Scotia, contain lesser amounts of pyrite (Fortin et al., 2000). In addition, Hg levels in Cu-Zn tailings generally originate from the ore sulfides (in the case of the Kidd tailings, Hg is present as micro-inclusions in pyrite (M.Hannington, pers. comm.)), whereas Hg in Au tailings often originates from the ore extraction process (Boudou et al. 2005). The analysis of the original tailings used in this study indicated that the Cu-Zn tailings contained more total Hg in the solid fraction than the old Au tailings (Tables 4 and 7), but there was more soluble Hg in the Au tailings than in the Cu-Zn tailings (Tables 2 and 5). There was no methylmercury in the original tailings.

During the course of the experiment, Hg was remobilized within the solid fraction of both the Cu-Zn and Au tailings (Figures 8 b and 22 b), more specifically, Hg accumulated near the surface of both columns in the presence of active and non-active SRB populations. MeHg accumulation near the surface corresponded to organic carbon accumulation at the same depth (Figures 23 a and b). There was a weak relationship between soluble Hg and MeHg (Figure 26 a), solid total Hg and MeHg (Figure 26 b) and solid MeHg and organic carbon (Figure 24 a) in the Au tailings, but not in the Cu-Zn tailings. In the Au tailings, percent methylmercury in the soluble fraction was 1%, whereas it was 10% in the solid fraction. These ratios are representative of other environments, including soils (Harmon et al., 2004) and wetlands (Regnell and Hammar,

2004). Recent studies have proposed that methylation increased the mobility of Hg (Regnell and Hammar, 2004; St-Louis et al., 2004). According to these authors, this would explain why Hg levels are poorly correlated to sulfide and dissolved organic material. Such relationship was not investigated in this study, but it is clear that in the Au tailings there was a larger production and mobility of MeHg and Hg in the sediments when compared to the Cu-Zn tailings, despite the fact that original total Hg concentration was greater in the Cu-Zn tailings. As proposed by Regnell and Hammar (2004), it is possible that Hg bound to organic matter in the Au tailings is released back to the porewater more easily than in the Cu-Zn tailings. This could be related to the fact that organic material in the Au tailings differs from the one in the Cu-Zn tailings from a chemical point of view. Au tailings are old and likely contain organic material from plant debris whereas Cu-Zn tailings are fresh from the metallurgical site and have never been exposed to the environment. This aspect of the research remains purely hypothetical but it certainly warrants more research on the relationship between Hg and MeHg and organic material in mine tailings.

The results from this study are not in agreement with the hypothesis stating that Au tailings should contain more Hg and potentially more MeHg than Cu-Zn tailings because of past ore extraction processes which used Hg amalgamation. It is true that more MeHg was present in the Au-tailings, but more Hg was originally present in the Cu-Zn tailings. It is believed that the difference in Hg cycling between the two types of tailings is related to the origin and structure of the organic material present within the tailings and not to mineralogical differences and ore extraction techniques.

6. Conclusion

The results of this study indicate that Hg was methylated in the columns containing Cu-Zn and Au mine tailings, but MeHg levels were not significantly enhanced by the activity of sulfate-reducing bacteria (SRB). In all the systems tested in this study, MeHg net production was the result of microbial activity and abiotic reactions. The results indicate that bacteria, other than SRB, could play an important role in the methylation of mercury in mine tailings. Geochemical evidence from the present study suggests that iron-reducing bacteria might be involved in MeHg formation. Such findings warrants more research on the potential role and importance of iron reducers in mine tailings and other types of environments. Abiotic methylation pathways also need to be further investigated, namely the role of acetate, a common electron donor in mine tailings.

Among the factors tested in this study, it was shown that temperature did not significantly affect SRB growth in the Cu-Zn mine tailings. However, the accidental freezing and thawing of one of the columns led to the production of MeHg in the aqueous phase, indicating that methylation did occur during the process. The exact mechanism responsible for MeHg formation remains unknown, but it might be important in natural mine tailings impoundment subjected to freezing and drying episodes on a regular basis. These unexpected results also warrant additional research on the effect of temperature on MeHg formation.

The results also showed that increased DOC and sulfate concentrations stimulated SRB activity, but not necessary by the MeHg formation in Cu-Zn tailings. The production of sulfides, as a result of microbial sulfate reduction, likely hindered Hg methylation.

There was however a correlation between the abundance of MeHg in the Au tailings and the quantity of organic material, but not in the Cu-Zn systems. The difference in behavior between the two types of tailings is likely due to the fact that fresh Cu-Zn tailings contained no naturally occurring organic carbon, whereas the old Au tailings were composed of organic material originating from vegetation. The association MeHg and organic carbon results from the affinity of MeHg for specific binding sites on organic material.

The tailings mineralogy had a direct effect on the amount of methyl mercury released into the overlying water and in the amount produced in the solid phase. Both the Cu-Zn and the Au tailings produced MeHg in the solid phase but the Au tailings released more MeHg into the aqueous phase, even though the Cu-Zn tailings had more Hg at the beginning of the experiment in the solid phase. The greater mobility of MeHg in Au tailings was the result of the *in situ* chemical conditions of the tailings (i.e., abundance of sulfide minerals, type of organic material) and possibly of the microbial diversity.

Ultimately, this study reinforces the fact that mercury can be and is being methylated in Cu-Zn and Au mine tailings. The processes involved in the net methylation rate are complex and not always directly linked to SRB activity, as previously thought. The implications of this study are that there might not be a need to worry about the role of SRB in natural Cu-Zn and Au tailings in Hg methylation, but at the same time, the results suggest that other bacteria, which are naturally occurring in the tailings, might be the important methylators. Since both microbial iron and sulfate reduction processes are being considered as promising bioremediation tools for mining sites, more research is obviously needed.

7. References

Adam, D., and Edyvean, R.G.J.,
(1997) The Use of Sulphate Reducing Bacteria to Assist the Removal of Heavy Metals from Acidic Mine Drainage. *International Biodeterioration and Biodegradation.* **37** (3-4), 241.

Al, T.A., Blowes, D.W., and Jambor, J.L.,
(1994) A Geochemical study of the main tailings impoundment at the Falconbridge Limited, Kidd Creek Division Metallurgical site, Timmins, Ontario. *Mineralogical Association of Canada Short Course Handbook on Environmental Geochemistry of Sulphide Oxidation.* (J.L. Jambor and D.W. Blowes, *editors*). **22**, 334-364.

Akagi, H., and Takabatake, E.,
(1973) Photochemical formation of Methylmercury compounds from mercuric acetate. *Chemosphere*. **3**, 131 –133.

Babiarz, C.L., Hurley, J.P., Benoit, J.M., Shafer, M.M., Andren, A.W., and Webb, D.A.,
(1998) Seasonal Influences on partitioning and transport of total and Methylmercury in rivers from contrasting watersheds. *Biogeochemistry.* **41**, 237-257.

Boening, D.W.,
(2000) Ecological effects, transport, and fate of mercury: a general review. *Chemosphere.* **40**, 1335-1351.

Boudou, A., Maury-Brachet, R., Coquery, M., Durrieu, G., Cossa, D.,
(2005) Synergic effect of gold mining and damming on mercury contamination in fish. *Environ. Sci. Technol.* **39**, 2448-2454.

Cai, Y., Jaffé, R., Alli, A., and R.D., Jones.,
(1996) Determination of organomercury compounds in aqueous samples by capillary gas chromatography-atomic fluorescence spectrometry following solid-phase extraction. *Analytica Chimica Acta.* **334**, 251-259.

Cochran, W.G.,
(1950) Estimation of Bacterial Densities by means of most probable number. *Biometrics*. **6**, 105-116.

Coleman, M.L., Hedrick, D.B., Lovley, D.R., White, D.C., Pye, K.,
(1993) Reduction of Fe(III) in Sediments by Sulphate-Reducing Bacteria. *Nature.* **361**, 436-344.

Compeau, G.C., and Bartha, R.,
(1985). "Sulfate-reducing bacteria" principal methylators of mercury in anoxic estuarine sediments. *Appl. Environ. Microbiol.* **50**, 498-502.

Cline, J.D.,
(1969). Spectrophotometric determination of hydrogen sulfide in natural waters. *Limnol. Oceanogr.* **14**, 454-458.

Drever, J.I.,
(1997) Geochemistry of Natural waters. Prentice Hall. 3rd Edition.

Environment Canada
(2004) Mercury website *http://www.ec.gc.ca/mercury/en/index.cfm*

Feasby, G., and Jones, R.K.,
(1994) Report of Results of a Workshop on Mine Reclamation, Toronto, Ontario March **10-11**.

Fortin, D., Rioux, J.P., and Roy, M.,
(2002) Geochemistry of Iron and Sulfur in the zone of microbial sulfate reduction in mine tailings. *Water, Air and Soil Pollution,* **2**, 37-56.

Fortin, D., Roy, M., Rioux, J.P., and Thibault, P.J.,
(2000a) Occurrence of sulfate-reducing bacteria under a wide range of physico-chemical conditions in Su and Cu-Zn mine tailings. *FEMS microbiology Ecolo.,* **33**, 197-208.

Fortin, D., Goulet, R., and Roy, M.,
(2000b) The effect of seasonal variations of sulfate- reducing bacteria populations on Fe and S cycling in a constructed wetland. *Geomicrobiology J.*, **17**, 221-235.

Fortin, D., Davis, B., and Beveridge, T.J.,
(1996) Role of *Thiobacillus* and sulfate-reducing bacteria on Fe biocycling in oxic and acidic mine tailings. *FEMS Microbiol. Ecol.* **21**, 11-24.

Gardfeldt, K., Munthe, J., Stromberg, D., and Lindqvist, O.,
(2003) A kinetic study on the abiotic methylation of divalent mercury in the aqueous phase. The Science of the Total Environment. **304**, 127-136.

Gilmour, C.C., Riedel, G.S., Ederington, M.C., Bell, J.T., Benoit, J.M., Gill, G.A., and Stordal, M.C.,
(1998) Methylmercury concentrations and production rates across a trophic gradient in the northern Everglades. *Biogeochemistry.* **40**, 327-345.

Gilmour, C.C., Henry, E.A., and Mitchell, R.,
(1992) Sulfate stimulation of mercury methylation in freshwater sediments. *Enviro. Sci. Technol.* **26**, 2281-2287.

Gould, W. D., Bettered, G., and Lortie, L.,
(1994) The nature and role of micro-organisms in the tailings environment. *Mineralogical Association of Canada Short Course Handbook on Environmental Geochemistry of Sulphide Oxidation.* (J.L. Jambor and D.W. Blowes, *editors*). **22**, 185-199.

Government of Canada.
(1991) State of Canada's Environment. Ministry of Supply and Services, Ottawa.

Grossman, E.L., Desrocher, S.,
(2001) Microbial sulfur cycling in terrestrial subsurface environments. In: Fredrickson JK, Fletcher M editors. *Subsurface Microbiology and Biogeochemistry*, New York: Wiley-Liss. p. 219–248.

Hakanson, L.,
(1980) The quantitative impact of pH, bioproduction, and Hg-contamination on the Hg-content of fish (pike). *Environmental Pollution (Series B).* **1**, 285-304.

Harmon, S.M., King, J.K., Gladden, J.B., Chandler, G.T., and Newman, L.A.,
(2004) Methylmercury formation in a wetland mesocosm amended with sulfate. *Environ. Sci. Technol.* **38,** 650-656.

Hintelmann, H., Welbourn, P.M., and Evans, R.D.,
(1997) Measurement of complexation of methylmercury(II) compounds by freshwater humic substances using equilibrium dialysis. *Environ. Sci. Technol.* **31**: 489–495.

Ifill, C.,
(1999) The Isolation and Purification of sulphate-reducing bacteria from the colon of patients suffering from Ulcerative Colitis. University of Portsmouth, School of Pharmacy and Biomedical Science. BSc (Hons) Biomedical Science. 29 pages.

Jurjovec, J., Ptacek, C.J., Blowes, D.W., and Jambor, J.L.,
(2003) The effect of Natrojarosite addition to mine tailings. *Environmental Science and Technology.* **37**, 158-164.

Karlsson, T., and Skyllberg, U.,
(2003) Bonding of ppb levels of methyl mercury to reduce sulfur groups in soil organic matter. *Environ. Sci. Technol.* **37**, 4912-4918.

Karnachuck, O.V., Pimenov, N.V., Yusupov, S.K., Frank. Y.A., Kaksonen, A.H., Puhakka, J.A., Ivanov, M.V., Lindstrom, E.B. and Tuovinen, O.H.
(2005) Sulfate Reduction Potential in Sediments in the Norilsk Mining Area, Northern Siberia. *Geomicrobiol. J.*, **22**, 11-25.

Karnachuck, O.V., Kurochkina, S.Y., and Tuovinen, O.H.,
(2002) Growth of sulfate-reducing bacteria with solid-phase electron acceptors. *Appl Microbiol Biotechnol.*, **58**, 482–486.

King, J.K., Harmon, S.M., Fu, T.T., and Gladden, J.B.,
(2002) Mercury removal, methylmercury formation, and sulfate-reducing bacteria profiles in wetland mesocosms. *Chemosphere.* **46**, 859-870.

Knoblauch, C., Jorgensen, B.B., and Harder, J.,

(1999) Community size and metabolic rates of psychrophilic sulfate-reducing bacteria in Arctic marine sediments. *App. Environ. Microbiol.*, **65**, 4230-4233.

Kolmert, A., and Johnson, D.B.,
(2001) Remediation of acidic waste waters using immobilized, acidophilic sulfate-reducing bacteria. *Journal of Chemical Technology and Biotechnology*. **76**, 836-843.

Koretsky, C.M., Moore, C.M., Lowe, K.L., Meile, C., DiChristina, T.J. and Van Cappellen, P.
(2003) Seasonal oscillation of microbial iron and sulfate reduction in saltmarsh sediments (Sapelo Island, GA, USA). *Biogeochemistry*, **64**, 179-203.

Koschorreck, M., Wendt-Potthoff, K., and Geller, W.,
(2003) Microbial Sulfate Reduction at Low pH in Sediments of an Acidic Lake in Argentina. *Environ. Sci. Technol.* **37**, 1159-1162.

Ku, Y., Wu, M.H., and Shen, Y.S.,
(2002) Mercury removal from aqueous solutions by zinc cementation. *Waste Management*. **22**, 721-726.

Küsel, K., and Dorsch, T.,
(2000) Effect of supplemental electron donors on the microbial reduction of Fe(III), sulfate, and CO_2 in coal mining-impacted freshwater lake sediments. *Microbial Ecology*, **40**, 238-249.

Langer, C.S., Fitzgerald, W.F., Visscher, P.T., and Vandal, G.M.,
(2001) Biogeochemical cycling of methylmercury at Barn Island Salt Marsh, Stonington, CT, USA. *Wetlands Ecol. And Manag.* **9**, 295-310

Macalady, J.L., Mack, E.E., Nelson, D.C., and Scow, K.M.,
(2000). Sediment microbial community structure and mercury methylation in mercury-polluted Clear Lake, California. *Appl. Environ. Microbiol.*, **66**, 1479-1488.

MacKasey, W.O.,
(2000) Mining Watch Canada. WOM Geological Associates Inc. Sudbury,Ontario http://www.miningwatch.ca/publications/Mackasey_abandoned_mines.html

MacKenzie,T.G.,
(1907) Notes on the Mining Property of the Seal Harbour Mining Company. Transactions of the Mining Society of Nova Scotia. Graduate thesis from Dalhousie University. 63-81.

Malm, O.,
(1998) Gold Mining as a Source of Mercury exposure in the Brazilian Amazon. *Environ. Research, Sec A.* **77**, 73-78.

Mauro, J.B.N., Guimaraes, J.R.D., Hintelmann, H., Watras, C.J., Haack, E.A., and Coelho-Souza, S.A.,
(2002) Mercury methylation in macrophytes, periphyton, and water-comparitive studies with stable and radio-mercury additions. *Anal Bioanal Chem.* **374**, 983-989.

Morel, F.M.M., Kraepiel, A.M.L., and Amyot, M.,
(1998) The chemical cycling and bioaccumulation of mercury. *Annual Review of Ecological Systems.* **29**, 543-566.

Morse, J. W., Millero, F. J., Cornwell, J. C., and Rickard, D.,
(1987) The Chemistry of the hydrogen sulfide and iron sulfide systems in natural waters. *Earth Sci. Rev.* **24**, 1–42.

Nordstrom, D.K.,
(1977) Thermochemical redox equilibria of ZoBell's solution. *Geochim. Cosmochim. Acta.* **41**, 1835-1841.

Oremland, R.S., Culbertson, C.W., and Winfrey, M.R.,
(1991) Methylmercury decomposition in sediments and bacterial cultures: involvement of methanogens and sulfate reducers in oxidative demethylation. *Appl. Environ. Microbiol.* **57**, 130-137.

Pak, K-R., and Bartha, R.,
(1998) Mercury methylation and demethylation in anoxic lake sediments and by strictly anaerobic bacteria. *Appl. Environ. Microbiol.* **64,** 1013-1017.

Pirrone, N., Allegrini, I., Keeler, G.J., Nriagus, J.O., Rossmann, R., and Robbins, J.A.,
(1998) Historical atmospheric mercury emissions and depositions in North America compared to mercury accumulations in sedimentary records. *Atmospheric Environment.* **32**. 929-940.

Poissant, L.,
(2004) Mercury Processes: Fate from Southern and Northern Locations. *Ottawa Carleton Geoscience Center Seminar Series.* Presented at the University of Ottawa; March 25, 2004.

Pomeroy, L.R., and Wiebe, W.J.,
(2001) Temperature and substrates as interactive limiting factors for marine heterotrophic bacteria. Aquatic Microb. Ecol. **23**,187-204.

Postgate, J.R.
(1984) The Sulphate-reducing bacteria. 2nd edition. Cambridge University Press. Cambridge. 208 pages.

Praharaj, T., and Fortin, D.,
(2004a) Determination of acid volatile sulfides and chromium reducible sulfides in Cu-Zn and Au mine tailings. *Water, Air, and Soil Pollution.* 155. 35-50.

Praharaj, T., and Fortin, D.

(2004b) Indicators of bacterial sulfate reduction in acidic sulfide-rich mine tailings. *Geomicrobiology J.*, **21**, 457-467.

Regnell, O., Hammar, T., Helgée, A., and Troedsson, B.,
(2001) Effects of anoxia and sulfide on concentrations of total and methyl mercury in sediment and waterin two Hg-polluted lakes. *Can J. Fish Aquat. Sci.*, **58,** 506-517.

Regnell, O., and Hammar, T.,
(2004). Coupling of methyl and total mercury in a minerotrophic peat bog in southeastern Sweden. *Can. J. Fish. Aquat. Sci.*, **61**, 2014-2023.

Renzoni, A., Zino, F., and Franchi, E.,
(1998) Mercury levels along the food chain and risk for exposed populations. *Environmental Research.*, Section A. **77**, 68-72.

Rioux, J-P.,
(2004) Microbial activity of iron-reducing bacteria and sulfate-reducing bacteria isolated. M.Sc. Thesis, University of Ottawa, 75 pages.

Roach, A.G.,
(1937) The Seal Harbour Mill. *Transactions from the Mining Society of Nova Scotia.* **XL**. 263-277.

Roach, A.G.,
(1940) Cyanide treatment of Auriferous concentrate from Nova Scotian Ores. *Transactions from the Mining Society of Nova Scotia.* **XLIII**. 709-731.

Roden, E.E., and Wetzel, R.G.,
(2003) Competition between Fe(III)-reducing bacteria and methanogenic bacteria for acetate in iron-rich freshwater sediments. *Microb. Ecol.*, **45**, 252-25.

Samuels, M.L., and Witmer, J.A.,
(1999) Statistics for the Life Sciences. 2nd edition. Prentice Hall. New Jersey. 683 pages.

Sass, H., Cypionka, H., and Babenzien, H.D.,
(1997) Vertical distribution of sulfate-reducing bacteria at the oxic-anoxic interface in sediments of the oligotrophic Lake Stechlin. *Microbiology Ecology.* **22**, 245-255.

Sellers P., Kelly C.A., Rudd J.W.M.,
(2001) Fluxes of methylmercury to the water column of a drainage lake: The relative importance of internal and external sources. Limnol. Oceanogr. **46**(3) 623-631.

St-Louis, V.L., Rudd, J.W.M., Kelly, C.A., Bodaly, R.A., Paterson, M.J., Beaty, K.G., Hesslein, R.H., Heyes, A., and Majeski, A.R.,

(2004) The rise and fall of mercury methylation in an experimental reservoir. *Environ. Sci. Technol.*, **38**, 1348-1358.

Stumm, W., and Morgan, J.,

(1996) Aquatic chemistry equilibria and rates in natural waters. 4th Edition. John, Wiley & sons Inc. New York.

Tsukamoto, T. K., and Miller, G. C.,

(1999) Methanol as a carbon source for microbiological treatment of acid mine drainage. *Water Research*. **33**(6), 1365-1370.

Veiga, M., Baker, R.

(2004) Protocols for Environmental and Health Assessment of Mercury Released by Artisanal and Small-Scale Gold Miners. *Global Mercury Project UNIDO*. 170 pages.

Warner, K.A., Roden, E.E., and Bonzongo, J-C.,

(2003) Microbial mercury transformation in anoxic freshwater sediments under iron-reducing and other electron-accepting conditions. *Environ. Sci. Technol.* **37**, 2159-2165.

Waybrant, K. R., Blowes, D.W., and Ptacek, C.J.,

(1995). Selection of reactive mixtures for the prevention of acid mine drainage using porous reactive walls. *In: Sudbury '95, Mining and the Environment*, **3**, 945-953.

Weber, J.H.,

(1993) Review of possible paths for abiotic methylation of mercury (II) in the aquatic environment. *Chemosphere*, **26**, 2063-2077.

Wendt-Potthoff, K., Frömmichen, R., Herzsprung, P., and Koschorreck, M.,

(2002) Microbial Fe(III) reduction in acidic mining lake sediments after addition of an organic substrate and lime. *Water, Air, and Soil Pollution: Focus*, **2**, 81-96.

Wood, L-A.,

(2004) L'effet du gel et du dégel sur la méthylation du Hg de résidus miniers de Cu et de Zn. B. Sc. Thesis, University of Ottawa, 32 p.

Appendix A

A-1. Warm Active SRB Cu-Zn and the Non-active SRB Cu-Zn columns

Table A-1. Statistical results of Warm Active SRB Cu-Zn and Non-active SRB Cu-Zn aqueous ICP results.

	same	different
Ca	•	
K	•	
Mg	•	
Mn		•
Na		•
Fe (tot)		•

The amount of dissolved Ca originally present in both columns (T = 0) significantly dropped shortly after the beginning of the experiment and remained low until day 106 and then slightly increased near the end (Figure A-1 a). In addition, the concentration of Ca in the aqueous phase of both columns was very similar. On the other hand, dissolved K concentrations increased in both the Warm Active SRB and the Non-active SRB Cu-Zn columns over time (Figure A-1 b). Concentrations slightly varied over the course of the experiment and remained similar for both columns. There was also a small release of soluble Mg into solution in both columns, especially after day 28 (Figure A-1 c). The level of Mg in both systems was comparable. The same release trend was also observed for soluble Mn in both the Warm Active and the Non-active SRB Cu-Zn columns (Figure A-2 a), but the Non-active column has 3 times more Mn being released into solution. Soluble Na concentrations were very high in both the Warm Active SRB and the Non-active SRB Cu-Zn columns (Figure A-2 b), but there was a considerable amount of Na added to the matrix and the Non-active SRB column has a higher concentration because of the added Na-molybdate. Total iron concentrations in the aqueous phase of the two columns was very different (Figure A-2 c), the Warm Active SRB Cu-Zn column did not release any iron over the course of the experiment, whereas Fe levels increased in the non-active SRB Cu-Zn column.

a)

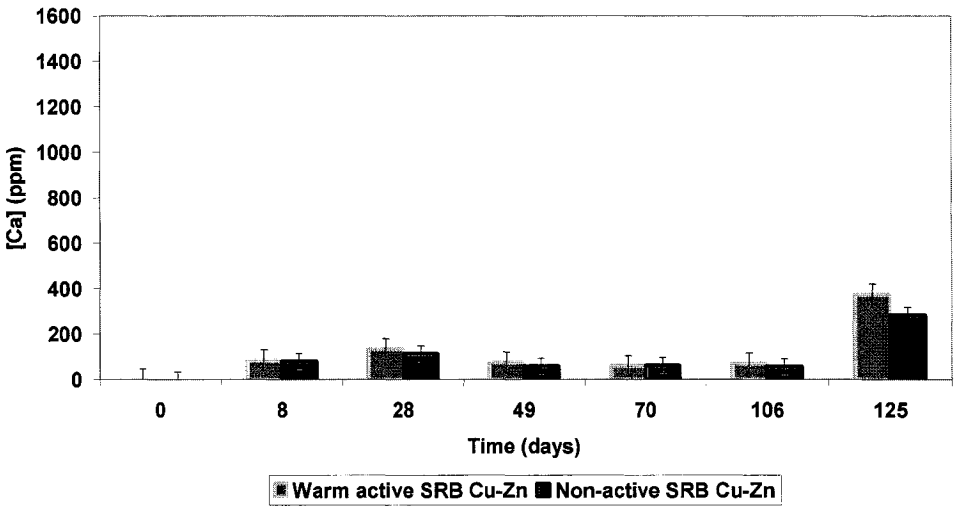

b)

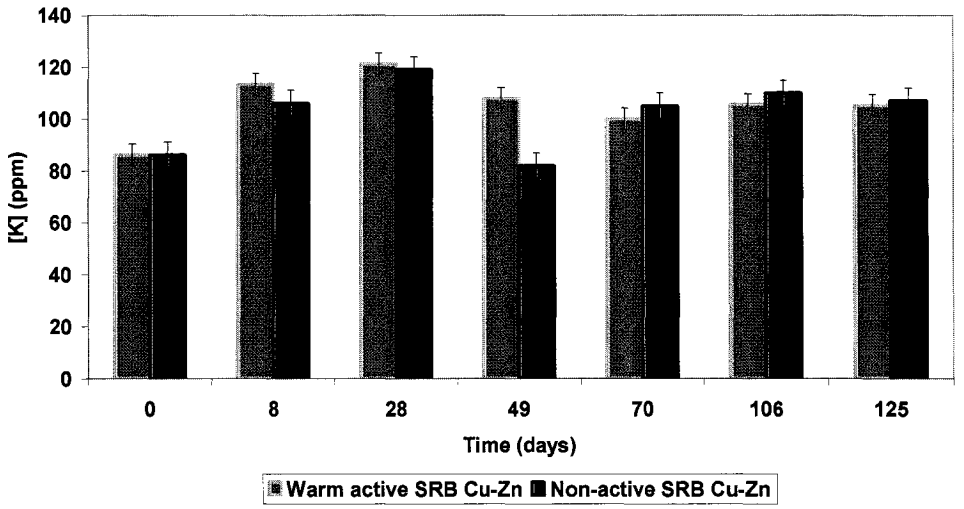

c)

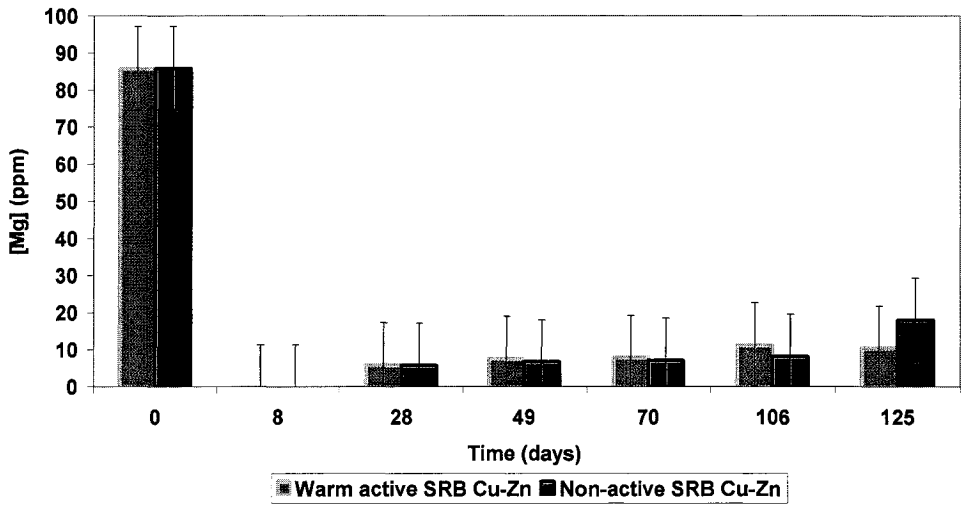

Figure A-1. Calcium (a), potassium (b), and magnesium (c) concentrations in the aqueous phase of the Warm Active SRB and the Non-active SRB Cu-Zn columns over 125 days.

a)

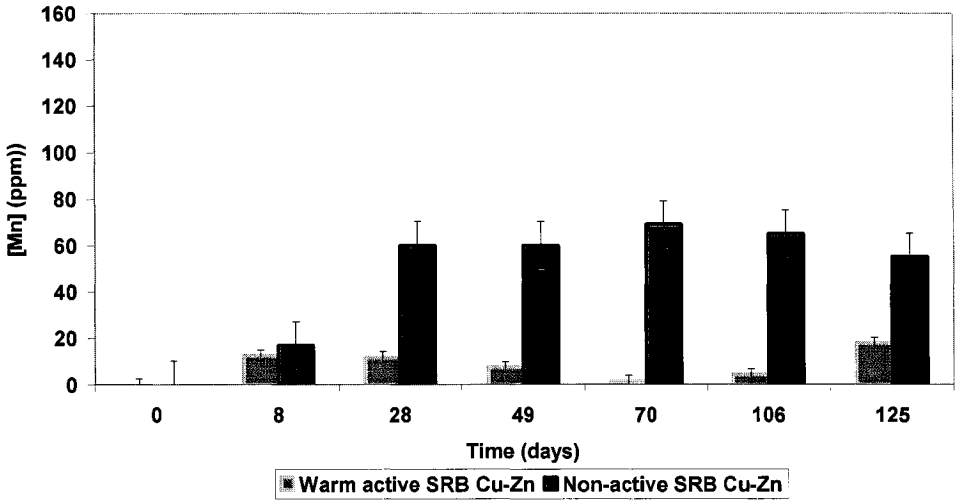

b)

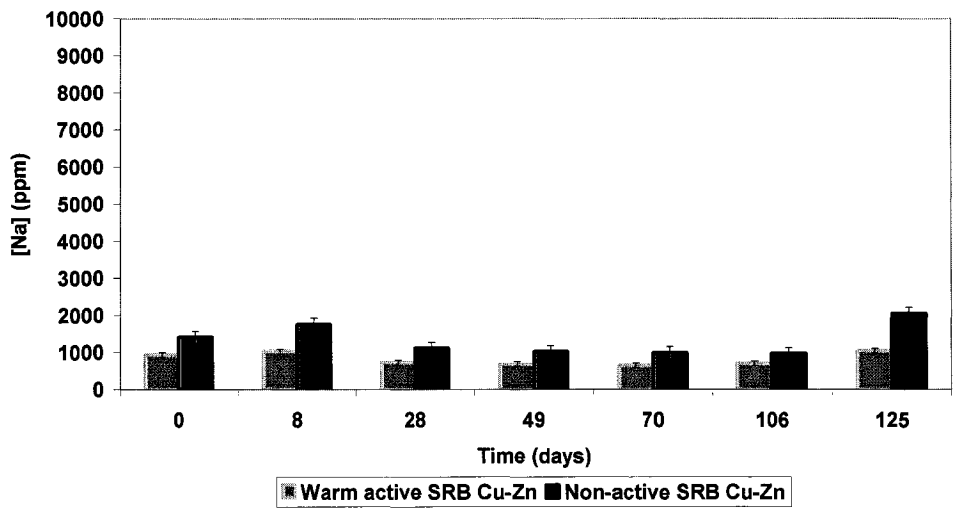

c)

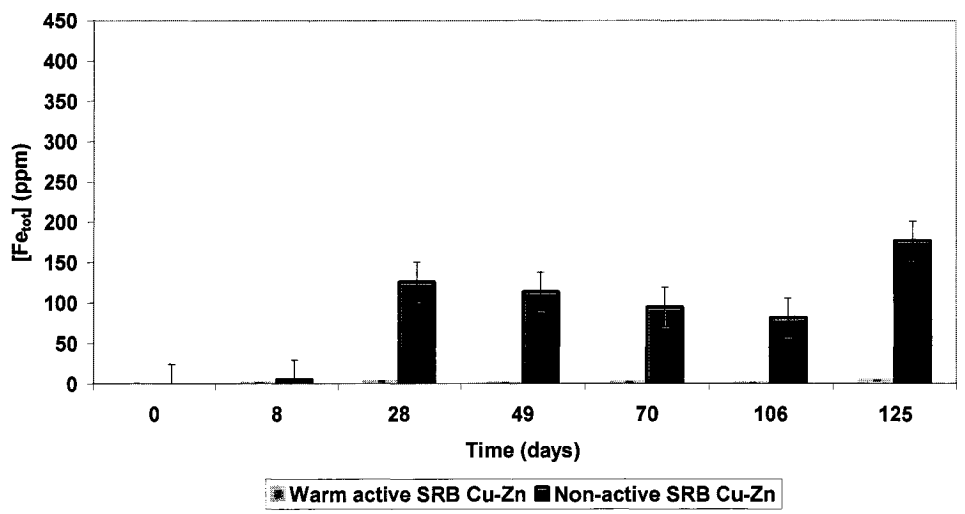

Figure A-2. Manganese (a), sodium (b), and total iron (c) concentrations in the aqueous phase of the Warm Active SRB and the Non-active SRB Cu-Zn columns over 125 days.

A-2. Warm Active SRB Cu-Zn and the Cold Active SRB Cu-Zn columns

Table A-2. Statistical results of Warm Active SRB Cu-Zn and Cold Active SRB Cu-Zn aqueous ICP results.

	same	different
Ca	•	
K		•
Mg	•	
Mn	•	
Na		•
Fe (tot)		•

The concentration of soluble Ca dropped in both the Warm Active SRB Cu-Zn and the Cold Active SRB Cu-Zn columns (Figure A-3 a) shortly after the beginning of the experiment. The Ca levels in both columns remained relatively similar, with the exception of time 70 days when the concentration of Ca in the Cold Active column (which was frozen by accident) was greater than the one in the Warm Active column. Soluble K levels increased over time in both the Warm Active SRB and the Cold Active SRB Cu-Zn columns (Figure A-3 b), with the exception of the data point at 70 days, when the cold Active column was frozen by accident. Soluble Mg concentrations increased slightly over time in both the Warm Active and the Cold Active SRB Cu-Zn columns (Figure A-3 c). Concentrations were similar for both systems, except near the end of the experiments when Mg was not detected in the aqueous phase of the Warm Active SRB column. There was also a slight release of soluble Mn in both columns over time (Figure A-4 a). Soluble Na levels were very high in both the Warm Active SRB Cu-Zn and the Cold Active SRB Cu-Zn columns (Figure A-4 b) and remained high for the entire experiment. There was no release of Fe over time in both the Warm Active SRB and the Cold Active SRB Cu-Zn columns (Figure A-4 c).

a)

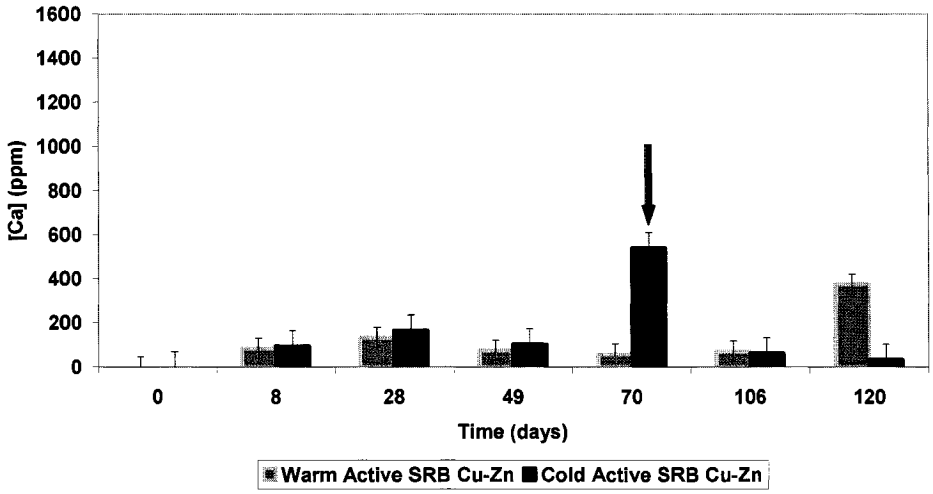

b)

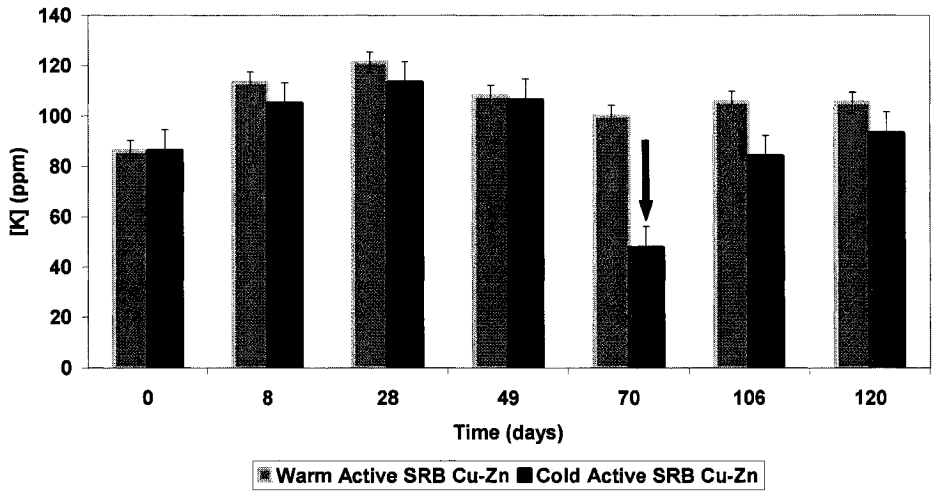

c)

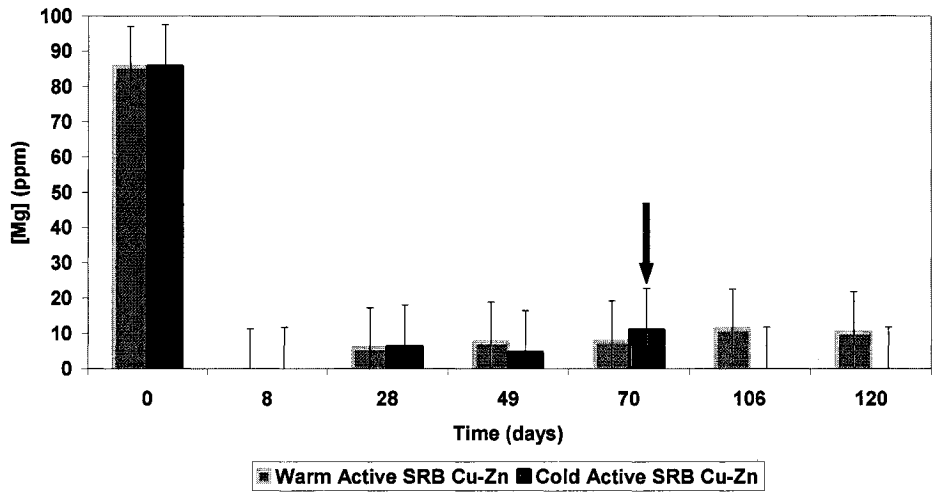

Figure A-3. Calcium (a), potassium (b), and magnesium (c) concentrations in the aqueous phase of the Warm Active SRB and the Cold Active SRB Cu-Zn columns over 125 days. Blue arrow corresponds to sample taken after accidental freezing of the Cold Active SRB Cu-Zn column.

a)

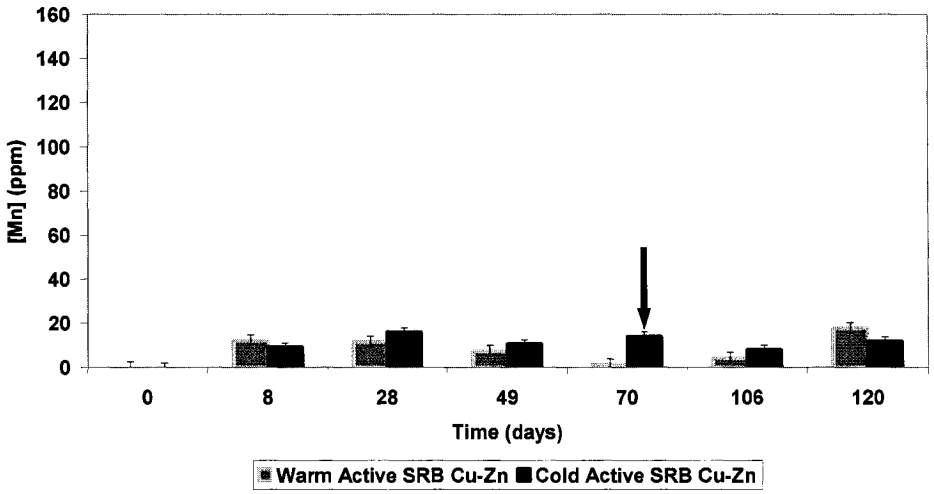

b)

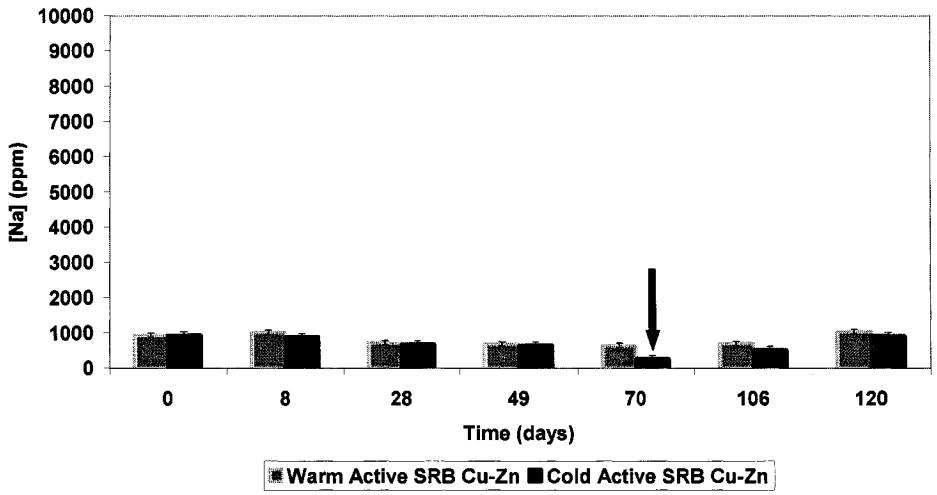

c)

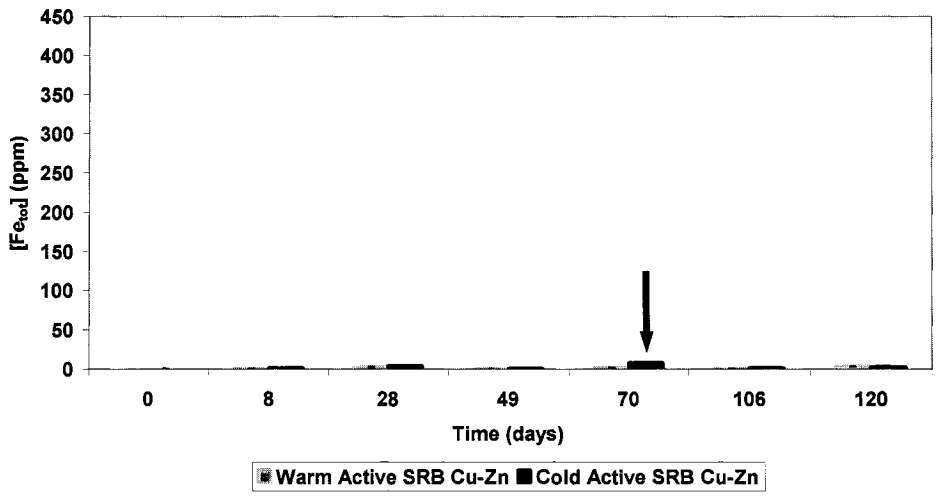

Figure A-4. Manganese (a), sodium (b), and total iron (c), concentrations in the aqueous phase of the Warm Active SRB and the Cold Active SRB Cu-Zn columns over 125 days. Blue arrow corresponds to sample taken after accidental freezing of the Cold Active SRB Cu-Zn column.

A-3. High Sulfate Cu-Zn and the Low Sulfate Cu-Zn columns

Table A-3. Statistical results of High Sulfate Cu-Zn and the Low Sulfate Cu-Zn aqueous ICP results.

	same	different
Ca		•
K	•	
Mg	•	
Mn	•	
Na		•
Fe (tot)	•	

The level of soluble Ca in the Low Sulfate Cu-Zn column remained stable over time, with the exception of time 110 days when it declined (Figure A-5 a). In the High Sulfate column, Ca concentrations fluctuated over time, but remained lower that the levels observed in the Low Sulfate column. There was a release of both soluble Mg and K in the aqueous phase of both columns over time (Figure A-5 b and c). Concentrations of both Mg and K were similar between the 2 systems, but some fluctuations occurred over time. Mn was initially released into solution in both columns, but the concentrations declined after day 71 and remained low for the remainder of the experiment (Figure A-6 a). Soluble Na levels were high in both columns, but higher in the High Sulfate column than in the Low Sulfate column because $NaSO_4$ was used to increase the sulfate level (Figure A-6 b). Small amount of iron was released into solution in both the High Sulfate Cu-Zn and Low Sulfate Cu-Zn columns (Figure A-6 c) until 41 days, then the iron was almost undetectable.

a)

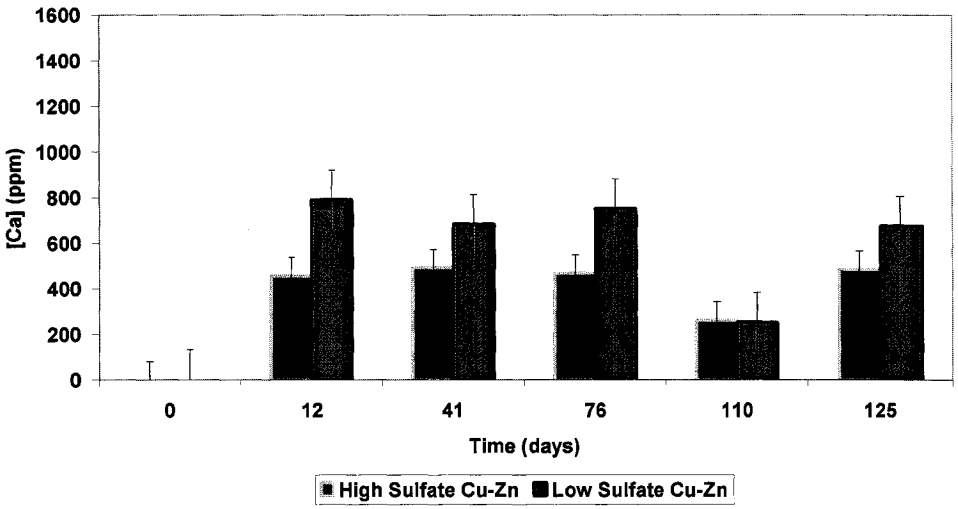

b)

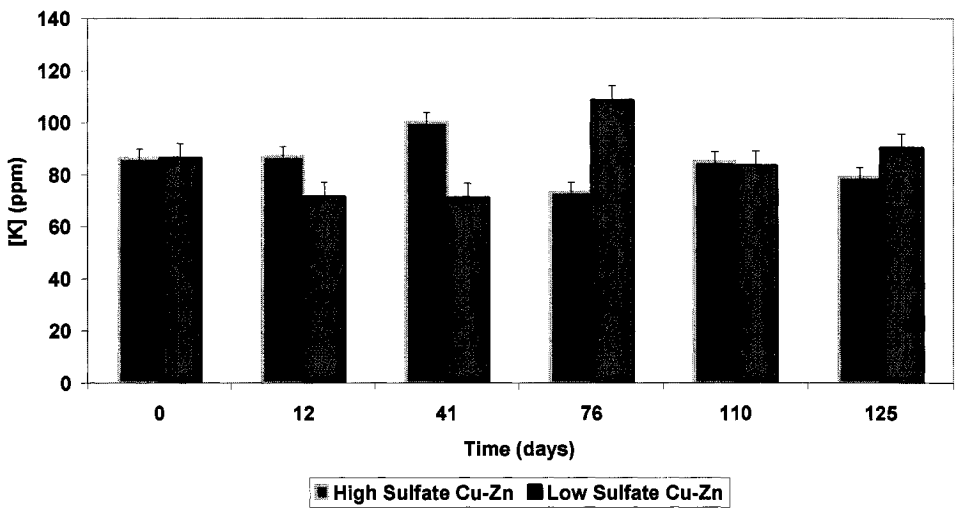

c)

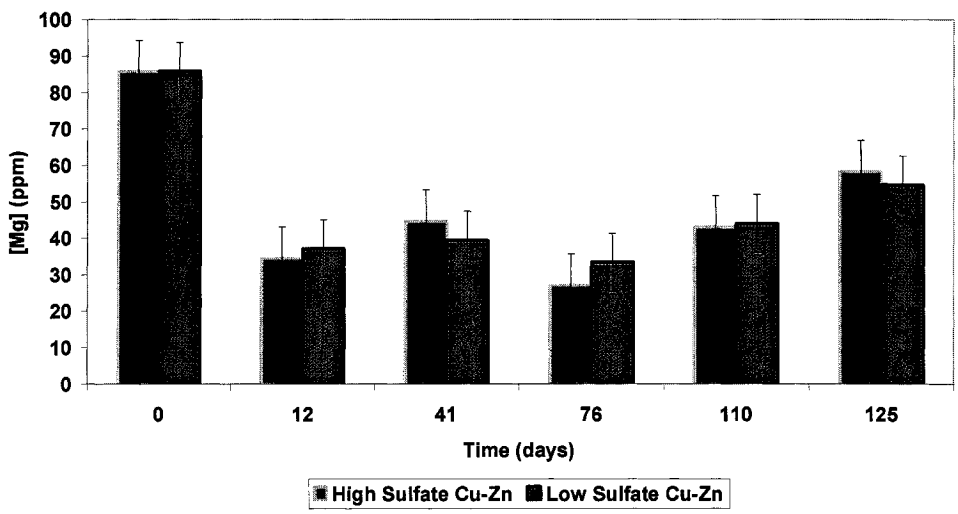

Figure A-5. Calcium (a), potassium (b), and magnesium (c) concentrations in the aqueous phase of the High Sulfate and the Low Sulfate Cu-Zn columns over 125 days.

a)

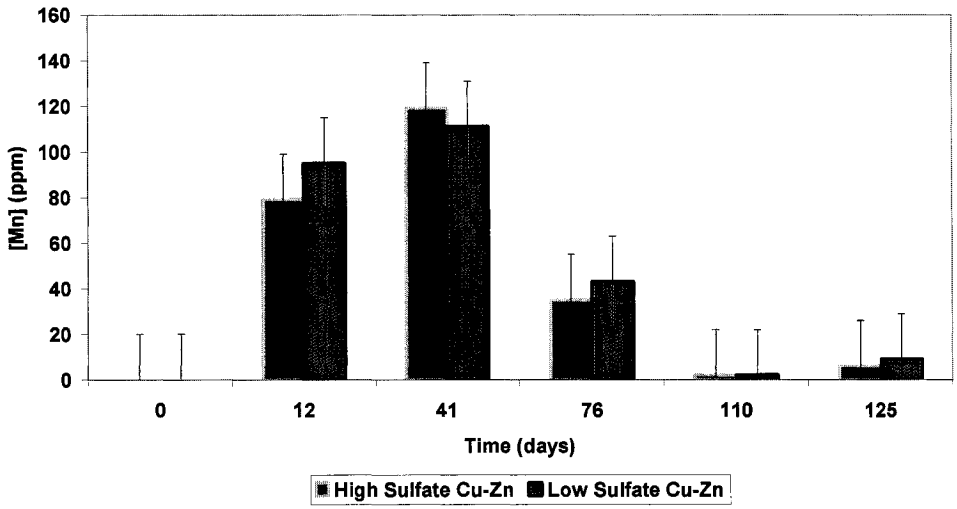

b)

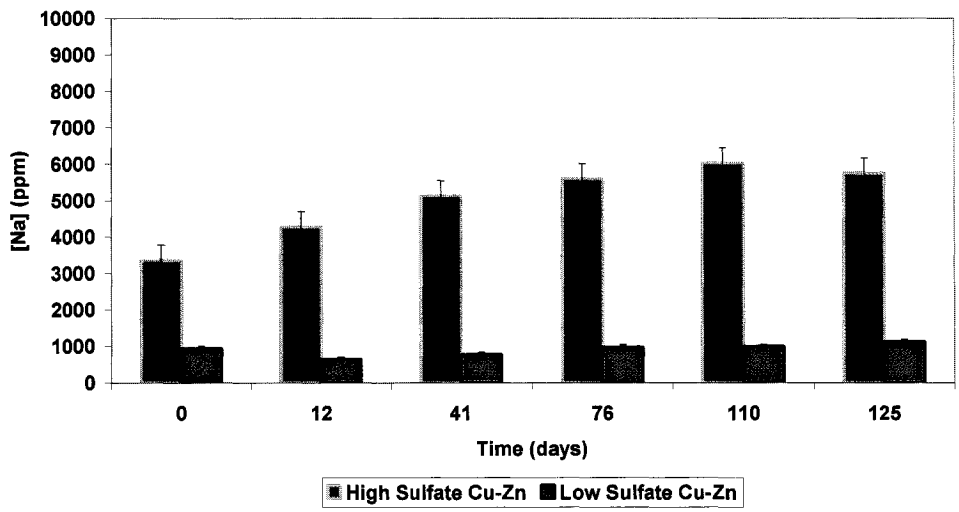

c)

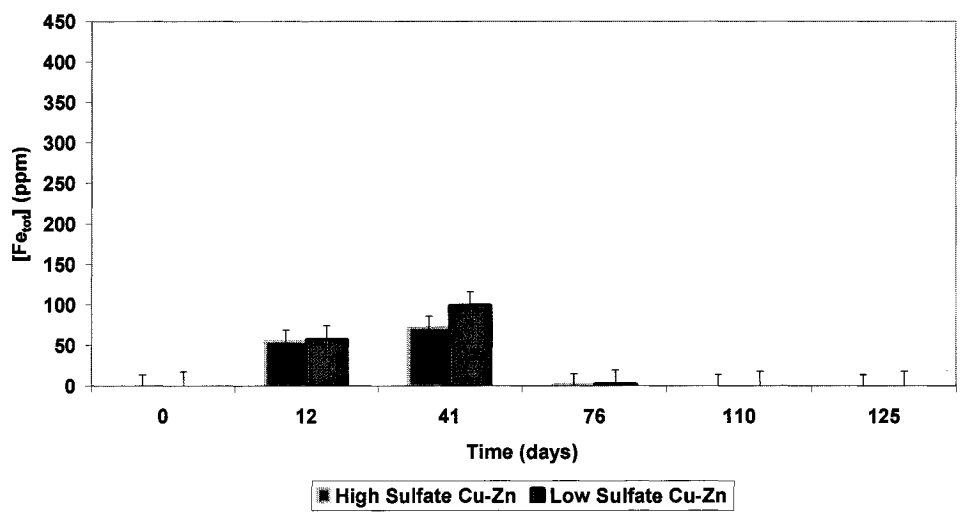

Figure A-6. Manganese (a), sodium (b), and total iron (c) concentrations in the aqueous phase of the High Sulfate and the Low Sulfate Cu-Zn columns over 125 days.

A-4. High DOC Cu-Zn and the Low DOC Cu-Zn columns

Table A-4. Statistical results of High DOC Cu-Zn and the Low DOC Cu-Zn aqueous ICP results.

	same	different
Ca		•
K	•	
Mg	•	
Mn		•
Na		•
Fe (tot)		•

Ca concentrations in the High DOC Cu-Zn column after the first 2 weeks exceeded the ICP-OES calibration curve, even when the samples were diluted 1000 times (Figure A-7 a). It is estimated that soluble Ca levels in the column over the course of the experiments were somewhere over 1500 ppm. The Low DOC Cu-Zn column had an average Ca concentration that slightly fluctuated over time and remained very similar to the original concentration in the medium (Figure A-7 a). Dissolved K concentrations increased at the beginning of the experiment and then remained fairly stable over time for both the Low and High DOC columns (Figure A-7 b). There was a obvious release of soluble Mg in both columns over the course of the experiments (Figure A-7 c). Results also indicated the concentrations of both columns were similar with the exception of the sampling day 41. The Low DOC Cu-Zn column released Mn into solution over time, whereas no Mn was measured in the High DOC Cu-Zn column, except after 12 days (Figure A-8 a). Na concentrations were higher in the High DOC Cu-Zn column than in the Low DOC column because of the higher concentration of Na-Lactate, Na-Pyruvate, Na-Formate, and Na-Acetate in the growth medium (Figure A-8 b). The Low DOC column released soluble iron over time, especially up to 41 days (Figure A-8 c), then the concentrations decreased until the end of the experiment. On the other hand, High DOC column did not have any significant total iron release.

a)

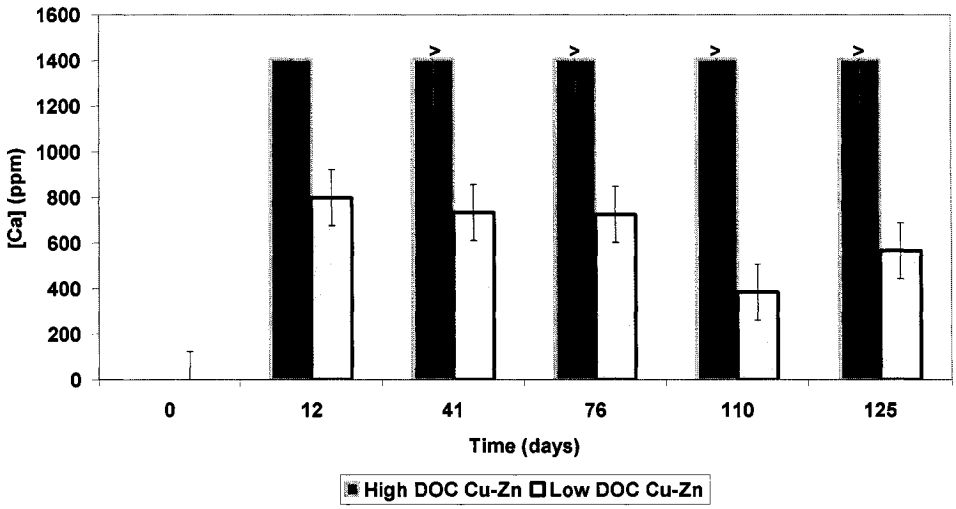

b)

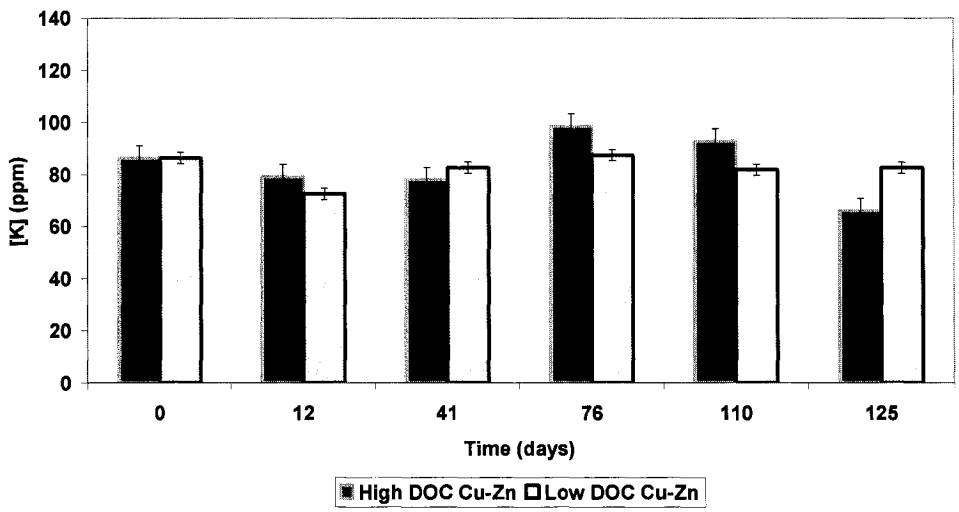

c)

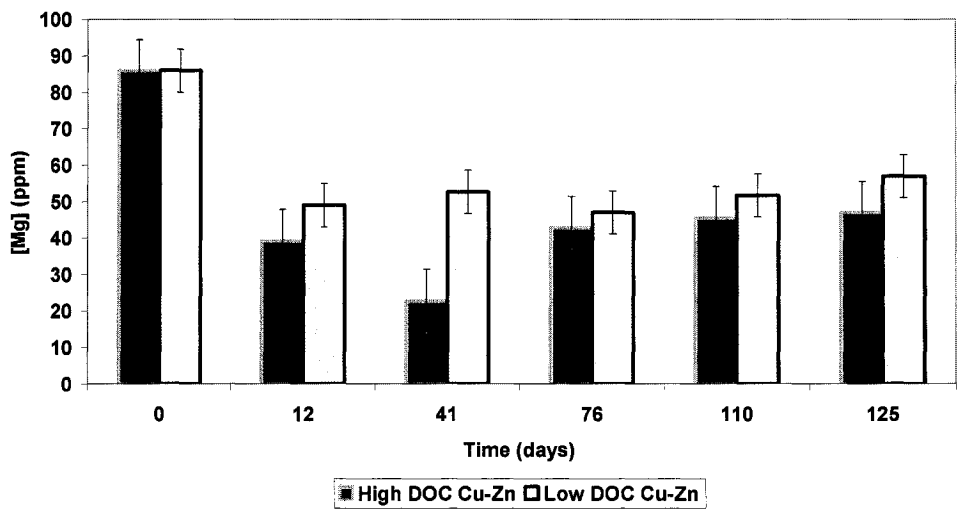

Figure A-7. Calcium (a), potassium (b), and magnesium (c) concentrations in the aqueous phase of the High DOC and the Low DOC Cu-Zn columns over 125 days.

a)

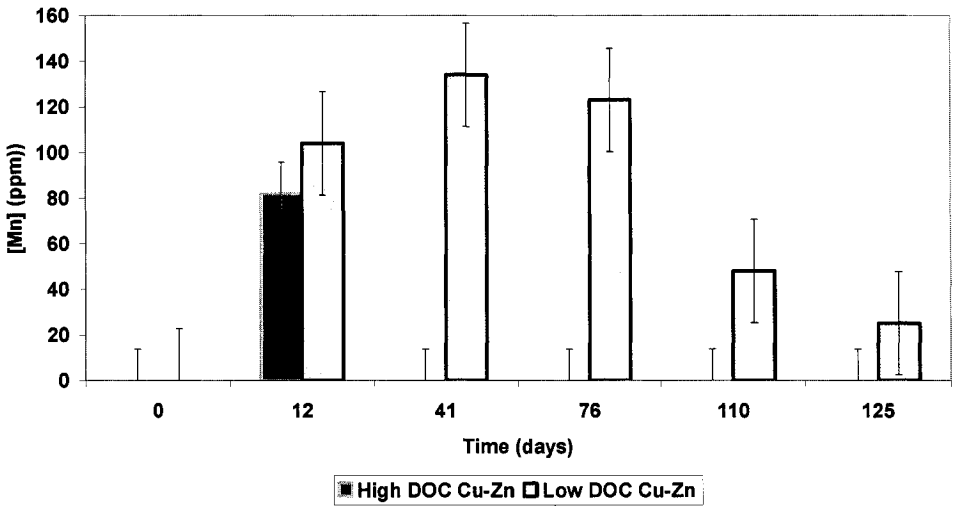

b)

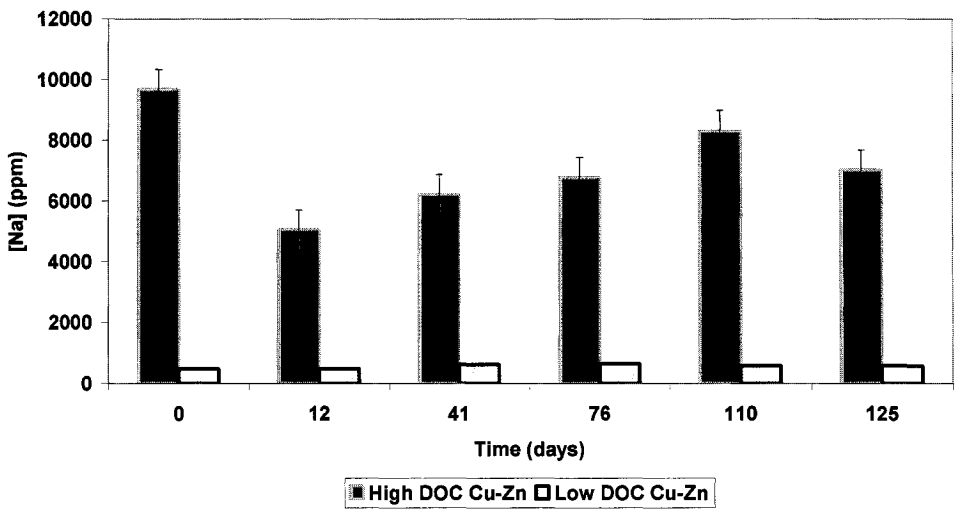

c)

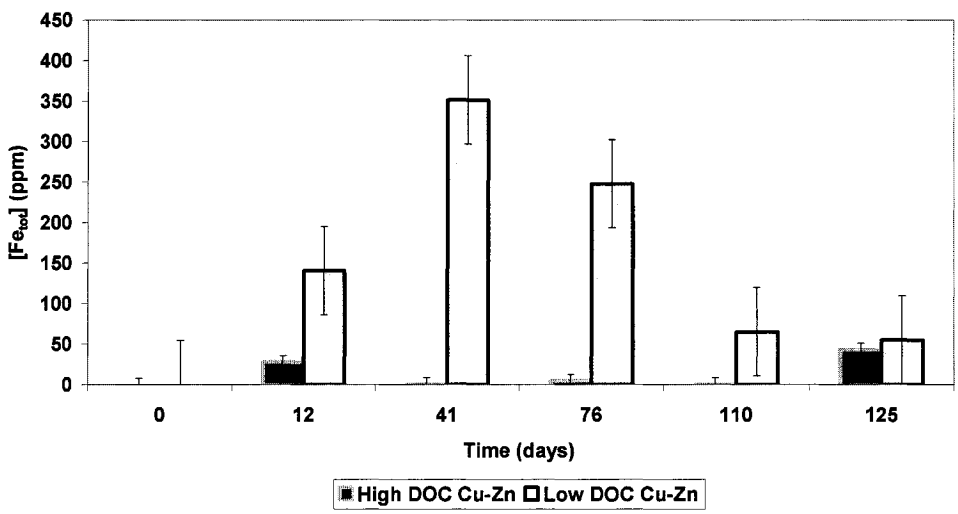

Figure A-8. Manganese (a), sodium (b), and total iron (c) concentrations in the aqueous phase of the High DOC and the Low DOC Cu-Zn columns over 125 days.

A-5. Active SRB Au and the Non-active SRB Au columns

Table A-5. Statistical results of Active SRB Au and the Non-active SRB Au aqueous ICP results.

	same	different
Ca	•	
K		•
Mg	•	
Mn		•
Na		•
Fe (tot)		•

There was little to no soluble Ca in the Active SRB and Non-active SRB Au columns overtime (Figure A-9 a) indicating that Ca was quickly removed from solution through precipitation. The results show that large levels of dissolved K were present into solution over time in both columns (Figure A-9 b), but a large portion of K was actually from the matrix solution. There was little to no Mg measured in both columns (Figure A-9 c). The initial concentration of Mn was very elevated in both columns (Table 6), but the concentration drastically declined after the first 2 weeks for the remainder of the experiment (Figure A-10 a). Large levels of Na were present in both columns (Figure A-10 b), but the concentrations were slightly higher in the inhibited Non-Active SRB Au column Na-Molybdate was added to the matrix. As observed in the SRB inhibited Cu-Zn columns, dissolved Fe was released over time in the Non-active SRB Au column compared to the Active SRB (Figure A-10 c).

a)

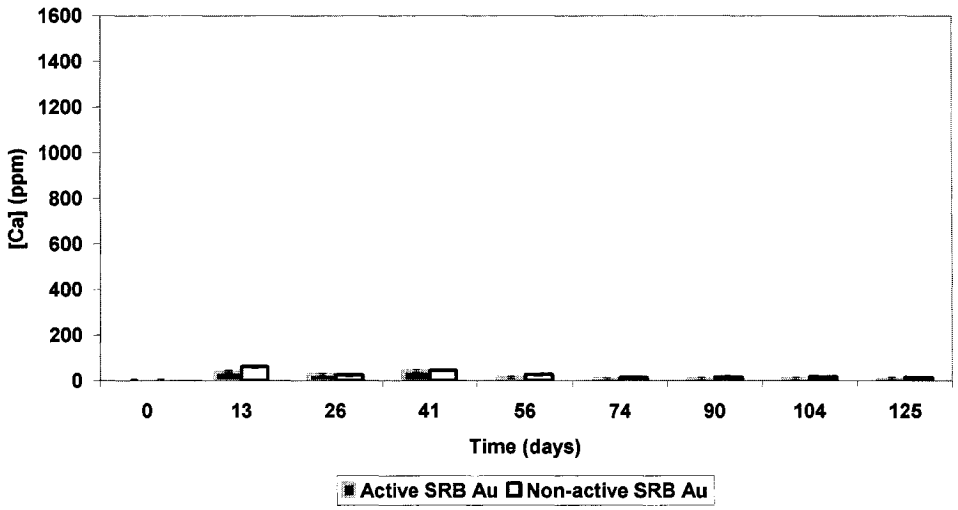

b)

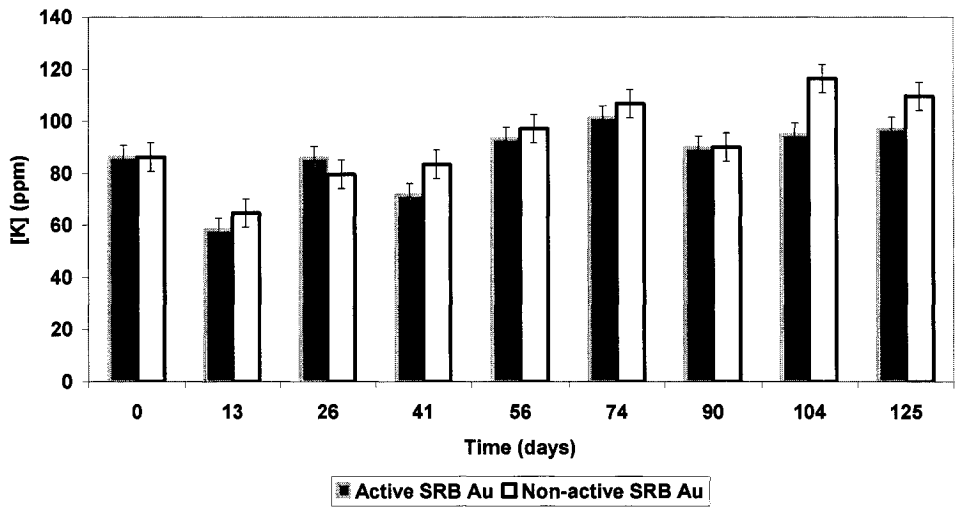

c)

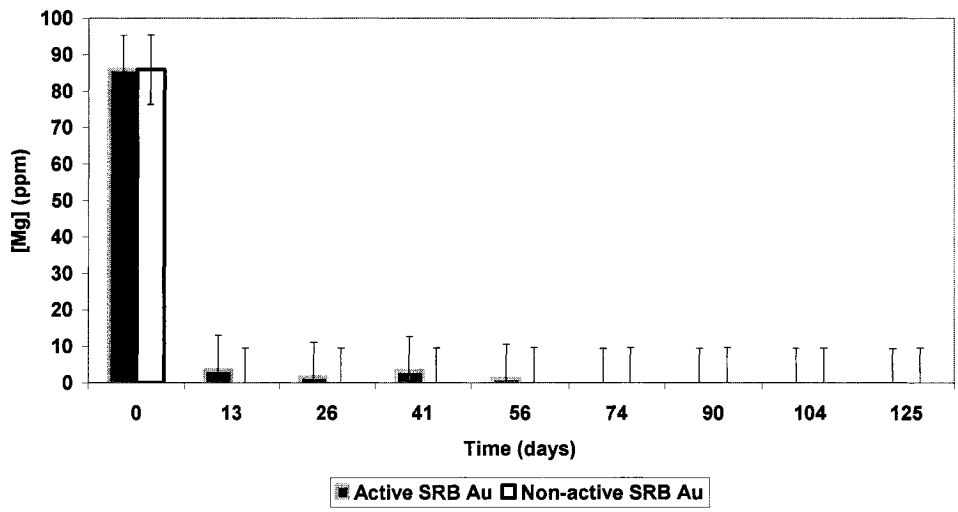

Figure A-9. Calcium (a), potassium (b), and magnesium (c) concentrations in the aqueous phase of the Active SRB and the Non-active SRB Au columns over 125 days.

a)

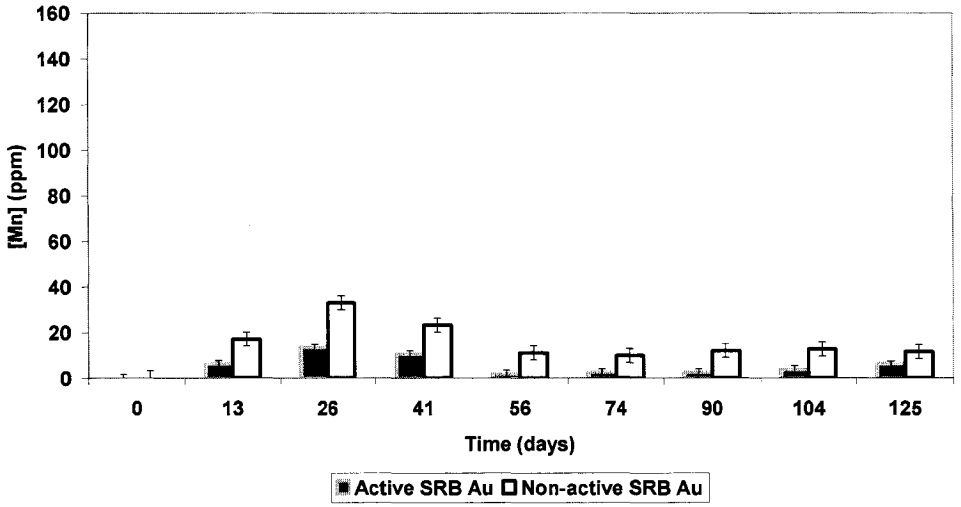

b)

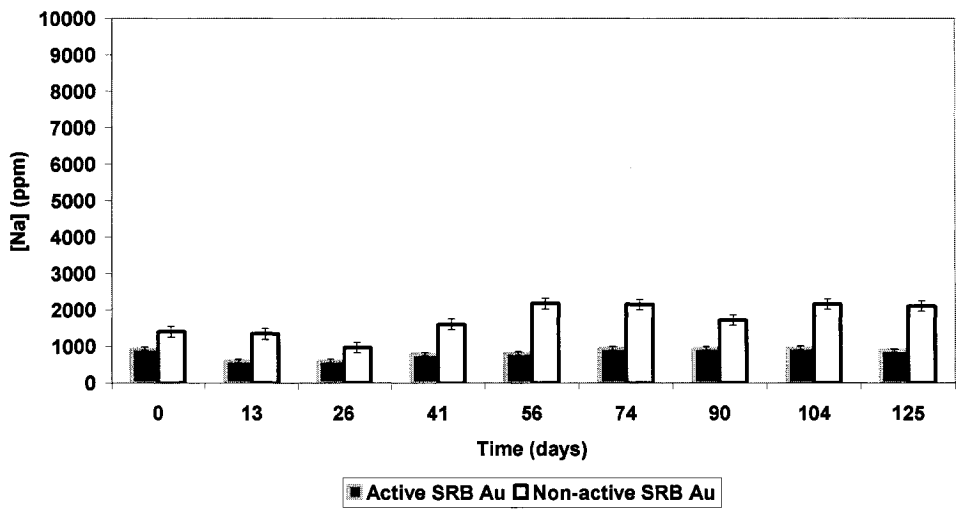

c)

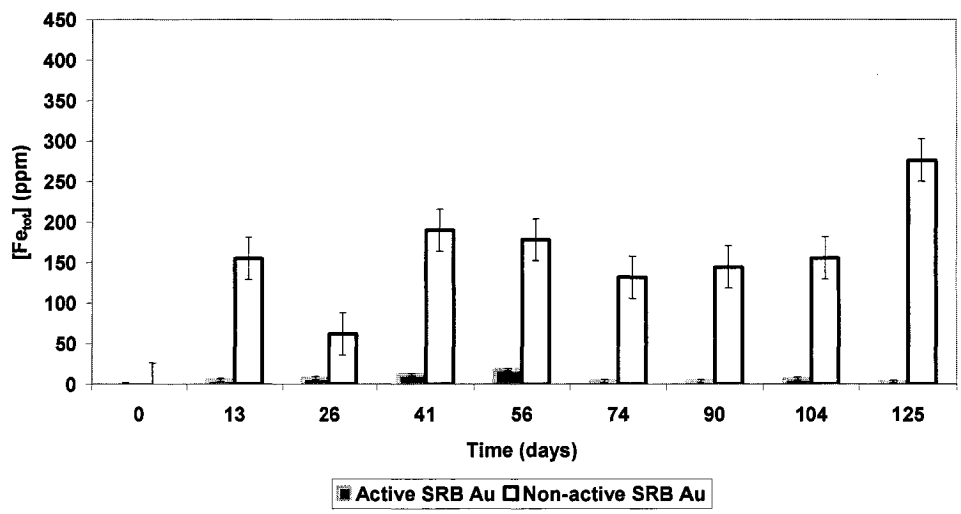

Figure A-10. Manganese (a), sodium (b), and total iron (c) concentrations in the aqueous phase of the Active SRB and the Non-active SRB Au columns over 125 days.

Appendix B

B-1. **Statistical analysis of the Acid Volatile Sulfide values in the Cu-Zn sediment cores:**

depth	name	n	S^{2-} (ppm)	
1.5	Cu-Zn active 0-3	1	0.286	
4.5	Cu-Zn active 3-6	1	0.280	
7.5	Cu-Zn active 6-9	1	0.254	
10.5	Cu-Zn active 9-12	1	0.241	
13.5	Cu-Zn active 12-15	1	0.189	
16.5	Cu-Zn active 15-18	1	0.183	

n_a	6		
x_a		0.239	
sd_a			0.044

depth	name	n	S^{2-} (ppm)	
1.5	Cu-Zn nonactive 0-3	1	0.222	
4.5	Cu-Zn nonactive 3-6	1	0.273	
7.5	Cu-Zn nonactive 6-9	1	0.176	
10.5	Cu-Zn nonactive 9-12	1	0.299	
13.5	Cu-Zn nonactive 12-15	1	0.215	
16.5	Cu-Zn nonactive 15-18	1	0.196	

n_n	6		
x_n		0.230	
sd_n			0.047

The *t* Statistic

μ_a = The Active SRB Cu-Zn values

μ_n = The Non-active SRB Cu-Zn values

The following null hypothesis is considered	$H_o: \mu_a = \mu_n$
The following alternative hypothesis is also considered	$H_a: \mu_a \neq \mu_n$

The *t test* is a standard method of choosing between the two hypotheses.

$$t_s = \frac{|X_a - X_n| - 0}{SE_{(Xa-Xn)}} \qquad \text{where; } SE_{(Xa-Xn)} = \sqrt{[((sd_a)^2/n_a) + ((sd_n)^2/n_n)]}$$

If $t_s < 1$ do not reject the null hypothesis

If $t_s > 1$ reject the null hypothesis and accept the alternative hypothesis

Note that the $|X_a - X_n|$ is subtracted from zero because H_o states that μ_a - μ_n equals zero; writing "$|X_a - X_n| - 0$" reminds us of what we are testing.

$$t_s = \frac{|0.239 - 0.230| - 0}{\sqrt{[((0.044)^2/6)+((0.047)^2/6)]}}$$

$t_s = 0.34$

$t_s < 1$ Therefore the null hypothesis is not rejected and $\mu_a = \mu_n$

The acid volatile sulfide (S^{2-}) values measured in the Active SRB Cu-Zn column are the same as the acid volatile sulfide (S^{2-}) values measured in the Non-Active SRB Cu-Zn column.

B-2. **Statistical analysis of the total mercury values in the Cu-Zn sediment cores:**

depth	name	n	Total $_{Hg}$	sd
1.5	Cu-Zn active 0-3	2	186.1	9.8
4.5	Cu-Zn active 3-6	2	140.4	13.9
7.5	Cu-Zn active 6-9	2	147.3	9.8
10.5	Cu-Zn active 9-12	2	139.3	0.7
13.5	Cu-Zn active 12-15	2	147.5	7.7
16.5	Cu-Zn active 15-18	2	147.8	5.7

n_a	**12**		
x_a		**151.4**	
sd_a			**17.4**

depth	name	n	Total $_{Hg}$	sd
1.5	Cu-Zn nonactive 0-3	2	192.9	4.8
4.5	Cu-Zn nonactive 3-6	2	129.2	6.3
7.5	Cu-Zn nonactive 6-9	2	163.0	39.5
10.5	Cu-Zn nonactive 9-12	2	134.0	14.1
13.5	Cu-Zn nonactive 12-15	2	152.4	12.5
16.5	Cu-Zn nonactive 15-18	2	171.2	34.3

n_n	**12**		
x_n		**157.1**	
sd_n			**23.9**

The *t* Statistic

μ_a = The Active SRB Cu-Zn values

μ_n = The Non-active SRB Cu-Zn values

The following null hypothesis is considered	$H_o: \mu_a = \mu_n$
The following alternative hypothesis is also considered	$H_a: \mu_a \neq \mu_n$

The *t test* is a standard method of choosing between the two hypotheses.

$$t_s = \frac{|X_a - X_n| - 0}{SE_{(Xa - Xn)}} \qquad \text{where; } SE_{(Xa-Xn)} = \sqrt{[((sd_a)^2/n_a) + ((sd_n)^2/n_n)]}$$

If $t_s < 1$ do not reject the null hypothesis

If $t_s > 1$ reject the null hypothesis and accept the alternative hypothesis

Note that the $|X_a - X_n|$ is subtracted from zero because H_o states that μ_a - μ_n equals zero; writing "$|X_a - X_n| - 0$" reminds us of what we are testing.

$$t_s = \frac{|151.4 - 157.1| - 0}{\sqrt{[((17)^2/12)+((24)^2/12)]}}$$

$t_s = 0.67$

$t_s < 1$ Therefore the null hypothesis is not rejected and $\mu_a = \mu_n$

The Total mercury values measured in the Active SRB Cu-Zn column are the same as the total mercury values measured in the Non-Active SRB Cu-Zn column.

B-3. **Statistical analysis of the methylmercury values in the Cu-Zn sediment cores:**

depth	name	n	MeHg (ppt)	sd
1.5	Cu-Zn active 0-3	3	0.0	0.0
4.5	Cu-Zn active 3-6	3	0.0	0.0
7.5	Cu-Zn active 6-9	3	14.7	0.9
10.5	Cu-Zn active 9-12	3	19.8	0.1
13.5	Cu-Zn active 12-15	3	17.5	1.7
16.5	Cu-Zn active 15-18	2	19.6	0.0

n_a	**17**		
x_a		**11.9**	
sd_a			**9.4**

depth	name	n	MeHg (ppt)	sd
1.5	Cu-Zn nonactive 0-3	3	11.9	2.6
4.5	Cu-Zn nonactive 3-6	3	11.1	1.6
7.5	Cu-Zn nonactive 6-9	2	8.2	1.3
10.5	Cu-Zn nonactive 9-12	2	13.6	4.2
13.5	Cu-Zn nonactive 12-15	3	19.7	3.2
16.5	Cu-Zn nonactive 15-18	3	25.9	2.6

n_n	**16**		
x_n		**15.1**	
sd_n			**6.5**

The *t* Statistic

μ_a = The Active SRB Cu-Zn values

μ_n = The Non-active SRB Cu-Zn values

The following null hypothesis is considered	$H_o: \mu_a = \mu_n$
The following alternative hypothesis is also considered	$H_a: \mu_a \neq \mu_n$

The *t test* is a standard method of choosing between the two hypotheses.

$$t_s = \frac{|X_a - X_n| - 0}{SE_{(Xa - Xn)}} \qquad \text{where; } SE_{(Xa - Xn)} = \sqrt{[((sd_a)^2/n_a) + ((sd_n)^2/n_n)]}$$

If $t_s < 1$ do not reject the null hypothesis

If $t_s > 1$ reject the null hypothesis and accept the alternative hypothesis

Note that the $|X_a - X_n|$ is subtracted from zero because H_o states that μ_a - μ_n equals zero; writing "$|X_a - X_n| - 0$" reminds us of what we are testing.

$$t_s = \frac{|11.9-15.1| - 0}{\sqrt{[((9.4)^2/17)+((6.5)^2/16)]}}$$

$t_s = 1.14$

$t_s > 1$ Therefore the null hypothesis is rejected and the alternative hypothesis is accepted $\mu_a \neq \mu_n$

The methylmercury values measured in the Active SRB Cu-Zn column are **not** the same as the methylmercury values measured in the Non-Active SRB Cu-Zn column.

B-4. Statistical analysis of the % Organics in the Cu-Zn sediment cores:

depth	name	n	%Organics	
1.5	Cu-Zn active 0-3	1	2.15	
4.5	Cu-Zn active 3-6	1	1.81	
7.5	Cu-Zn active 6-9	1	1.89	
10.5	Cu-Zn active 9-12	1	1.58	
13.5	Cu-Zn active 12-15	1	1.24	
16.5	Cu-Zn active 15-18	1	1.76	

n_a	6		
x_a		1.74	
sd_a			0.31

depth	name	n	%Organics	
1.5	Cu-Zn nonactive 0-3	1	3.54	
4.5	Cu-Zn nonactive 3-6	1	2.18	
7.5	Cu-Zn nonactive 6-9	1	1.61	
10.5	Cu-Zn nonactive 9-12	1	2.28	
13.5	Cu-Zn nonactive 12-15	1	2.09	
16.5	Cu-Zn nonactive 15-18	1	2.10	

n_n	6		
x_n		2.30	
sd_n			0.65

The *t* Statistic

μ_a = The Active SRB Cu-Zn values

μ_n = The Non-active SRB Cu-Zn values

The following null hypothesis is considered	$H_o: \mu_a = \mu_n$
The following alternative hypothesis is also considered	$H_a: \mu_a \neq \mu_n$

The *t test* is a standard method of choosing between the two hypotheses.

$$t_s = \frac{|X_a - X_n| - 0}{SE_{(Xa-Xn)}} \qquad \text{where; } SE_{(Xa-Xn)} = \sqrt{[((sd_a)^2/n_a) + ((sd_n)^2/n_n)]}$$

If $t_s < 1$ do not reject the null hypothesis

If $t_s > 1$ reject the null hypothesis and accept the alternative hypothesis

Note that the $|X_a - X_n|$ is subtracted from zero because H_o states that μ_a - μ_n equals zero; writing "$|X_a - X_n| - 0$" reminds us of what we are testing.

$$t_s = \frac{|1.74 - 2.30| - 0}{\sqrt{[((0.31)^2/6)+((0.65)^2/6)]}}$$

$t_s = 1.90$

$t_s > 1$ Therefore the null hypothesis is rejected and the alternative hypothesis is accepted $\mu_a \neq \mu_n$

The % organic carbon measured in the Active SRB Cu-Zn column are **not** the same as the % organic carbon measured in the Non-Active SRB Cu-Zn column.

Summary:
The total mercury and acid volatile sulfides do not differ depending on whether the column was inhibited or not. The Methylmercury and % organics do differ from the active and non-active columns.

Appendix C

C-1. Statistical analysis of the Acid Volatile Sulfide values in the Au sediment cores:

depth	name	n	S^{2-} (ppm)	
1.5	Au active 0-3	1	0.211	
4.5	Au active 3-6	1	0.223	
7.5	Au active 6-9	1	0.254	
10.5	Au active 9-12	1	0.266	
13.5	Au active 12-15	1	0.211	
16.5	Au active 15-18	1	0.211	

n_a	6		
x_a		0.229	
sd_a			0.025

depth	name	n	S^{2-} (ppm)	
1.5	Au nonactive 0-3	1	0.260	
4.5	Au nonactive 3-6	1	0.280	
7.5	Au nonactive 6-9	1	0.215	
10.5	Au nonactive 9-12	1	0.163	
13.5	Au nonactive 12-15	1	0.131	
16.5	Au nonactive 15-18	1	0.131	

n_n	6		
x_n		0.197	
sd_n			0.065

The *t* Statistic

μ_a = The Active SRB Au values

μ_n = The Non-active SRB Au values

The following null hypothesis is considered	$H_o: \mu_a = \mu_n$
The following alternative hypothesis is also considered	$H_a: \mu_a \neq \mu_n$

The *t test* is a standard method of choosing between the two hypotheses.

$$t_s = \frac{|X_a - X_n| - 0}{SE_{(Xa - Xn)}} \qquad \text{where; } SE_{(Xa - Xn)} = \sqrt{[((sd_a)^2/n_a) + ((sd_n)^2/n_n)]}$$

If $t_s < 1$ do not reject the null hypothesis

If $t_s > 1$ reject the null hypothesis and accept the alternative hypothesis

Note that the $|X_a - X_n|$ is subtracted from zero because H_o states that $\mu_a - \mu_n$ equals zero; writing "$|X_a - X_n| - 0$" reminds us of what we are testing.

$$t_s = \frac{|0.229 - 0.197| - 0}{\sqrt{[((0.025)^2/6)+((0.065)^2/6)]}}$$

$t_s = 1.15$

$t_s > 1$ Therefore the null hypothesis is rejected and $\mu_a \neq \mu_n$

The acid volatile sulfide (S^{2-}) values measured in the Active SRB Au column are not the same as the acid volatile sulfide (S^{2-}) values measured in the Non-Active SRB Au column.

C-2. Statistical analysis of the Total Mercury values in the Au sediment cores:

depth	name	n	Total $_{Hg}$ (ppb)	
1.5	Au active 0-3	2	526.8	2.9
4.5	Au active 3-6	2	67.2	1.6
7.5	Au active 6-9	2	55.2	3.1
10.5	Au active 9-12	2	56.2	10.3
13.5	Au active 12-15	2	58.1	6.8
16.5	Au active 15-18	2	53.5	1.6

n_a	12		
x_a		136.1	
sd_a			191.4

depth	name	n	Total $_{Hg}$ (ppb)	
1.5	Au nonactive 0-3	2	860.8	20.7
4.5	Au nonactive 3-6	2	177.2	1.3
7.5	Au nonactive 6-9	2	61.9	2.5
10.5	Au nonactive 9-12	2	58.0	4.1
13.5	Au nonactive 12-15	2	52.2	3.4
16.5	Au nonactive 15-18	2	46.9	4.8

n_n	12		
x_n		209.5	
sd_n			322.8

The *t* Statistic

μ_a = The Active SRB Au values

μ_n = The Non-active SRB Au values

The following null hypothesis is considered	$H_o: \mu_a = \mu_n$
The following alternative hypothesis is also considered	$H_a: \mu_a \neq \mu_n$

The *t test* is a standard method of choosing between the two hypotheses.

$$t_s = \frac{|X_a - X_n| - 0}{SE_{(Xa-Xn)}} \qquad \text{where; } SE_{(Xa-Xn)} = \sqrt{[((sd_a)^2/n_a) + ((sd_n)^2/n_n)]}$$

If $t_s < 1$ do not reject the null hypothesis

If $t_s > 1$ reject the null hypothesis and accept the alternative hypothesis

Note that the $|X_a - X_n|$ is subtracted from zero because H_o states that μ_a - μ_n equals zero; writing "$|X_a - X_n| - 0$" reminds us of what we are testing.

$$t_s = \frac{|136.18 - 209.51| - 0}{\sqrt{[((191.44)^2/12)+((322.83)^2/12)]}}$$

$t_s = 0.68$

$t_s < 1$ Therefore the null hypothesis is not rejected and $\mu_a = \mu_n$

The Total mercury values measured in the Active SRB Au column are the same as the total mercury values measured in the Non-Active SRB Au column.

C-3. Statistical analysis of the methylmercury values in the Au sediment cores:

depth	name	n	MeHg (ppt)	sd
1.5	Au active 0-3	3	6.8	1.5
4.5	Au active 3-6	3	0.0	0
7.5	Au active 6-9	3	0.0	0
10.5	Au active 9-12	3	0.0	0
13.5	Au active 12-15	3	0.0	0
16.5	Au active 15-18	3	0.0	0

n_a	18		
x_a		1.1	
sd_a			2.7

depth	name	n	MeHg (ppt)	sd
1.5	Au nonactive 0-3	3	92.7	9.4
4.5	Au nonactive 3-6	3	3.5	3.5
7.5	Au nonactive 6-9	3	0.0	0
10.5	Au nonactive 9-12	2	0.0	0
13.5	Au nonactive 12-15	3	0.0	0
16.5	Au nonactive 15-18	3	0.0	0

n_n	17		
x_n		16.0	
sd_n			37.5

The *t* Statistic

μ_a = The Active SRB Au values

μ_n = The Non-active SRB Au values

The following null hypothesis is considered	$H_o: \mu_a = \mu_n$
The following alternative hypothesis is also considered	$H_a: \mu_a \neq \mu_n$

The *t test* is a standard method of choosing between the two hypotheses.

$$t_s = \frac{|X_a - X_n| - 0}{SE_{(Xa - Xn)}} \qquad \text{where; } SE_{(Xa-Xn)} = \sqrt{[((sd_a)^2/n_a) + ((sd_n)^2/n_n)]}$$

If $t_s < 1$ do not reject the null hypothesis

If $t_s > 1$ reject the null hypothesis and accept the alternative hypothesis

Note that the $|X_a - X_n|$ is subtracted from zero because H_o states that μ_a - μ_n equals zero; writing "$|X_a - X_n| - 0$" reminds us of what we are testing.

$$t_s = \frac{|1.1 - 16.0| - 0}{\sqrt{[((2.7)^2/18)+((16.0)^2/17)]}}$$

$t_s = 1.63$

$t_s > 1$ Therefore the null hypothesis is rejected and the alternative hypothesis is accepted $\mu_a \neq \mu_n$

The methylmercury values measured in the Active SRB Au column are **not** the same as the methylmercury values measured in the Non-Active SRB Au column.

C-4. Statistical analysis of the % Organics in the Au sediment cores:

depth	name	n	%Organics	
1.5	Au active 0-3	1	3.2	
4.5	Au active 3-6	1	0.2	
7.5	Au active 6-9	1	0.1	
10.5	Au active 9-12	1	0.1	
13.5	Au active 12-15	1	0.1	
16.5	Au active 15-18	1	0.2	

n_a	6		
x_a		0.664	
sd_a			1.255

depth	name	n	%Organics	
1.5	Au nonactive 0-3	1	4.0	
4.5	Au nonactive 3-6	1	1.5	
7.5	Au nonactive 6-9	1	0.2	
10.5	Au nonactive 9-12	1	0.2	
13.5	Au nonactive 12-15	1	0.2	
16.5	Au nonactive 15-18	1	0.1	

n_n	6		
x_n		1.022	
sd_n			1.538

The *t* Statistic

μ_a = The Active SRB Cu-Zn values

μ_n = The Non-active SRB Cu-Zn values

The following null hypothesis is considered	$H_o: \mu_a = \mu_n$
The following alternative hypothesis is also considered	$H_a: \mu_a \neq \mu_n$

The *t test* is a standard method of choosing between the two hypotheses.

$$t_s = \frac{|X_a - X_n| - 0}{SE_{(Xa - Xn)}} \qquad \text{where; } SE_{(Xa-Xn)} = \sqrt{[((sd_a)^2/n_a) + ((sd_n)^2/n_n)]}$$

If $t_s < 1$ do not reject the null hypothesis

If $t_s > 1$ reject the null hypothesis and accept the alternative hypothesis

Note that the $|X_a - X_n|$ is subtracted from zero because H_o states that $\mu_a - \mu_n$ equals zero; writing "$|X_a - X_n| - 0$" reminds us of what we are testing.

$$t_s = \frac{|0.664 - 1.022| - 0}{\sqrt{[((0.1.25)^2/6)+((01.54)^2/6)]}}$$

$t_s = 0.44$

$t_s < 1$ Therefore the null hypothesis is not rejected and $\mu_a = \mu_n$

The % Organics values measured in the Active SRB Au column are the same as the % Organics values measured in the Non-Active SRB Au column.

Summary:
The total mercury and % Organics do *not* differ depending on whether the column was inhibited or not. The AVS and Methyl mercury do differ from the active and non-active SRB Au columns.

Appendix D

D-1. Warm Active SRB Cu-Zn and Non-active SRB Cu-Zn Columns

The grain size distribution of the initial Cu-Zn slurry was different than the one observed for both the Warm Active SRB and Non-active SRB Cu-Zn columns, at the end of the 4 month-experiment (Figure D-1 (a), (b), and (c)). The dominant grain size fraction in the fresh tailings was the 63-250 μm, whereas the sediments in both columns had a greater proportion of particles with a diameter greater than 250μm.

D-2. Active SRB Au and Non-active SRB Au Columns

The grain size distribution pattern of the initial old Au tailings was also different that the one observed in both the Warm Active SRB and Non-active SRB Au columns (Figure D-2 (a), (b), and (c)). The initial Au tailings contained a large fraction of particles between 63 and 250 μm, whereas the sediments in both columns displayed a larger abundance of larger particles (i.e., > 250 μm). In addition, the relative abundance of large particles (> 250 μm) appeared to increase with depth in both columns.

a)

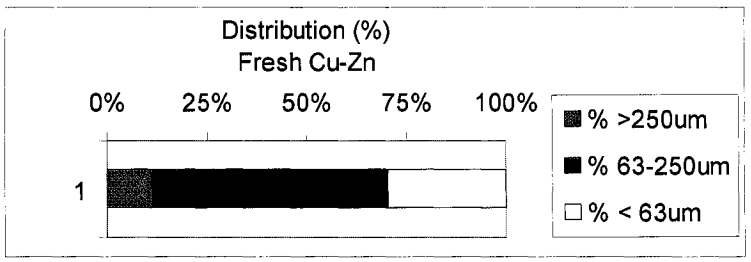

b)

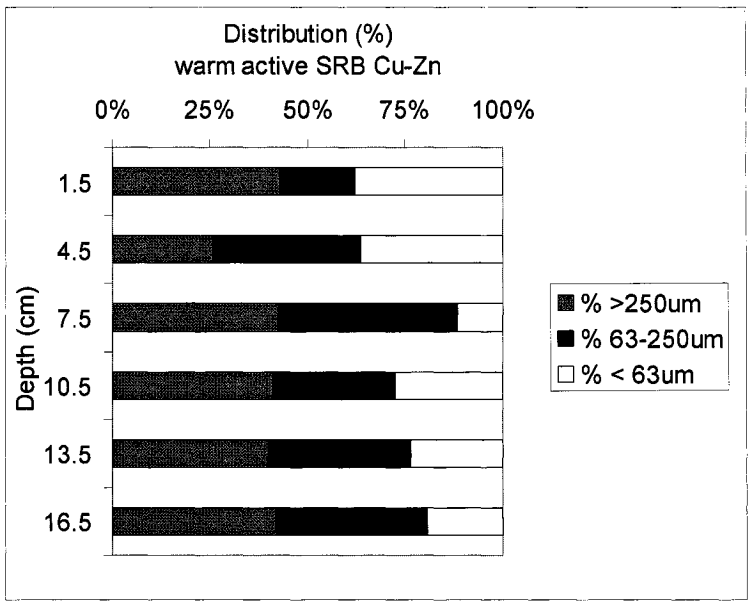

c)

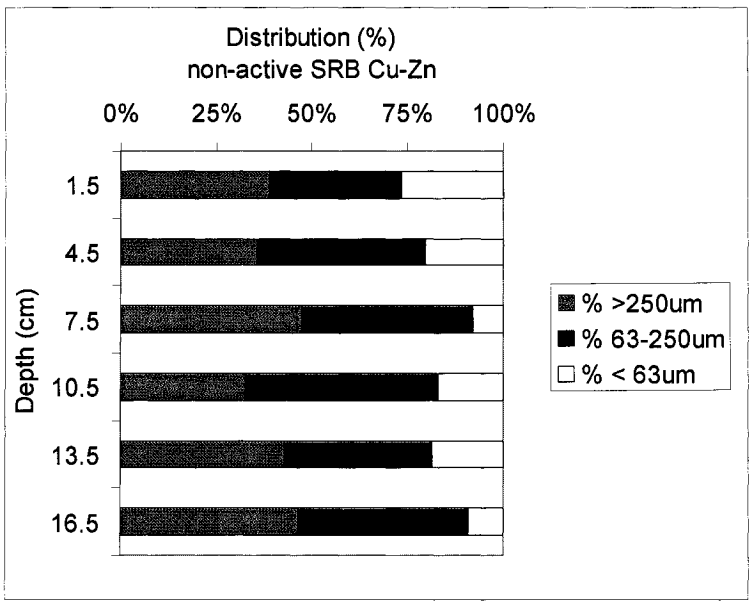

Figure D-1. Grain size distribution in the fresh Cu-Zn tailings (a) Warm Active SRB Cu-Zn (b) and Non-active SRB Cu-Zn columns (c).

a)

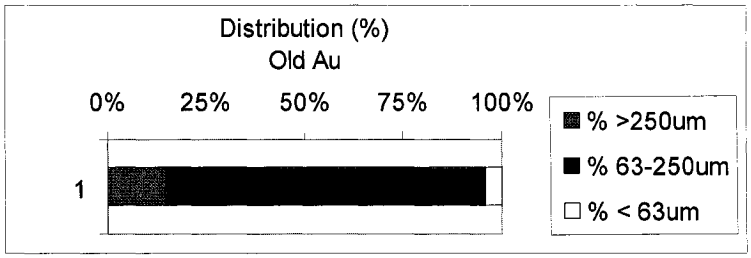

b)

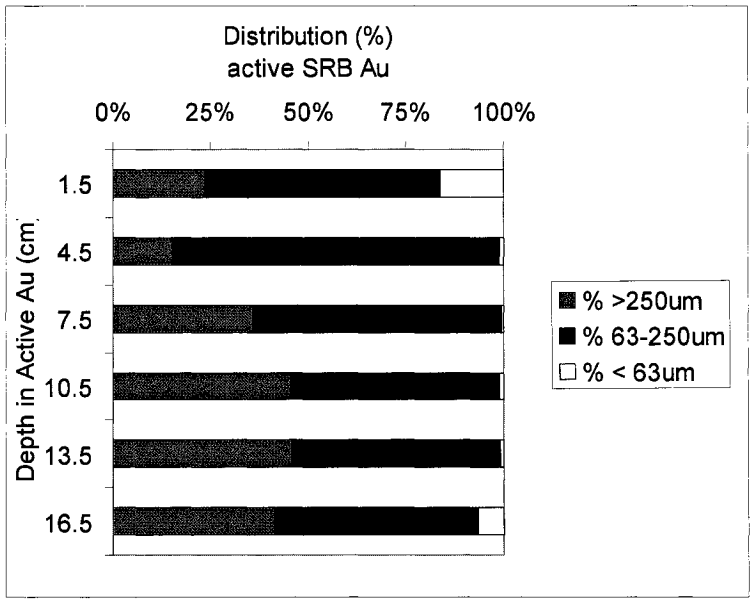

c)

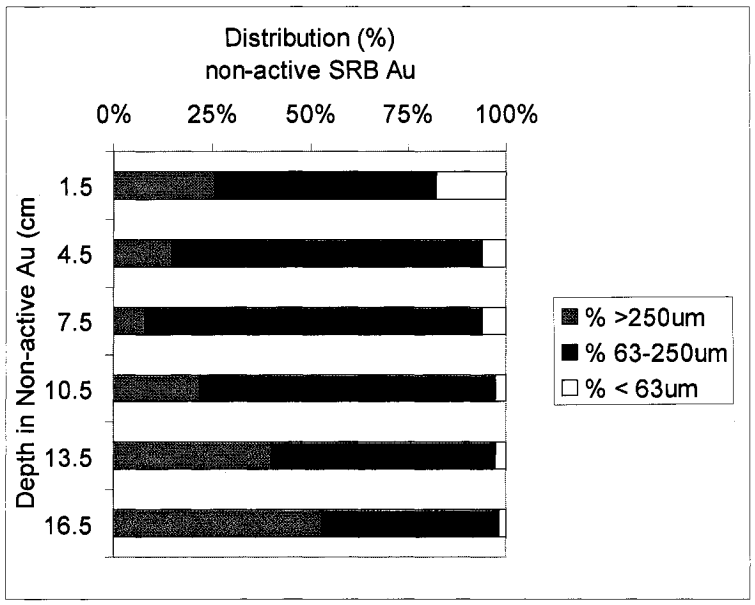

Figure D-2. Grain size distribution in the initial old Au tailings (a) Active SRB Au (b) and Non-active SRB Au columns (c).

Appendix E

E-1. The t Statistics of the Warm active SRB and the Non-active SRB Cu-Zn aqueous phases.

μ_a = The Warm Active SRB Cu-Zn values
μ_n = The Non-active SRB Cu-Zn values

The following null hypothesis is considered	H_o: $\mu_a = \mu_n$
The following alternative hypothesis is also considered	H_a: $\mu_a \neq \mu_n$

The t test is a standard method of choosing between the two hypotheses.

$$t_s = \frac{|X_a - X_n| - 0}{SE_{(Xa - Xn)}} \qquad \text{where; } SE_{(Xa - Xn)} = \sqrt{[((sd_a)^2/n_a) + ((sd_n)^2/n_n)]}$$

If $t_s < 1$ do not reject the null hypothesis
If $t_s > 1$ reject the null hypothesis and accept the alternative hypothesis

Note that the $|X_a - X_n|$ is subtracted from zero because H_o states that μ_a - μ_n equals zero; writing "$|X_a - X_n| - 0$" reminds us of what we are testing.

E-1.1 Statistical analysis of pH in the aqueous phase of the Warm Active SRB and Non-active SRB Cu-Zn columns:

Warm active SRB Cu-Zn	Day	n	pH	
	8	1	7.26	
	28	1	7.03	
	49	1	7.35	
	70	1	7.79	
	106	1	8.09	
	125	1	8.09	
	n_a	**6**		
	x_a		**7.60**	
	sd_a			**0.45**

Non-active SRB Cu-Zn	Day	n	pH	
	8	1	6.63	
	28	1	6.39	
	49	1	6.26	
	70	1	6.16	
	106	1	6.54	
	125	1	6.77	
	n_n	**6**		
	x_n		**6.46**	
	sd_n			**0.23**

Xn-Xa	1.14
$(sd_a)^2/n_a)$	0.03
$(sd_n)^2/n_n)$	0.01
$\sqrt{[((sd_a)^2/n_a) + ((sd_n)^2/n_n)]}$	0.21
ts	5.52

t_s = 5.52
$t_s > 1$ Therefore the null hypothesis is rejected and $\mu_a \neq \mu_n$

The pH values measured in the Warm active SRB Cu-Zn column are not the same as the pH values measured in the Non-active SRB Cu-Zn column.

E-1.2 Statistical analysis of Eh in the aqueous phase of the Warm Active SRB and Non-active SRB Cu-Zn columns:

Warm active SRB Cu-Zn	Day	n	Eh (mv)	
	8	1	55.1	
	28	1	81	
	49	1	146	
	70	1	66	
	106	1	144	
	125	1	223	
	n_a	6		
	x_a		**119.18**	
	sd_a			**64.04**

Non-active SRB Cu-Zn	Day	n	Eh (mv)	
	8	1	138.4	
	28	1	64	
	49	1	95	
	70	1	71	
	106	1	58	
	125	1	208.47	
	n_n	6		
	x_n		**105.81**	
	sd_n			**58.25**

Xn-Xa	13.37
$(sd_a)^2/n_a)$	683.53
$(sd_n)^2/n_n)$	565.45
$\sqrt{[((sd_a)^2/n_a) + ((sd_n)^2/n_n)]}$	35.34
ts	0.38

$t_s = 0.38$
$t_s < 1$ Therefore the null hypothesis is not rejected and $\mu_a = \mu_n$

The Eh values measured in the Warm active SRB Cu-Zn column are the same as the Eh values measured in the Non-active SRB Cu-Zn column.

E-1.3 Statistical analysis of SO_4^{2-} in the aqueous phase of the Warm Active SRB and Non-active SRB Cu-Zn columns:

Warm active SRB Cu-Zn	Day	n	SO_4^{2-} (ppm)	
	8	1	130	
	28	1	175	
	49	1	95	
	70	1	200	
	106	1	300	
	125	1	1152	
	n_a	6		
	x_a		**342.00**	
	sd_a			**402.96**

Non-active SRB Cu-Zn	Day	n	SO_4^{2-} (ppm)	
	8	1	78	
	28	1	250	
	49	1	450	
	70	1	489.9	
	106	1	537.5	
	125	1	1405.6	
	n_n	6		
	x_n		**535.17**	
	sd_n			**459.84**

Xn-Xa	193.17
$(sd_a)^2/n_a)$	27062.33
$(sd_n)^2/n_n)$	35242.78
$\sqrt{[((sd_a)^2/n_a) + ((sd_n)^2/n_n)]}$	249.61
ts	0.77

$t_s = 0.77$
$t_s < 1$ Therefore the null hypothesis is not rejected and $\mu_a = \mu_n$

The SO_4^{2-} values measured in the Warm active SRB Cu-Zn column are the same as the SO_4^{2-} values measured in the Non-active SRB Cu-Zn column.

E-1.4 Statistical analysis of S^{2-} in the aqueous phase of the Warm Active SRB and Non-active SRB Cu-Zn columns:

Warm active SRB Cu-Zn	Day	n	S^{2-} (ppm)	
	8	1	0.644	
	28	1	0.052	
	49	1	0.198	
	70	1	0.09	
	106	1	0.004	
	125	1	0.127	
n_a	**6**			
x_a		**0.19**		
sd_a			**0.23**	

Non-active SRB Cu-Zn	Day	n	S^{2-} (ppm)	
	8	1	1.292	
	28	1	0.168	
	49	1	0.196	
	70	1	0.109	
	106	1	0.128	
	125	1	0.9754	
n_n	**6**			
x_n		**0.48**		
sd_n			**0.52**	

Xn-Xa	0.29
$(sd_a)^2/n_a)$	0.01
$(sd_n)^2/n_n)$	0.04
$\sqrt{[((sd_a)^2/n_a) + ((sd_n)^2/n_n)]}$	0.23
ts	1.26

$t_s = 1.62$
$t_s > 1$ Therefore the null hypothesis is not rejected and $\mu_a \neq \mu_n$

The S^{2-} values measured in the Warm active SRB Cu-Zn column are not the same as the S^{2-} values measured in the Non-active SRB Cu-Zn column.

E-1.5 Statistical analysis of Fe_{diss} in the aqueous phase of the Warm Active SRB and Non-active SRB Cu-Zn columns:

Warm active SRB Cu-Zn	Day	n	Fe_{diss} (ppm)	
	8	1	0.66	
	28	1	1.84	
	49	1	0.3	
	70	1	1.54	
	106	1	0.44	
	125	1	1.771	
n_a	**6**			
x_a		**1.09**		
sd_a			**0.70**	

Non-active SRB Cu-Zn	Day	n	Fe_{diss} (ppm)	
	8	1	2.82	
	28	1	119	
	49	1	107.1	
	70	1	90.9	
	106	1	79.8	
	125	1	138.8	
n_n	**6**			
x_n		**89.74**		
sd_n			**47.37**	

Xn-Xa	88.64
$(sd_a)^2/n_a)$	0.08

$(sd_n)^2/n_n)$	373.99
$\sqrt{[((sd_a)^2/n_a) + ((sd_n)^2/n_n)]}$	19.34
ts	4.58

$t_s = 4.58$
$t_s > 1$ Therefore the null hypothesis is rejected and $\mu_a \neq \mu_n$

The Fe_{diss} values measured in the Warm active SRB Cu-Zn column are not the same as the Fe_{diss} values measured in the Non-active SRB Cu-Zn column.

E-1.6 Statistical analysis of DOC in the aqueous phase of the Warm Active SRB and Non-active SRB Cu-Zn columns:

Warm active SRB Cu-Zn	Day	n	DOC (ppm)	
	8	1	309.6	
	28	1	179.6	
	49	1	62.3	
	70	1	3.1	
	106	1	1.9	
	125	1	247.9	
	n_a	**6**		
	x_a		**134.07**	
	sd_a			**130.85**

Non-active SRB Cu-Zn	Day	n	DOC (ppm)	
	8	1	388.3	
	28	1	136	
	49	1	71.1	
	70	1	70	
	106	1	48.8	
	125	1	412.1	
	n_n	**6**		
	x_n		**187.72**	
	sd_n			**167.34**

Xn-Xa	53.65
$(sd_a)^2/n_a)$	2853.80
$(sd_n)^2/n_n)$	4667.02
$\sqrt{[((sd_a)^2/n_a) + ((sd_n)^2/n_n)]}$	86.72
ts	0.62

$t_s = 0.62$
$t_s < 1$ Therefore the null hypothesis is not rejected and $\mu_a = \mu_n$

The DOC values measured in the Warm active SRB Cu-Zn column are the same as the DOC values measured in the Non-active SRB Cu-Zn column.

E-1.7 Statistical analysis of Hg_{tot} in the aqueous phase of the Warm Active SRB and Non-active SRB Cu-Zn columns:

Warm active SRB Cu-Zn	Day	n	Hg_{tot} (ppt)	
	8	1	14.9	
	28	1	11.75	
	49	1	8.62	
	70	1	43.2	
	106	1	7.24	
	125	1	0	
	n_a	**6**		

Non-active SRB Cu-Zn	Day	n	Hg_{tot} (ppt)	
	8	1	6.26	
	28	1	86.36	
	49	1	11.64	
	70	1	3.05	
	106	1	0	
	125	1	0	
	n_n	**6**		

	x_a		14.29		x_n		17.89	
	sd_a			15.02	sd_n			33.83

Xn-Xa	3.60
$(sd_a)^2/n_a)$	37.62
$(sd_n)^2/n_n)$	190.76
$\sqrt{[((sd_a)^2/n_a) + ((sd_n)^2/n_n)]}$	15.11
ts	0.24

$t_s = 0.24$
$t_s < 1$ Therefore the null hypothesis is not rejected and $\mu_a = \mu_n$

The Hg_{tot} values measured in the Warm active SRB Cu-Zn column are the same as the Hg_{tot} values measured in the Non-active SRB Cu-Zn column.

E-1.8 Statistical analysis of MeHg in the aqueous phase of the Warm Active SRB and Non-active SRB Cu-Zn columns:

Warm active SRB Cu-Zn	Day	n	MeHg (ppt)	
	8	1	0	
	28	1	0	
	49	1	0	
	70	1	0	
	106	1	0	
	125	1	0.45	
	n_a	6		
	x_a		0.08	
	sd_a			0.18

Non-active SRB Cu-Zn	Day	n	MeHg (ppt)	
	8	1	0	
	28	1	0	
	49	1	0	
	70	1	0	
	106	1	0	
	125	1	0.48	
	n_n	6		
	x_n		0.08	
	sd_n			0.20

Xn-Xa	0.01
$(sd_a)^2/n_a)$	0.01
$(sd_n)^2/n_n)$	0.01
$\sqrt{[((sd_a)^2/n_a) + ((sd_n)^2/n_n)]}$	0.11
ts	0.05

$t_s = 0.05$
$t_s < 1$ Therefore the null hypothesis is not rejected and $\mu_a = \mu_n$

The MeHg values measured in the Warm active SRB Cu-Zn column are the same as the MeHg values measured in the Non-active SRB Cu-Zn column.

E-1.9 Statistical analysis of SRB populations in the aqueous phase of the Warm Active SRB and Non-active SRB Cu-Zn columns:

Warm active SRB Cu-Zn	Day	n	SRB CFU/g dry wt. sed.	
	0	5	2.80E+04	
	28	5	2.70E+06	

Non-active SRB Cu-Zn	Day	n	SRB CFU/g dry wt. sed.	
	0	5	2.80E+04	
	28	5	4.30E+04	

	49	5	1.30E+07		49	5	4.30E+05	
	125	5	4.60E+06		125	5	9.40E+03	
n_a	20			n_n	20			
x_a		5.08E+06		x_n		1.28E+05		
sd_a			5.60E+06	sd_n			2.02E+05	

Xn-Xa	4.95E+06
$(sd_a)^2/n_a)$	1.57E+12
$(sd_n)^2/n_n)$	2.04E+09
$\sqrt{[((sd_a)^2/n_a) + ((sd_n)^2/n_n)]}$	1.25E+06
ts	3.95

$t_s = 3.95$
$t_s > 1$ Therefore the null hypothesis is not rejected and $\mu_a \neq \mu_n$

The SRB populations at the sediment/water interface of the Warm active SRB Cu-Zn column are not the same as the SRB populations at the sediment/water interface of the Non-active SRB Cu-Zn columns.

E-2. The t Statistics of the Warm active SRB and the Cold active Cu-Zn aqueous phases.

μ_a = The Warm Active SRB Cu-Zn values
μ_n = The Cold active SRB Cu-Zn values

The following null hypothesis is considered	H_o: $\mu_a = \mu_n$
The following alternative hypothesis is also considered	H_a: $\mu_a \neq \mu_n$

The t test is a standard method of choosing between the two hypotheses.

$$t_s = \frac{|X_a - X_n| - 0}{SE_{(Xa - Xn)}} \qquad \text{where; } SE_{(Xa - Xn)} = \sqrt{[((sd_a)^2/n_a) + ((sd_n)^2/n_n)]}$$

If $t_s < 1$ do not reject the null hypothesis
If $t_s > 1$ reject the null hypothesis and accept the alternative hypothesis

Note that the $|X_a - X_n|$ is subtracted from zero because H_o states that μ_a - μ_n equals zero; writing "$|X_a - X_n| - 0$" reminds us of what we are testing.

E-2.1 Statistical analysis of pH in the aqueous phase of the Warm Active SRB and Cold active SRB Cu-Zn columns:

Warm active SRB Cu-Zn	Day	n	pH	
	8	1	7.26	
	28	1	7.03	
	49	1	7.35	
	70	1	7.79	
	106	1	8.09	

Cold active SRB Cu-Zn	Day	n	pH	
	8	1	7.58	
	28	1	7.3	
	49	1	7.17	
	70	1	7.46	
	106	1	6.89	

	125	1	8.09			125	1	6.95	
	n_a	6				n_n	6		
	x_a		7.60			x_n		7.23	
	sd_a			0.45		sd_n			0.27

Xn-Xa	0.38
$(sd_a)^2/n_a)$	0.03
$(sd_n)^2/n_n)$	0.01
$\sqrt{[((sd_a)^2/n_a) + ((sd_n)^2/n_n)]}$	0.22
ts	1.75

$t_s = 1.75$
$t_s > 1$ Therefore the null hypothesis is rejected and $\mu_a \neq \mu_n$

The pH values measured in the Warm active SRB Cu-Zn column are not the same as the pH values measured in the Cold active SRB Cu-Zn column.

E-2.2 Statistical analysis of Eh in the aqueous phase of the Warm Active SRB and Cold active SRB Cu-Zn columns:

Warm active SRB Cu-Zn	Day	n	Eh (mv)	
	8	1	55.1	
	28	1	81	
	49	1	146	
	70	1	66	
	106	1	144	
	125	1	223	
	n_a	6		
	x_a		119.18	
	sd_a			64.04

Cold active SRB Cu-Zn	Day	n	Eh (mv)	
	8	1	36.1	
	28	1	27	
	49	1	129	
	70	1	105	
	106	1	89	
	125	1	160.4	
	n_n	6		
	x_n		91.08	
	sd_n			52.10

Xn-Xa	28.10
$(sd_a)^2/n_a)$	683.53
$(sd_n)^2/n_n)$	452.34
$\sqrt{[((sd_a)^2/n_a) + ((sd_n)^2/n_n)]}$	33.70
ts	0.83

$t_s = 0.83$
$t_s < 1$ Therefore the null hypothesis is not rejected and $\mu_a = \mu_n$

The Eh values measured in the Warm active SRB Cu-Zn column are the same as the Eh values measured in the Cold active SRB Cu-Zn column.

E-2.3 Statistical analysis of SO_4^{2-} in the aqueous phase of the Warm Active SRB and Cold active SRB Cu-Zn columns:

Warm active	Day	n	SO_4^{2-} (ppm)	

Cold active	Day	n	SO_4^{2-} (ppm)	

SRB Cu-Zn				
	8	1	130	
	28	1	175	
	49	1	95	
	70	1	200	
	106	1	300	
	125	1	1152	
	n_a	6		
	x_a		342.00	
	sd_a			402.96

SRB Cu-Zn				
	8	1	195	
	28	1	200	
	49	1	195	
	70	1	1623	
	106	1	200	
	125	1	104.8	
	n_n	6		
	x_n		419.63	
	sd_n			590.70

Xn-Xa	77.63
$(sd_a)^2/n_a)$	27062.33
$(sd_n)^2/n_n)$	58153.64
$\sqrt{[((sd_a)^2/n_a) + ((sd_n)^2/n_n)]}$	291.92
ts	0.27

$t_s = 0.26$
$t_s < 1$ Therefore the null hypothesis is not rejected and $\mu_a = \mu_n$

The SO_4^{2-} values measured in the Warm active SRB Cu-Zn column are the same as the SO_4^{2-} values measured in the Cold active SRB Cu-Zn column.

E-2.4 Statistical analysis of S^{2-} in the aqueous phase of the Warm Active SRB and Cold active SRB Cu-Zn columns:

Warm active SRB Cu-Zn	Day	n	S^{2-} (ppm)	
	8	1	0.644	
	28	1	0.052	
	49	1	0.198	
	70	1	0.09	
	106	1	0.004	
	125	1	0.127	
	n_a	6		
	x_a		0.19	
	sd_a			0.23

Cold active SRB Cu-Zn	Day	n	S^{2-} (ppm)	
	8	1	0.172	
	28	1	0.336	
	49	1	0.278	
	70	1	0.65	
	106	1	0.029	
	125	1	0.132	
	n_n	6		
	x_n		0.27	
	sd_n			0.22

Xn-Xa	0.08
$(sd_a)^2/n_a)$	0.01
$(sd_n)^2/n_n)$	0.01
$\sqrt{[((sd_a)^2/n_a) + ((sd_n)^2/n_n)]}$	0.13
ts	0.62

$t_s = 0.62$
$t_s < 1$ Therefore the null hypothesis is not rejected and $\mu_a = \mu_n$

The S^{2-} values measured in the Warm active SRB Cu-Zn column are the same as the S^{2-} values measured in the Cold active SRB Cu-Zn column.

E-2.5 Statistical analysis of Fe_{diss} in the aqueous phase of the Warm Active SRB and Cold active SRB Cu-Zn columns:

Warm active SRB Cu-Zn	Day	n	Fe_{diss} (ppm)	
	8	1	0.66	
	28	1	1.84	
	49	1	0.3	
	70	1	1.54	
	106	1	0.44	
	125	1	1.771	
	n_a	6		
	x_a		**1.09**	
	sd_a			**0.70**

Cold active SRB Cu-Zn	Day	n	Fe_{diss} (ppm)	
	8	1	1.48	
	28	1	3.54	
	49	1	0.7	
	70	1	2.61	
	106	1	1.4	
	125	1	2.22	
	n_n	6		
	x_n		**1.99**	
	sd_n			**1.01**

Xn-Xa	0.90
$(sd_a)^2/n_a)$	0.08
$(sd_n)^2/n_n)$	0.17
$\sqrt{[((sd_a)^2/n_a) + ((sd_n)^2/n_n)]}$	0.50
ts	1.79

$t_s = 1.79$
$t_s > 1$ Therefore the null hypothesis is rejected and $\mu_a \neq \mu_n$

The Fe_{diss} values measured in the Warm active SRB Cu-Zn column are not the same as the Fe_{diss} values measured in the Cold active SRB Cu-Zn column.

E-2.6 Statistical analysis of DOC in the aqueous phase of the Warm Active SRB and Cold active SRB Cu-Zn columns:

Warm active SRB Cu-Zn	Day	n	DOC (ppm)	
	8	1	309.6	
	28	1	179.6	
	49	1	62.3	
	70	1	3.1	
	106	1	1.9	
	125	1	247.9	
	n_a	6		
	x_a		**134.07**	
	sd_a			**130.85**

Cold active SRB Cu-Zn	Day	n	DOC (ppm)	
	8	1	260.7	
	28	1	91.5	
	49	1	63.4	
	70	1	2.9	
	106	1	0.9	
	125	1	238.6	
	n_n	6		
	x_n		**109.67**	
	sd_n			**114.14**

Xn-Xa	24.40
$(sd_a)^2/n_a)$	2853.80
$(sd_n)^2/n_n)$	2171.16
$\sqrt{[((sd_a)^2/n_a) + ((sd_n)^2/n_n)]}$	70.89
ts	0.34

$t_s = 0.34$
$t_s < 1$ Therefore the null hypothesis is not rejected and $\mu_a = \mu_n$

The DOC values measured in the Warm active SRB Cu-Zn column are the same as the DOC values measured in the Cold active SRB Cu-Zn column.

E-2.7 Statistical analysis of Hg_{tot} in the aqueous phase of the Warm Active SRB and Cold active SRB Cu-Zn columns:

Warm active SRB Cu-Zn	Day	n	Hg_{tot} (ppt)	
	8	1	14.9	
	28	1	11.7	
	49	1	8.62	
	70	1	43.2	
	106	1	7.24	
	125	1	0	
	n_a	6		
	x_a		**14.28**	
	sd_a			**15.03**

Cold active SRB Cu-Zn	Day	n	Hg_{tot} (ppt)	
	8	1	2.38	
	28	1	11.3	
	49	1	10.2	
	70	1	0	
	106	1	3.8	
	125	1	0	
	n_n	6		
	x_n		**4.61**	
	sd_n			**4.98**

Xn-Xa	9.66
$(sd_a)^2/n_a)$	37.63
$(sd_n)^2/n_n)$	4.14
$\sqrt{[((sd_a)^2/n_a) + ((sd_n)^2/n_n)]}$	6.46
ts	1.50

$t_s = 1.50$
$t_s > 1$ Therefore the null hypothesis is rejected and $\mu_a \neq \mu_n$

The Hg_{tot} values measured in the Warm active SRB Cu-Zn column are not the same as the Hg_{tot} values measured in the Cold active SRB Cu-Zn column.

E-2.8 Statistical analysis of MeHg in the aqueous phase of the Warm Active SRB and Cold active SRB Cu-Zn columns:

Warm active SRB Cu-Zn	Day	n	MeHg (ppt)	
	8	1	0	
	28	1	0	
	49	1	0	
	70	1	0	
	106	1	0	
	125	1	0.45	
	n_a	6		
	x_a		**0.08**	
	sd_a			**0.18**

Cold active SRB Cu-Zn	Day	n	MeHg (ppt)	
	8	1	0	
	28	1	0	
	49	1	0	
	70	1	0.89	
	106	1	0	
	125	1	0	
	n_n	6		
	x_n		**0.15**	
	sd_n			**0.36**

Xn-Xa	0.07
$(sd_a)^2/n_a)$	0.01
$(sd_n)^2/n_n)$	0.02
$\sqrt{[((sd_a)^2/n_a) + ((sd_n)^2/n_n)]}$	0.17
ts	0.44

t_s = 0.44
$t_s < 1$ Therefore the null hypothesis is not rejected and $\mu_a = \mu_n$

The MeHg values measured in the Warm active SRB Cu-Zn column are the same as the MeHg values measured in the Cold active SRB Cu-Zn column.

E-2.9 Statistical analysis of SRB populations in the aqueous phase of the Warm Active SRB and Cold active SRB Cu-Zn columns:

Warm active SRB Cu-Zn	Day	n	SRB CFU/g dry wt. sed.	
	0	5	2.80E+04	
	28	5	2.70E+06	
	49	5	1.30E+07	
	125	5	4.60E+06	
	n_a	**20**		
	x_a		**5.08E+06**	
	sd_a			**5.60E+06**

Cold active SRB Cu-Zn	Day	n	SRB CFU/g dry wt. sed.	
	0	5	2.80E+04	
	28	5	1.20E+07	
	49	5	9.00E+06	
	125	5	8.50E+06	
	n_n	**20**		
	x_n		**7.38E+06**	
	sd_n			**5.14E+06**

Xn-Xa	2.30E+06
$(sd_a)^2/n_a)$	1.57E+12
$(sd_n)^2/n_n)$	1.32E+12
$\sqrt{[((sd_a)^2/n_a) + ((sd_n)^2/n_n)]}$	1.70E+06
ts	1.35

t_s = 1.35
$t_s > 1$ Therefore the null hypothesis is rejected and $\mu_a \neq \mu_n$

The SRB populations at the sediment/water interface of the Warm active SRB Cu-Zn column are not the same as the SRB populations at the sediment/water interface of the Cold active SRB Cu-Zn column.

E-3. The t Statistics of the High Sulfate and the Low Sulfate Cu-Zn aqueous phases.

μ_a = The High Sulfate Cu-Zn values
μ_n = The Low Sulfate Cu-Zn values

The following null hypothesis is considered	H_o: $\mu_a = \mu_n$
The following alternative hypothesis is also considered	H_a: $\mu_a \neq \mu_n$

The t test is a standard method of choosing between the two hypotheses.

$$t_s = \frac{|X_a - X_n| - 0}{SE_{(Xa - Xn)}} \qquad \text{where; } SE_{(Xa - Xn)} = \sqrt{[((sd_a)^2/n_a) + ((sd_n)^2/n_n)]}$$

If $t_s < 1$ do not reject the null hypothesis
If $t_s > 1$ reject the null hypothesis and accept the alternative hypothesis

Note that the $|X_a - X_n|$ is subtracted from zero because H_o states that μ_a - μ_n equals zero; writing "$|X_a - X_n| - 0$" reminds us of what we are testing.

E-3.1 Statistical analysis of pH in the aqueous phase of the High Sulfate and Low Sulfate Cu-Zn columns:

High Sulfate Cu-Zn	Day	n	pH		Low Sulfate Cu-Zn	Day	n	pH	
	12	1	7.9			12	1	7.76	
	41	1	7.33			41	1	7.3	
	76	1	8.07			76	1	8.14	
	110	1	8.9			110	1	8.59	
	125	1	8.22			125	1	8.6	
n_a	5				n_n	5			
x_a		8.08			x_n		8.08		
sd_a			0.57		sd_n			0.56	

Xn-Xa	0.01
$(sd_a)^2/n_a)$	0.06
$(sd_n)^2/n_n)$	0.06
$\sqrt{[((sd_a)^2/n_a) + ((sd_n)^2/n_n)]}$	0.36
ts	0.02

$t_s = 0.02$
$t_s < 1$ Therefore the null hypothesis is not rejected and $\mu_a = \mu_n$

The pH values measured in the High Sulfate Cu-Zn column are the same as the pH values measured in the Low Sulfate Cu-Zn column.

E-3.2 Statistical analysis of Eh in the aqueous phase of the High Sulfate and Low Sulfate Cu-Zn columns:

High Sulfate Cu-Zn	Day	n	Eh (mv)		Low Sulfate Cu-Zn	Day	n	Eh (mv)	
	12	1	5			12	1	59	
	41	1	64			41	1	74	
	76	1	211			76	1	157	
	110	1	276			110	1	338.7	
	125	1	189.4			125	1	271.7	
n_a	5				n_n	5			
x_a		149.08			x_n		180.08		
sd_a			111.32		sd_n			122.48	

Xn-Xa	31.00
$(sd_a)^2/n_a)$	2478.31
$(sd_n)^2/n_n)$	3000.03
$\sqrt{[((sd_a)^2/n_a) + ((sd_n)^2/n_n)]}$	74.02
ts	0.42

$t_s = 0.42$
$t_s < 1$ Therefore the null hypothesis is not rejected and $\mu_a = \mu_n$

The Eh values measured in the High Sulfate Cu-Zn Zn column are the same as the Eh values measured in the Low Sulfate Cu-Zn column.

E-3.3 Statistical analysis of SO_4^{2-} in the aqueous phase of the High Sulfate and Low Sulfate Cu-Zn columns:

High Sulfate Cu-Zn	Day	n	SO_4^{2-} (ppm)	
	12	1	35729	
	41	1	12158	
	76	1	12431	
	110	1	123133	
	125	1	12106.8	
n_a	**5**			
x_a		**39111.56**		
sd_a			**48058.94**	

Low Sulfate Cu-Zn	Day	n	SO_4^{2-} (ppm)	
	12	1	2457	
	41	1	2724	
	76	1	2226	
	110	1	588	
	125	1	1763	
n_n	**5**			
x_n		**1951.60**		
sd_n			**839.99**	

Xn-Xa	37159.96
$(sd_a)^2/n_a)$	461932391.65
$(sd_n)^2/n_n)$	141115.06
$\sqrt{[((sd_a)^2/n_a) + ((sd_n)^2/n_n)]}$	21495.90
ts	1.73

$t_s = 1.73$
$t_s > 1$ Therefore the null hypothesis is rejected and $\mu_a \neq \mu_n$

The SO_4^{2-} values measured in the High Sulfate Cu-Zn column are not same as the SO_4^{2-} values measured in the Low Sulfate Cu-Zn column.

E-3.4 Statistical analysis of S^{2-} in the aqueous phase of the High Sulfate and Low Sulfate Cu-Zn columns:

High Sulfate Cu-Zn	Day	n	S^{2-} (ppm)	
	12	1	0.004	
	41	1	0.01	
	76	1	0.582	
	110	1	0.635	
	125	1	4.116	
n_a	**5**			
x_a		**1.07**		
sd_a			**1.73**	

Low Sulfate Cu-Zn	Day	n	S^{2-} (ppm)	
	12	1	0.01	
	41	1	0.001	
	76	1	0.071	
	110	1	0.9695	
	125	1	1.404	
n_n	**5**			
x_n		**0.49**		
sd_n			**0.65**	

Xn-Xa	0.58
$(sd_a)^2/n_a)$	0.60
$(sd_n)^2/n_n)$	0.09
$\sqrt{[((sd_a)^2/n_a) + ((sd_n)^2/n_n)]}$	0.83

ts	0.70	

$t_s = 0.70$
$t_s < 1$ Therefore the null hypothesis is not rejected and $\mu_a = \mu_n$

The S^{2-} values measured in the High Sulfate Cu-Zn column are the same as the S^{2-} values measured in the Low Sulfate Cu-Zn column.

E-3.5 Statistical analysis of Fe_{diss} in the aqueous phase of the High Sulfate and Low Sulfate Cu-Zn columns:

High Sulfate Cu-Zn	Day	n	Fe_{diss} (ppm)	
	12	1	54.57	
	41	1	71.01	
	76	1	0.42	
	110	1	0.02	
	125	1	0	
	n_a	**5**		
	x_a		**25.20**	
	sd_a			**34.80**

Low Sulfate Cu-Zn	Day	n	Fe_{diss} (ppm)	
	12	1	45.3	
	41	1	91.34	
	76	1	0.89	
	110	1	0.07	
	125	1	0.02	
	n_n	**5**		
	x_n		**27.52**	
	sd_n			**40.64**

Xn-Xa	2.32
$(sd_a)^2/n_a)$	242.21
$(sd_n)^2/n_n)$	330.40
$\sqrt{[((sd_a)^2/n_a) + ((sd_n)^2/n_n)]}$	23.93
ts	0.10

$t_s = 0.10$
$t_s < 1$ Therefore the null hypothesis is not rejected and $\mu_a = \mu_n$

The Fe_{diss} values measured in the High Sulfate Cu-Zn column are the same as the Fe_{diss} values measured in the Low Sulfate Cu-Zn column.

E-3.6 Statistical analysis of DOC in the aqueous phase of the High Sulfate and Low Sulfate Cu-Zn columns:

High Sulfate Cu-Zn	Day	n	DOC (ppm)	
	12	1	10.2	
	41	1	4.9	
	76	1	11.1	
	110	1	16.2	
	125	1	85.4	
	n_a	**5**		
	x_a		**25.56**	
	sd_a			**33.69**

Low Sulfate Cu-Zn	Day	n	DOC (ppm)	
	12	1	9.8	
	41	1	3.4	
	76	1	4.5	
	110	1	7.7	
	125	1	7.6	
	n_n	**5**		
	x_n		**6.60**	
	sd_n			**2.60**

Xn-Xa	18.96

$(sd_a)^2/n_a)$	227.01
$(sd_n)^2/n_n)$	1.36
$\sqrt{[((sd_a)^2/n_a) + ((sd_n)^2/n_n)]}$	15.11
ts	1.25

$t_s = 1.25$
$t_s > 1$ Therefore the null hypothesis is rejected and $\mu_a \neq \mu_n$

The DOC values measured in the High Sulfate Cu-Zn column are not the same as the DOC values measured in the Low Sulfate Cu-Zn column.

E-3.7 Statistical analysis of Hg_{tot} in the aqueous phase of the High Sulfate and Low Sulfate Cu-Zn columns:

High Sulfate Cu-Zn	Day	n	Hg_{tot} (ppt)	
	12	1	48.5	
	41	1	0	
	76	1	3	
	110	1	4.6	
	125	1	6	
	n_a	**5**		
	x_a		**12.42**	
	sd_a			**20.29**

Low Sulfate Cu-Zn	Day	n	Hg_{tot} (ppt)	
	12	1	7.6	
	41	1	0	
	76	1	4.1	
	110	1	9.5	
	125	1	10.3	
	n_n	**5**		
	x_n		**6.30**	
	sd_n			**4.26**

Xn-Xa	6.12
$(sd_a)^2/n_a)$	82.36
$(sd_n)^2/n_n)$	3.62
$\sqrt{[((sd_a)^2/n_a) + ((sd_n)^2/n_n)]}$	9.27
ts	0.66

$t_s = 0.66$
$t_s < 1$ Therefore the null hypothesis is not rejected and $\mu_a = \mu_n$

The Hg_{tot} values measured in the High Sulfate Cu-Zn column are the same as the Hg_{tot} values measured in the Low Sulfate Cu-Zn column.

E-3.8 Statistical analysis of MeHg in the aqueous phase of the High Sulfate and Low Sulfate Cu-Zn columns:

High Sulfate Cu-Zn	Day	n	MeHg (ppt)	
	12	1	0	
	41	1	0	
	76	1	0	
	110	1	0	
	125	1	0	
	n_a	**5**		
	x_a		**0.00**	

Low Sulfate Cu-Zn	Day	n	MeHg (ppt)	
	12	1	0	
	41	1	0	
	76	1	0	
	110	1	0	
	125	1	0	
	n_n	**5**		
	x_n		**0.00**	

	sd_a			0.00	sd_n		0.00

Xn-Xa	0.00
$(sd_a)^2/n_a)$	0.00
$(sd_n)^2/n_n)$	0.00
$\sqrt{[((sd_a)^2/n_a) + ((sd_n)^2/n_n)]}$	0.00
ts	0

$t_s = 0$
$t_s < 1$ Therefore the null hypothesis is not rejected and $\mu_a = \mu_n$

There was no MeHg measured in either the High Sulfate or Low Sulfate Cu-Zn aqueous phases. They are statistically the same.

E-3.9 Statistical analysis of SRB populations in the aqueous phase of the High Sulfate and Low Sulfate Cu-Zn columns:

High Sulfate Cu-Zn	Day	n	SRB CFU/g dry wt. sed.	
	0	5	2.80E+04	
	12	5	1.30E+06	
	110	5	1.00E+06	
	125	5	5.50E+06	
	n_a	**20**		
	x_a		**1.96E+06**	
	sd_a			**2.42E+06**

Low Sulfate Cu-Zn	Day	n	SRB CFU/g dry wt. sed.	
	0	5	2.80E+04	
	12	5	3.40E+07	
	110	5	4.50E+07	
	125	5	7.50E+07	
	n_n	**20**		
	x_n		**3.85E+07**	
	sd_n			**3.10E+07**

Xn-Xa	3.66E+07
$(sd_a)^2/n_a)$	2.94E+11
$(sd_n)^2/n_n)$	4.79E+13
$\sqrt{[((sd_a)^2/n_a) + ((sd_n)^2/n_n)]}$	6.94E+06
ts	5.26

$t_s = 5.26$
$t_s > 1$ Therefore the null hypothesis is rejected and $\mu_a \neq \mu_n$

The SRB populations at the sediment/water interface of the High Sulfate Cu-Zn column are not the same as the SRB populations at the sediment/water interface of the Low Sulfate Cu-Zn column.

E-4. The t Statistics of the High DOC and the Low DOC Cu-Zn aqueous phases.

μ_a = The High DOC Cu-Zn values
μ_n = The Low DOC Cu-Zn values

The following null hypothesis is considered	H_o: $\mu_a = \mu_n$
The following alternative hypothesis is also considered	H_a: $\mu_a \neq \mu_n$

The t test is a standard method of choosing between the two hypotheses.

$$|X_a - X_n| - 0$$

$t_s = \dfrac{}{SE_{(Xa - Xn)}}$ where; $SE_{(Xa - Xn)} = \sqrt{[((sd_a)^2/n_a) + ((sd_n)^2/n_n)]}$

If $t_s < 1$ do not reject the null hypothesis
If $t_s > 1$ reject the null hypothesis and accept the alternative hypothesis

Note that the $|X_a - X_n|$ is subtracted from zero because H_o states that $\mu_a - \mu_n$ equals zero; writing "$|X_a - X_n| - 0$" reminds us of what we are testing.

E-4.1 Statistical analysis of pH in the aqueous phase of the High DOC and Low DOC Cu-Zn columns:

High DOC Cu-Zn	Day	n	pH	
	12	1	8.23	
	41	1	8.2	
	76	1	8.8	
	110	1	9.43	
	125	1	8.8	
	n_a	**5**		
	x_a		**8.69**	
	sd_a			**0.51**

Low DOC Cu-Zn	Day	n	pH	
	12	1	7.05	
	41	1	6.07	
	76	1	3.51	
	110	1	4.1	
	125	1	6	
	n_n	**5**		
	x_n		**5.35**	
	sd_n			**1.48**

Xn-Xa	3.35
$(sd_a)^2/n_a)$	0.05
$(sd_n)^2/n_n)$	0.44
$\sqrt{[((sd_a)^2/n_a) + ((sd_n)^2/n_n)]}$	0.70
ts	4.78

$t_s = 4.78$
$t_s > 1$ Therefore the null hypothesis is rejected and $\mu_a \neq \mu_n$

The pH values measured in the High DOC Cu-Zn column are not the same as the pH values measured in the Low DOC Cu-Zn column.

E-4.2 Statistical analysis of Eh in the aqueous phase of the High DOC and Low DOC Cu-Zn columns:

High DOC Cu-Zn	Day	n	Eh (mv)	
	12	1	-44	
	41	1	-26	
	76	1	130	
	110	1	277.9	
	125	1	-91.5	
	n_a	**5**		
	x_a		**49.28**	
	sd_a			**152.45**

Low DOC Cu-Zn	Day	n	Eh (mv)	
	12	1	133	
	41	1	203	
	76	1	351	
	110	1	294.2	
	125	1	28.8	
	n_n	**5**		
	x_n		**202.00**	
	sd_n			**127.93**

Xn-Xa	152.72
$(sd_a)^2/n_a)$	4648.50
$(sd_n)^2/n_n)$	3273.10
$\sqrt{[((sd_a)^2/n_a) + ((sd_n)^2/n_n)]}$	89.00

ts	1.72

$t_s = 1.72$
$t_s > 1$ Therefore the null hypothesis is rejected and $\mu_a \neq \mu_n$

The Eh values measured in the High DOC Cu-Zn Zn column are not the same as the Eh values measured in the Low DOC Cu-Zn column.

E-4.3 Statistical analysis of SO_4^{2-} in the aqueous phase of the High DOC and Low DOC Cu-Zn columns:

High DOC Cu-Zn	Day	n	SO_4^{2-} (ppm)	
	12	1	3442.5	
	41	1	1445	
	76	1	3300	
	110	1	1223.6	
	125	1	1233	
	n_a	**5**		
	x_a		**2128.82**	
	sd_a			**1138.74**

Low DOC Cu-Zn	Day	n	SO_4^{2-} (ppm)	
	12	1	2700	
	41	1	2735	
	76	1	2838	
	110	1	1286.4	
	125	1	1561.6	
	n_n	**5**		
	x_n		**2224.20**	
	sd_n			**738.67**

Xn-Xa	95.38
$(sd_a)^2/n_a)$	259347.21
$(sd_n)^2/n_n)$	109128.02
$\sqrt{[((sd_a)^2/n_a) + ((sd_n)^2/n_n)]}$	607.02
ts	0.16

$t_s = 0.16$
$t_s < 1$ Therefore the null hypothesis is not rejected and $\mu_a = \mu_n$

The SO_4^{2-} values measured in the High DOC Cu-Zn column are the same as the SO_4^{2-} values measured in the Low DOC Cu-Zn column.

E-4.4 Statistical analysis of S^{2-} in the aqueous phase of the High DOC and Low DOC Cu-Zn columns:

High DOC Cu-Zn	Day	n	S^{2-} (ppm)	
	12	1	0.002	
	41	1	3.33	
	76	1	0.05	
	110	1	0.933	
	125	1	0.16	
	n_a	**5**		
	x_a		**0.90**	
	sd_a			**1.41**

Low DOC Cu-Zn	Day	n	S^{2-} (ppm)	
	12	1	0.006	
	41	1	0.006	
	76	1	0.002	
	110	1	0.006	
	125	1	0.024	
	n_n	**5**		
	x_n		**0.01**	
	sd_n			**0.01**

Xn-Xa	0.89
$(sd_a)^2/n_a)$	0.40
$(sd_n)^2/n_n)$	0.00

$\sqrt{[((sd_a)^2/n_a) + ((sd_n)^2/n_n)]}$	0.63
ts	1.40

$t_s = 1.40$
$t_s > 1$ Therefore the null hypothesis is rejected and $\mu_a \neq \mu_n$

The S^{2-} values measured in the High DOC Cu-Zn column are not the same as the S^{2-} values measured in Low DOC Cu-Zn column.

E-4.5 Statistical analysis of Fe_{diss} in the aqueous phase of the High DOC and Low DOC Cu-Zn columns:

High DOC Cu-Zn	Day	n	Fe_{diss} (ppm)	
	12	1	26.1	
	41	1	0.2	
	76	1	4.1	
	110	1	0.2	
	125	1	40.2	
	n_a	**5**		
	x_a		**14.16**	
	sd_a			**18.11**

Low DOC Cu-Zn	Day	n	Fe_{diss} (ppm)	
	12	1	123.3	
	41	1	302.4	
	76	1	228.5	
	110	1	64.9	
	125	1	47.7	
	n_n	**5**		
	x_n		**153.36**	
	sd_n			**109.26**

Xn-Xa	139.20
$(sd_a)^2/n_a)$	65.58
$(sd_n)^2/n_n)$	2387.59
$\sqrt{[((sd_a)^2/n_a) + ((sd_n)^2/n_n)]}$	49.53
ts	2.81

$t_s = 2.81$
$t_s > 1$ Therefore the null hypothesis is rejected and $\mu_a \neq \mu_n$

The Fe_{diss} values measured in the High DOC Cu-Zn column are not the same as the Fe_{diss} values measured in the Low DOC Cu-Zn column.

E-4.6 Statistical analysis of DOC in the aqueous phase of the High DOC and Low DOC Cu-Zn columns:

High DOC Cu-Zn	Day	n	DOC (ppm)	
	12	1	1113.3	
	41	1	1952.9	
	76	1	1702.2	
	110	1	1792.6	
	125	1	1767	
	n_a	**5**		
	x_a		**1665.60**	
	sd_a			**322.23**

Low DOC Cu-Zn	Day	n	DOC (ppm)	
	12	1	2.4	
	41	1	1.5	
	76	1	1.2	
	110	1	0.7	
	125	1	0.7	
	n_n	**5**		
	x_n		**1.30**	
	sd_n			**0.70**

Xn-Xa	1664.30
$(sd_a)^2/n_a)$	20766.35
$(sd_n)^2/n_n)$	0.10

$\sqrt{[((sd_a)^2/n_a) + ((sd_n)^2/n_n)]}$	144.11
ts	11.55

$t_s = 11.55$
$t_s > 1$ Therefore the null hypothesis is rejected and $\mu_a \neq \mu_n$

The DOC values measured in the High DOC Cu-Zn column are not the same as the DOC values measured in the Low DOC Cu-Zn column.

E-4.7 Statistical analysis of Hg_{tot} in the aqueous phase of the High DOC and Low DOC Cu-Zn columns:

High DOC Cu-Zn	Day	n	Hg_{tot} (ppt)	
	12	1	7.1	
	41	1	0	
	76	1	0	
	110	1	0	
	125	1	0	
	n_a	**5**		
	x_a		**1.42**	
	sd_a			**3.18**

Low DOC Cu-Zn	Day	n	Hg_{tot} (ppt)	
	12	1	0	
	41	1	0	
	76	1	0	
	110	1	0	
	125	1	11	
	n_n	**5**		
	x_n		**2.20**	
	sd_n			**4.92**

Xn-Xa	0.78
$(sd_a)^2/n_a)$	2.02
$(sd_n)^2/n_n)$	4.84
$\sqrt{[((sd_a)^2/n_a) + ((sd_n)^2/n_n)]}$	2.62
ts	0.30

$t_s = 0.30$
$t_s < 1$ Therefore the null hypothesis is not rejected and $\mu_a = \mu_n$

The Hg_{tot} values measured in the High DOC Cu-Zn column are the same as the Hg_{tot} values measured in the Low DOC Cu-Zn column.

E-4.8 Statistical analysis of MeHg in the aqueous phase of the High DOC and Low DOC Cu-Zn columns:

High DOC Cu-Zn	Day	n	MeHg (ppt)	
	12	1	0	
	41	1	0.07	
	76	1	0.04	
	110	1	0.07	
	125	1	0.03	
	n_a	**5**		
	x_a		**0.04**	
	sd_a			**0.03**

Low DOC Cu-Zn	Day	n	MeHg (ppt)	
	12	1	0	
	41	1	0	
	76	1	0	
	110	1	0.11	
	125	1	0	
	n_n	**5**		
	x_n		**0.02**	
	sd_n			**0.05**

Xn-Xa	0.02
$(sd_a)^2/n_a)$	0.00
$(sd_n)^2/n_n)$	0.00

$\sqrt{[((sd_a)^2/n_a) + ((sd_n)^2/n_n)]}$	0.03
ts	0.78

$t_s = 0.78$
$t_s < 1$ Therefore the null hypothesis is not rejected and $\mu_a = \mu_n$

The MeHg values measured in the High DOC Cu-Zn column are the same as the MeHg values measured in the Low DOC Cu-Zn column.

E-4.9 Statistical analysis of SRB populations in the aqueous phase of the High DOC and Low DOC Cu-Zn columns:

High DOC Cu-Zn	Day	n	SRB CFU/g dry wt. sed.	
	0	5	2.80E+04	
	12	5	2.80E+04	
	110	5	2.30E+05	
	125	5	2.20E+08	
	n_a	**20**		
	x_a		**5.51E+07**	
	sd_a			**1.10E+08**

Low DOC Cu-Zn	Day	n	SRB CFU/g dry wt. sed.	
	0	5	2.80E+04	
	12	5	4.10E+04	
	110	5	1.60E+05	
	125	5	1.50E+06	
	n_n	**20**		
	x_n		**4.32E+05**	
	sd_n			**7.14E+05**

Xn-Xa	5.46E+07
$(sd_a)^2/n_a)$	6.04E+14
$(sd_n)^2/n_n)$	2.55E+10
$\sqrt{[((sd_a)^2/n_a) + ((sd_n)^2/n_n)]}$	2.46E+07
ts	2.22

$t_s = 2.22$
$t_s > 1$ Therefore the null hypothesis is rejected and $\mu_a \neq \mu_n$

The SRB populations at the sediment/water interface of the High DOC Cu-Zn column are not the same as the SRB populations at the sediment/water interface of the Low DOC Cu-Zn column.

E-5. The t Statistics of the Active SRB and the Non-active SRB Au aqueous phases.

μ_a = The Active SRB Au values
μ_n = The Non-active SRB Au values

The following null hypothesis is considered	H_o: $\mu_a = \mu_n$
The following alternative hypothesis is also considered	H_a: $\mu_a \neq \mu_n$

The t test is a standard method of choosing between the two hypotheses.

$$t_s = \frac{|X_a - X_n| - 0}{SE_{(Xa - Xn)}} \qquad \text{where; } SE_{(Xa - Xn)} = \sqrt{[((sd_a)^2/n_a) + ((sd_n)^2/n_n)]}$$

If $t_s < 1$ do not reject the null hypothesis
If $t_s > 1$ reject the null hypothesis and accept the alternative hypothesis

Note that the $|X_a - X_n|$ is subtracted from zero because H_o states that $\mu_a - \mu_n$ equals zero; writing

"$|X_a - X_n| - 0$" reminds us of what we are testing.

E-5.1 Statistical analysis of pH in the aqueous phase of the Active SRB and Non-active SRB Au columns:

Active SRB Au	Day	n	pH	
	13	1	7.94	
	26	1	7.07	
	41	1	8.05	
	56	1	8.21	
	74	1	8.5	
	90	1	9.27	
	104	1	8.22	
	125	1	8.12	
	n_a	8		
	x_a		8.17	
	sd_a			0.61

Non-active SRB Au	Day	n	pH	
	13	1	6.85	
	26	1	7.02	
	41	1	6.9	
	56	1	7.78	
	74	1	7.83	
	90	1	8.15	
	104	1	7.98	
	125	1	8.12	
	n_n	8		
	x_n		7.58	
	sd_n			0.56

Xn-Xa	0.59
$(sd_a)^2/n_a)$	0.05
$(sd_n)^2/n_n)$	0.04
$\sqrt{[((sd_a)^2/n_a) + ((sd_n)^2/n_n)]}$	0.29
ts	2.03

$t_s = 2.03$
$t_s > 1$ Therefore the null hypothesis is rejected and $\mu_a \neq \mu_n$

The pH values measured in the Active SRB Au column are not the same as the pH values measured in the Non-active SRB Au column.

E-5.2 Statistical analysis of Eh in the aqueous phase of the Active SRB and Non-active SRB Au columns:

Active SRB Au	Day	n	Eh (mv)	
	13	1	68.7	
	26	1	75.7	
	41	1	167.1	
	56	1	88	
	74	1	234.8	
	90	1	117	
	104	1	385	
	125	1	419	
	n_a	8		
	x_a		194.41	
	sd_a			139.57

Non-active SRB Au	Day	n	Eh (mv)	
	13	1	42.7	
	26	1	57.4	
	41	1	146.6	
	56	1	1	
	74	1	179	
	90	1	112	
	104	1	80	
	125	1	390	
	n_n	8		
	x_n		126.09	
	sd_n			121.01

Xn-Xa	68.33

$(sd_a)^2/n_a)$	2434.87
$(sd_n)^2/n_n)$	1830.56
$\sqrt{[((sd_a)^2/n_a) + ((sd_n)^2/n_n)]}$	65.31
ts	1.05

$t_s = 1.05$
$t_s > 1$ Therefore the null hypothesis is rejected and $\mu_a \neq \mu_n$

The Eh values measured in the Active SRB Au column are not the same as the Eh values measured in the Non-active SRB Au column.

E-5.3 Statistical analysis of SO_4^{2-} in the aqueous phase of the Active SRB and Non-active SRB Au columns:

Active SRB Au	Day	n	SO_4^{2-} (ppm)	
	13	1	0	
	26	1	0	
	41	1	0	
	56	1	0	
	74	1	0	
	90	1	0	
	104	1	0	
	125	1	0	
	n_a	**8**		
	x_a		**0.00**	
	sd_a			**0.00**

Non-active SRB Au	Day	n	SO_4^{2-} (ppm)	
	13	1	16	
	26	1	8	
	41	1	1	
	56	1	0	
	74	1	1	
	90	1	1	
	104	1	0	
	125	1	0	
	n_n	**8**		
	x_n		**3.38**	
	sd_n			**5.76**

Xn-Xa	3.38
$(sd_a)^2/n_a)$	0.00
$(sd_n)^2/n_n)$	4.14
$\sqrt{[((sd_a)^2/n_a) + ((sd_n)^2/n_n)]}$	2.03
ts	1.66

$t_s = 1.66$
$t_s > 1$ Therefore the null hypothesis is rejected and $\mu_a \neq \mu_n$

The SO_4^{2-} values measured in the Active SRB Au column are not the same as the SO_4^{2-} values measured in the Non-active SRB Au column.

E-5.4 Statistical analysis of S^{2-} in the aqueous phase of the Active SRB and Non-active SRB Au columns:

Active SRB Au	Day	n	S^{2-} (ppm)	
	13	1	0.053	
	26	1	0.115	
	41	1	0.016	
	56	1	0.022	
	74	1	0.008	

Non-active SRB Au	Day	n	S^{2-} (ppm)	
	13	1	1.394	
	26	1	0.248	
	41	1	0.131	
	56	1	0.241	
	74	1	0.184	

	90	1	0.95		90	1	0.267	
	104	1	0.067		104	1	0.026	
	125	1	0.071		125	1	0.04	
n_a	8			n_n	8			
x_a		0.16		x_n		0.32		
sd_a			0.32	sd_n			0.45	

Xn-Xa	0.15
$(sd_a)^2/n_a)$	0.01
$(sd_n)^2/n_n)$	0.02
$\sqrt{[((sd_a)^2/n_a) + ((sd_n)^2/n_n)]}$	0.19
ts	0.79

$t_s = 0.79$
$t_s < 1$ Therefore the null hypothesis is not rejected and $\mu_a = \mu_n$

The S^{2-} values measured in the Active SRB Au column are the same as the S^{2-} values measured in the Non-active SRB Au column.

E-5.5 Statistical analysis of Fe_{diss} in the aqueous phase of the Active SRB and Non-active SRB Au columns:

Active SRB Au	Day	n	Fe_{diss} (ppm)		Non-active SRB Au	Day	n	Fe_{diss} (ppm)	
	13	1	1.3			13	1	116.3	
	26	1	5.36			26	1	69.4	
	41	1	0.54			41	1	158	
	56	1	2.39			56	1	153.7	
	74	1	0.77			74	1	40.6	
	90	1	0.63			90	1	55.6	
	104	1	1.53			104	1	35.9	
	125	1	1.51			125	1	92	
n_a	8				n_n	8			
x_a		1.75			x_n		90.19		
sd_a			1.58		sd_n			48.33	

Xn-Xa	88.43
$(sd_a)^2/n_a)$	0.31
$(sd_n)^2/n_n)$	292.00
$\sqrt{[((sd_a)^2/n_a) + ((sd_n)^2/n_n)]}$	17.10
ts	5.17

$t_s = 5.17$
$t_s > 1$ Therefore the null hypothesis is rejected and $\mu_a \neq \mu_n$

The Fe_{diss} values measured in the Active SRB Au column are not the same as the Fe_{diss} values measured in the Non-active SRB Au column.

E-5.6 Statistical analysis of DOC in the aqueous phase of the Active SRB and Non-active SRB Au columns:

Active SRB Au	Day	n	DOC (ppm)	
	13	1	131.2	
	26	1	25.5	
	41	1	34.4	
	56	1	28.1	
	74	1	46.9	
	90	1	107.4	
	104	1	92.1	
	125	1	27.4	
	n_a	**8**		
	x_a		**61.63**	
	sd_a			**42.13**

Non-active SRB Au	Day	n	DOC (ppm)	
	13	1	192.6	
	26	1	17.9	
	41	1	210	
	56	1	231.6	
	74	1	231.6	
	90	1	239.4	
	104	1	218.1	
	125	1	167.7	
	n_n	**8**		
	x_n		**188.61**	
	sd_n			**72.90**

Xn-Xa	126.99
$(sd_a)^2/n_a)$	221.84
$(sd_n)^2/n_n)$	664.25
$\sqrt{[((sd_a)^2/n_a) + ((sd_n)^2/n_n)]}$	29.77
ts	4.27

$t_s = 4.27$
$t_s > 1$ Therefore the null hypothesis is rejected and $\mu_a \neq \mu_n$

The DOC values measured in the Active SRB Au column are not the same as the DOC values measured in the Non-active SRB Au column.

E-5.7 Statistical analysis of Hg_{tot} in the aqueous phase of the Active SRB and Non-active SRB Au columns:

Active SRB Au	Day	n	Hg_{tot} (ppt)	
	13	1	0	
	26	1	0.42	
	41	1	0.26	
	56	1	0	
	74	1	131.1	
	90	1	0	
	104	1	0	
	125	1	28.7	
	n_a	**8**		
	x_a		**20.06**	
	sd_a			**45.97**

Non-active SRB Au	Day	n	Hg_{tot} (ppt)	
	13	1	0	
	26	1	0	
	41	1	0	
	56	1	0	
	74	1	0	
	90	1	0	
	104	1	0	
	125	1	0	
	n_n	**8**		
	x_n		**0.00**	
	sd_n			**0.00**

Xn-Xa	20.06
$(sd_a)^2/n_a)$	264.14
$(sd_n)^2/n_n)$	0.00
$\sqrt{[((sd_a)^2/n_a) +}$	16.25

$((sd_n)^2/n_n)]$	
ts	1.23

$t_s = 1.23$
$t_s > 1$ Therefore the null hypothesis is not rejected and $\mu_a \neq \mu_n$

The Hg_{tot} values measured in the Active SRB Au column are not the same as the Hg_{tot} values measured in the Non-active SRB Au column.

E-5.8 Statistical analysis of MeHg in the aqueous phase of the Active SRB and Non-active SRB Au columns:

Active SRB Au	Day	n	MeHg (ppt)	
	13	1	0.07	
	26	1	0.13	
	41	1	0.23	
	56	1	0.96	
	74	1	1.45	
	90	1	0	
	104	1	0	
	125	1	0.9	
	n_a	**8**		
	x_a		**0.47**	
	sd_a			**0.56**

Non-active SRB Au	Day	n	MeHg (ppt)	
	13	1	0.17	
	26	1	0	
	41	1	0.35	
	56	1	0.48	
	74	1	0.11	
	90	1	0.09	
	104	1	0	
	125	1	0.08	
	n_n	**8**		
	x_n		**0.16**	
	sd_n			**0.17**

Xn-Xa	0.31
$(sd_a)^2/n_a)$	0.04
$(sd_n)^2/n_n)$	0.00
$\sqrt{[((sd_a)^2/n_a) + ((sd_n)^2/n_n)]}$	0.21
ts	1.50

$t_s = 1.50$
$t_s > 1$ Therefore the null hypothesis is rejected and $\mu_a \neq \mu_n$

The MeHg values measured in the Active SRB Au column are not the same as the MeHg values measured in the Non-active SRB Au column.

E-5.9 Statistical analysis of SRB populations in the aqueous phase of the Active SRB and Non-active SRB Au columns:

Active SRB Au	Day	n	SRB CFU/g dry wt. sed.	
	0	5	8.00E+05	
	13	5	7.10E+07	
	41	5	3.90E+05	
	125	5	9.80E+06	
	n_a	**20**		
	x_a		**2.05E+07**	

Non-active SRB Au	Day	n	SRB CFU/g dry wt. sed.	
	0	1	8.00E+05	
	13	1	1.20E+06	
	41	1	5.80E+04	
	125	1	8.80E+03	
	n_n	**4**		
	x_n		**5.17E+05**	

	sd_a			3.39E+07		sd_n		5.82E+05

Xn-Xa	2.00E+07
$(sd_a)^2/n_a)$	5.76E+13
$(sd_n)^2/n_n)$	8.46E+10
$\sqrt{[((sd_a)^2/n_a) + ((sd_n)^2/n_n)]}$	7.60E+06
ts	2.63

$t_s = 2.63$
$t_s > 1$ Therefore the null hypothesis is rejected and $\mu_a \neq \mu_n$

The SRB populations at the sediment/water interface of the Active SRB Au column are not the same as the SRB populations at the sediment/water interface of the Non-active SRB Au column.